Norwegian University
of Life Sciences

Master's Thesis 2020 60 ECTS
Faculty of Chemistry, Biotechnology and Food Sciences

Inosine-independent roles of human Endonuclease V

Hannah Winther Solbakk
Master of Science, Biotechnology

Inosine-independent roles of human Endonuclease V

Department of Microbiology,

Oslo University Hospital

And

The Norwegian University of Life Sciences

Faculty of Chemistry, Biotechnology and Food Science

Acknowledgements

The study presented in this master thesis was carried out between August 2019 and May 2020 at Oslo University Hospital, Rikshospitalet, Department of Microbiology and the Norwegian University of Life Sciences, Department of Chemistry, Biotechnology and Food Sciences.

First, I would like to thank my supervisor at Department of Microbiology, Dr. Ingrun Alseth. Your excellent guidance, feedback, support and enthusiasm throughout this year and while writing this thesis has been invaluable. You are a great role model and I am very much looking forward to continuing my work in your research group.

I would also like to thank Dr. Natalia Berges for all the help in the lab and for always taking the time to answer my questions. Thank you to Rune J. Forstrøm for the help with protein purification, and to other members of the staff for the help and guidance in the laboratory.

I also wish to express my gratitude towards my supervisor at Norwegian University of Life Sciences, Professor Dzung Bao Diep for being available for questions and for support throughout this study.

Thank you to all the people in the student office and especially Ida for making my year at the department much easier and funnier. Going through this experiment with you has been a delight.

A big thanks to my parents and family for their support and for believing in me, even though I didn´t always believe in myself.

Last, but not least, thank you to my husband Eirik for indispensable support and encouragement not only with the writing of this thesis, but throughout my whole studies. I am forever grateful for your love, patience and understanding.

Ås, May 2020
Hannah Winther Solbakk

Abstract

Endonuclease V (EndoV) is a highly conserved enzyme with specificity for inosines in nucleic acids. The bacterial EndoVs are active both on DNA and RNA, whereas the human (h) homolog (hEndoV) cleaves only at inosines in RNA. In DNA, inosine is regarded a damage and the role of hEndoV as a repair enzyme is well acknowledged. In contrast, the biological function of hEndoV upon RNA is still unknown. Non-coding RNAs are involved in many cellular processes, but the biological role and significance of many of them remains uncertain. Y RNAs are a family of non-coding RNAs conserved in vertebrates that are often components of ribonucleoproteins (RNPs) complexed with Ro60 (RoRNP). Ro60 is a conserved RNA-binding protein that was first characterized as an antigen targeted by autoantibodies from patients with systemic lupus erythematosus and Sjögren´s syndrome. No interaction between hEndoV and Ro60 is known, but both are found to interact with the RNA binding proteins Y-Box protein (YBX) and insulin-like growth factor-2 mRNA-binding protein 1 (IGF2BP1).

The goal for this thesis was to confirm an individual-nucleotide resolution crosslinking immunoprecipitation (IP) assay (iCLIP) where certain tRNAs and Y RNAs were found as possible targets for hEndoV. This was done by biochemical activity assays and electrophoretic mobility shift assays (EMSA) using tRNAs with and without inosine and Y RNA1 and Y RNA4 as substrates. Three variants of recombinant hEndoV were used. The Y RNA transcript levels of hEndoV were also studied in a quantative reverse transcriptase PCR (RT-qPCR) analysis. In addition, hEndoV interactions with YBX1, IGF2BP1 and Ro60 were investigated further by co-immunoprecipitation assay and immunocytochemistry (ICC).

The results show that hEndoV both bind and cleave all tRNAs and Y RNAs tested and this was independent of the presence of inosines. Moreover, interaction of hEndoV with YBX1 and IGF2BP1 but not Ro60, was confirmed. These data suggest that hEndoV may have a broader role in the cells beyond processing inosine-containing RNA. Though, inosine-containing RNA appears to be the best substrate for hEndoV.

Sammendrag

Endonuklease V er et godt konservert enzym med spesifisitet for inosin i nukleinsyrer. De bakterielle EndoV´er er aktive både på DNA og RNA, mens den humane homologen kun kutter ved inosin i RNA. I DNA blir inosin sett på som en skade, og rollen til hEndoV som et reparasjonsenzym er annerkjent. I motsetning er den biologiske funksjonen til hEndoV fortsatt ukjent. Ikke-kodende RNA er involvert i mange cellulære prosesser, men den biologiske rollen og signifikansen til mange av dem er fortsatt usikker. Y RNA er en familie av ikke-kodende RNA konservert i vertebrater og som ofte er komponenter av ribonuklein proteiner sammen med Ro60. Ro60 er et RNA-bindene protein som først ble karakterisert som et antigen for autoantistoffer fra pasienter med systemisk lupus erythematosus og Sjögren´s syndrom. Ingen interaksjon mellom hEndoV og Ro60 er kjent, men begge har blitt rapportert å interagere med de RNA bindende proteinene YBX1 og IGF2BP1.

I denne oppgaven var målet å bekrefte funnene i en iCLIP analyse der tRNA og YRNA ble funnet bundet til hEndoV. Dette ble gjort med biokjemisk aktivitetsassay og EMSA analyse hvor tRNA både med og uten inosin og Y RNA1 og Y RNA4 ble benyttet som substrater. Tre varianter av rekombinant hEndoV ble brukt. Om Y RNA transkript-nivåer ble påvirket av mengden hEndoV i cellene ble også undersøkt i en RT-qPCR analyse. I tillegg ble hEndoV´s interaksjoner med YBX1, IGF2BP1 og Ro60 undersøkt videre med co-immunopresipitering og ICC.

Resultatene viser at hEndoV både binder og kutter alle tRNA og Y RNA som ble undersøkt. Binding og aktivitet ble funnet å være uavhengig av tilstedeværelsen av inosin. Interaksjoner av hEndoV med YBX1 og IGF2BP1 ble bekreftet, men ingen interaksjon mellom hEndoV og Ro60 ble funnet. Disse dataene viser at hEndoV kanskje har en bredere rolle i cellene utover å prosessere inosinholdig RNA. Dog er inosinholdig RNA det foretrukne substratet til hEndoV

Table of contents

Abbreviations

3′OH	3′-hydroxyl
5′-P	5′-phosphate
ADAR	adenosine deaminase acting on RNA
ADAT	adenosine deaminase acting on tRNA
ATP	adenosine triphosphate
CCA	cytosin-cytosin-adenine
cDNA	complementary DNA
CSD	cold shock domain
DEN	diethylnitrosamine
DNA	deoxyribonucleic acid
ds	double-stranded
dsCTR RNA	double-stranded control RNA
E. coli	*Escherichia coli*
eIF4I	eukaryotic initiation factor 4F
EMSA	electrophoretic mobility shift assay
EndoV	Endonuclease V
e.g.	exempli gratia
FT	flow through
FRT	Flp Recombination Target
GAPDH	glyceraldehyde 3-phosphate dehydrogenase
GFP	green fluorescent protein
HCC	hepatocellular carcinoma
HeLa	Henrietta Lacks
HRP	horseradish peroxidase
Human Endonuclease V	hEndoV
ICC	immunocytochemistry
iCLIP	individual-nucleotide resolution crosslinking immunoprecipitation assay
IGF2BP1	insulin-like growth factor-2 mRNA-binding protein 1
KH	k-homology
KO	knockout
LB	Luria-Bertani
m^5C	5-methylcytosine
m^1A	N1-methyladenosine
MBP	maltose binding protein
mEndoV	mouse EndoV
mRNA	messenger RNA
MQ water	milli-Q water
MWCO	molecular weight cut-off
OD_{600}	optical density 600

ON	overnight
OUH	Oslo University Hospital
PAGE	polyacrylamide gel electrophoresis
pmol	picomole (10^{-12} mole)
PNK	polynucleotide kinase
Poly I:C	poly I: poly C
Pre-mRNA	precursor mRNA
Pre-tRNA	precursor tRNA
RNA	ribonucleic acid
RNase	ribonuclease
RNH	ribonuclease/angiogenin inhibitor 1
RNP	ribonucleoproteins
RRM	RNA recognition motifs
RT	room temperature
RT-qPCR	quantitative real time-polymerase chain reaction
SG	stress granules
ss	single stranded
TEV	Tobacco Etch Virus
Tma	*Thermotoga maritima*
Tb	*Trypansoma brucei*
tRF	tRNA derived fragments
tRNA	transfer RNA
tsRNA	tRNA-derived small fragments
UTR	untranslated region
UV	ultra-violet
UV-Vis	ultra-violet visible spectre
WT	wild type
YBX	Y-box protein

1 Introduction

Enzymes are a type of proteins that work as biological catalysts, and their function is to accelerate the speed of chemical reactions in living organisms (Robinson, 2015). A class of enzymes is nucleases that cleave the phosphodiester bonds of nucleic acids. The nucleases can be either endo- or exonucleases. Exonucleases cleaves at the 5′ or 3′endings, whereas endonucleases cleaves internal in the polynucleotide chain (Yang, 2011).

In 1977 Gates and Linn described an endonuclease encoded by the *nfi*- gene in *Escherichia coli,* called endonucleaseV (eEndoV) (Gates and Linn, 1977). EndoV cleaves the second phosphodiester bond 3′ to deoxyinosine in DNA and RNA (Yao et al., 1994). In DNA inosine, the deamination product of adenosine, is regarded as a damage , while in RNA it is an essential modification resulting in increased diversity of the transcriptome (Alseth et al., 2014).

Non-coding RNAs are involved in many different cellular processes, although most of them still have unknown biochemical functions (Kowalski and Krude, 2015). Often non-coding RNAs complex with proteins to regulate important cellular functions (Dhahbi et al., 2014) such as RNA processing and quality control and are essential factors for the first steps of chromosomal DNA replication in human cells (Kowalski and Krude, 2015). Two types of these RNAs are tRNA and cytoplasmic (Y) RNA. tRNAs have an important role in the protein synthesis where they functions as adapters between mRNA and corresponding amino acids (Tymoczko et al., 2015). Y RNAs together with Ro60 are components of RNPs complexes, and the subcellular localization of Ro60 is suggested to be regulated by Y RNA-protein complexes (Kowalski and Krude, 2015, Sim and wolin, 2011).

In an attempt to identify which RNAs are targeted by EndoV inside the cells, our research group performed an individual-nucleotide resolution cross-linking and immunoprecipitation (IP) assay (iCLIP) and it was found that both tRNA and Y RNA were bound to EndoV. In this thesis we want to confirm the finding of the iCLIP analysis and study the possible interaction between hEndoV and tRNA/Y RNA and associated proteins.

1.1 Inosine in RNA

Deamination of the nucleobases of DNA and RNA is a common event and a result of spontaneous hydrolysis, endogenous or environmental factors or deaminase enzymes (Cao, 2013, Gray, 2012). One of the four bases of the nucleic acids is adenosine (A), which for RNA can be deaminated to inosine (I) in a so-called A-to-I editing (Figure 1). This editing results in the conversion of the 6-aminopurine ring of adenosine to 6-oxopurine in inosine (Gray, 2012). Inosine resembles guanosine (G) which normally pairs with cytosine (C), and inosine will therefore pair most stably with cytosine (Schouten and Weiss, 1999, Hill-Perkins et al., 1986).

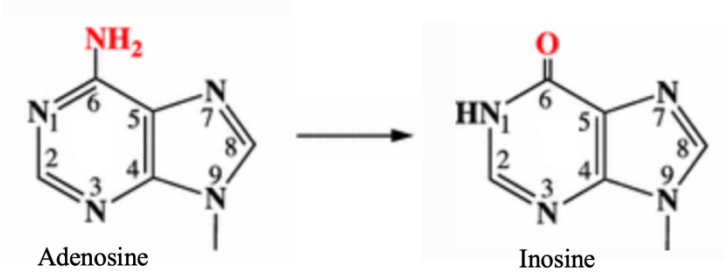

Figure 1. Deamination of adenosine yields inosine*. In the deamination of adenosine, the amino group is replaced by a keto group to form inosine. The 6-aminopurine ring is converted to 6-oxopurine. Adapted from (Cao, 2013).*

One major difference when regarding inosine is that in DNA, inosine is regarded a damage that needs to be fixed because of its miscoding properties. However, in RNA inosine is a normal and essential alteration introduced by specific deaminases that contributes to gene diversity. The four bases of RNA are often co- or post-transcriptionally modified, and the A-to-I editing is probably the most prevalent (Gray, 2012).

1.1.1 Deamination of adenosine in RNA

There are three mechanisms leading to deaminated adenosines in RNA, these are spontaneous deamination, nitrosative stress, misincorporation (Dedon et al., 2006) and deamination by specific enzymes called adenosine deaminases acting on RNA (ADAR). In mRNA and non-coding RNA like miRNA, the responsible enzymes are ADAR, whereas in tRNA the responsible enzymes are adenosine deaminases acting on tRNA (ADAT). Inosine has not been found in rRNA (Gray, 2012).

In tRNA, inosine is found in wobble position 34 and it is a necessity for protein translation. Because inosine has relaxed base pairing properties, multiple codons can be decoded by a single tRNA. $tRNA_{Arg}$ (the tRNA that binds L-arginine) is the only tRNA with inosine in bacteria, whereas eight different tRNAs have inosine at the wobble position in mammals. In mRNA inosine may lead to a re-coding of the genetic information or deletion/generation of stop codons and splice variants. This can result in protein diversity and is believed to have been fundamental for human development and cognitive complexity (Alseth et al., 2014).

1.2 tRNA

tRNA has an important role in the protein synthesis. They are a special class of small RNA molecules, about 80 nucleotides in length, that work as adaptors between mRNA and amino acids (Alberts et al., 2015). This function helps ribosomes to decode information in mRNA into amino acids, resulting in proteins. tRNAs is bound to the mRNA codon by the complimentary anticodon, a set of three consecutive nucleotides (Alberts et al., 2015). The activated amino acids are covalently attached to the 3´hydroxyl group of the adenosine residue located at the tail of the 3´cytosin-cytosin-adenine (CCA) component of the tRNA (Tymoczko et al., 2015, Ibba and Söll, 2000). The recognition and attachment of the amino acids is mediated by aminoacyl tRNA synthase, which specifically couple each amino acid to the corresponding tRNA containing the precise anticodon (Ibba and Söll, 2000).

Every codon is specific for one amino acid, but several codons may specify the same amino acid. Therefore, some tRNAs molecules can base-pair with more than one codon (Alberts et al., 2015, Crick, 1968).

tRNA molecules are arranged in a cloverleaf secondary structure. The structure includes a 3´amino acid acceptor stem, an extra variable arm, a DHU loop/arm, a TψC arm and a phosphorylated 5´end (Figure 2) (Tymoczko et al., 2015).

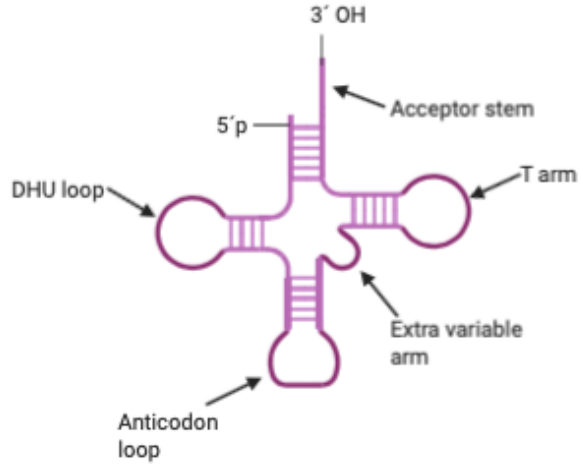

Figure 2. Structure of tRNA. *tRNA has a cloverleaf secondary structure with 3´amino acid acceptor stem, an extra variable arm, a DHU loop/arm, a TψC arm and a phosphorylated 5´end.*

1.2.1 tRNA maturations

Mature tRNAs has undergone vigorous processing. In the transcription, tRNAs are transcribed as precursor-tRNAs (pre-tRNA) in the nucleus by RNA-polymerase III (Robertson et al., 1972). The early steps in the biosynthesis for tRNAs are the same for most tRNAs while steps specific for different tRNAs often occur later (Hopper et al., 2011). An important component for the early tRNA processing is the ribonuclease P (RNase P) which cleaves the 5´leader of the tRNA, resulting in a 5´monophosphate end (Robertson et al., 1972). The 3´trailer is cleaved by another enzyme called RNase Z which results in a single 3´overhang acceptor stem and a 3´hydroxyl end (Schiffer et al., 2002).

In MODOMICS, a database for RNA modifications, over 170 RNA modifications are showed (Boccaletto et al., 2018). Nuclear encoded tRNA is the absolute most modified RNA, with an average of 13 modifications per molecule. Modifications of individual tRNAs are more uneven, for example are mitochondrial tRNAs generally less modified with five modifications per molecule on average (Pan, 2018). The modifications are most prevalent in the anticodon loop and where the DHU loop/arm and TψC arm interact in the tRNA core region (Lorenz et al., 2017). The most prominent tRNA modification is amongst others wybutosine, methylation (5-methylcytosine, m^5C or 1- methyladenosine, m^1A) or pseudouridylation (Boccaletto et al., 2018). tRNA modifications can alter or stabilize its tertiary structures and/or help the recognition of the codon-anticodon. For proper function of tRNAs, some of the modification are particularly important (Ishitani et al., 2003).

1.2.2 tRNA-derived small RNAs; tRFs and tRNA halves

The importance of the biological functions of tRNA derived small fragments (tsRNAs) has been gradually investigated in recent years (Shen et al., 2018). tsRNAs are on a general basis divided in tRNA derived fragments (tRFs) and tRNA halves (Sobala and Hutvanger, 2011). tsRNA refers to the cleavage of tRNAs by specific nucleases [e.g. Dicer, angiogenin (Ang) and RNAse Z] (Shen et al., 2018) (Figure 3). In 2019 Krishna et al. demonstrated that specific 5´tsRNAs can preferentially interact with zipcode-binding protein (IGF2BP1, an RNA-binding protein, which will be discussed later in this thesis (Krishna et al., 2019).

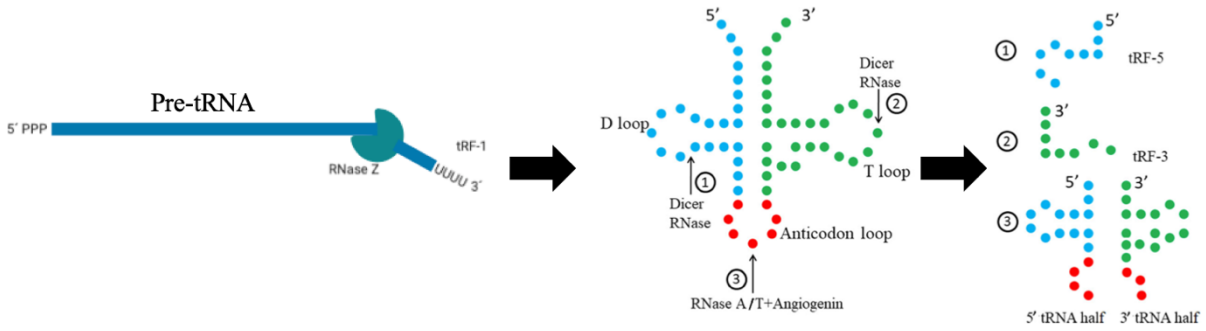

Figure 3. Biogenesis of tsRNAs. *tRNAs are cleaved by specific nucleases generating tRFs and tRNA halves. Adapted from (Shen et al., 2018).*

tRFs

tRFs are 14-30 nucleotides long and can mainly be separated into three subclasses: tRF-3, tRF-5 and tRF-1. tRFs-3 are derived from the 3´end of mature tRNA, tRFs-5 are derived from the 5´end of mature tRNA and tRF-1 corresponds to tRNA 3´trailers (Figure 3) (Tuck and Tollervey, 2011). The main enzymes responsible for generating the tRFs are Dicer and RNase Z. The tRFs can also be divided based on which enzyme that generates them, where group I are formed by Dicer and group II by RNase Z (Haussecker et al., 2010). Several groups have showed that the cleaving of mature tRNA into tRFs is surprisingly site-specific, causing tRFs with highly definite lengths among different cell lines. It has also been shown that the abundance of pre-tRNA does not correlate with the tRF expression (Keam and Hutvagner, 2015). tRFs have important roles in numerous biological contexts such as innate immunity, cancer, stress response and neurological disorders (Fu et al., 2015). In 2015 Lee et al., suggested that tRFs are not just by-products of tRNA degradation, but a novel class of small

RNAs with specific biological roles. Among others they found that one tRF in the tRF-1 series is required for cell proliferation (Lee et al., 2015).

tRNA halves

tRNA halves are slightly longer than tRFs with 31-40 nucleotides in length. They are generated by cleavage in the anticodon loop of mature tRNA, resulting in 5´and 3´fragments, (Figure 3) (Li and Hu, 2012, Shen et al., 2018) . Stress activates the protein Ang into generating tRNA halves (Yamasaki et al., 2009). Ang belongs to the RNAse A superfamily, and upon stress ang is released from the ribonuclease/ang inhibitor 1 (RNH1) to the cytoplasm to act on tRNA (Li and Hu, 2012). Ang has an important role in promoting cancer progression (Yoshioka et al., 2006). 5´tRNA halves, but not 3´tRNA halves inhibit translation (Emara et al., 2010, Ivanov et al., 2011). The translation is inhibited through blocking of the assembly of the cap-binding eukaryotic initiation factor 4F (eIF4F) complex (Ivanov et al., 2011). Both tRFs and tRNA halves have important roles in regulation of rRNA and protein biogenesis (Zhu et al., 2019).

1.3 Y RNA, Ro60 and related proteins

1.3.1 Y RNA and Ro60

Y RNA are a type of small non-coding RNAs that were first discovered in 1981 in the cytoplasm of mammalian cells. To distinguish them from other RNAs, they were given the prefix Y, for cytoplasmic RNA (Lerner et al., 1981).
In humans there are found four Y RNA genes; *hY1*, *hY3*, *hY4* and *hY5*, that are clustered together on chromosome 7q36. *hY2* was also originally described but was later found to be a degradation product of *hY1* and removed from the list. So far, all vertebrates investigated have had between one and four different Y RNA genes per species (Perreault et al., 2007, Maraia et al., 1996, Mosig et al., 2007). The vertebrate Y RNAs are not homologous with the bacterial Y RNA (Perreault et al., 2007).

The Y RNAs are relatively small being 100 ± 20 nucleotides long, and they fold into characteristic stem-loop secondary structures. Experiments have revealed that the termini hybridize to form the upper and lower stem domains, whereas the middle part form the internal loop domain (Figure 4) (Gelder et al., 1994, Teunissen et al., 2000). The sequence

and the predicted structure of the internal loop vary greatly, while the nucleotide sequence of the stems is highly conserved (Kowalski and Krude, 2015).

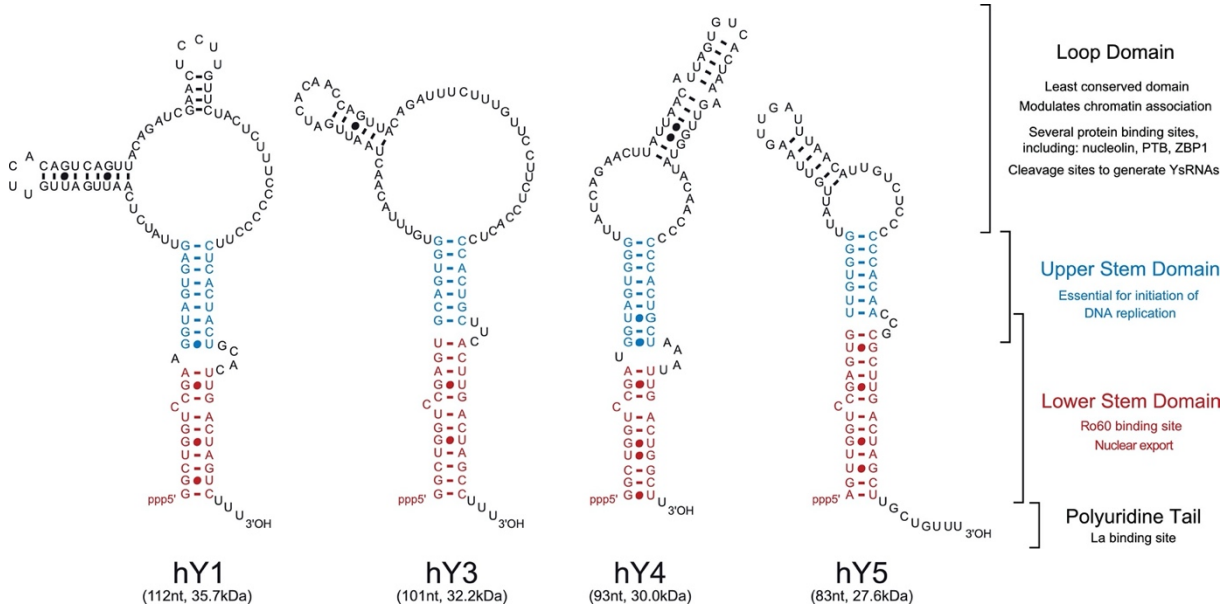

Figure 4. Non-coding human Y RNAs. *Structural RNA domains and their associated functions are shown in the right bar. For each RNA the nucleotides (nt) and molecular weight (kDa) are given. Adapted from (Kowalski and Krude, 2015).*

Y RNAs are often components of RNPs complexed with Ro60. Ro60 was first characterized as an antigen targeted by autoantibodies from patients with systemic lupus erythematosus and Sjögren´s syndrome, two systemic autoimmune rheumatic diseases (Kowalski and Krude, 2015) . The number of Y RNAs in the complexes vary, but in all studies Ro60 is found complexed with at least one Y RNA (Boccitto and Wolin, 2019). Binding of Ro60 to the internal stem loop in Y RNA, protects Y RNA from degradation (Sim et al., 2012).

In 2012 Sim *et al*. identified a number of Ro-associated proteins, among them La, YBX and the zipcode-binding protein IGF2BP1. IGF2BP1 was previously described to copurify with Ro60 (Sim et al., 2012, Jønson et al., 2007). The association of Ro60 with YBX1 and IGF2BP1 is RNA dependent (Sim et al., 2012) YBX1 and IGF2BP1 will be further studied in this thesis.

1.3.2 Y-box protein

The YBX family consist of three proteins YBX1, 2 and 3. The gene encoding *YBX1* is located on chromosome 1p34.2 while the *YBX2* and *YBX3* genes are found on other chromosomes (Prabhu et al., 2015). YBX1 is an RNA-binding protein with numerous of interacting partners. YBX1 is important in many cellular pathways as transcriptional and translational control as well as cell proliferation (Matsumoto and Bay, 2005). Research done with mouse shows that inactivation of YBX1 leads to embryonic lethality (Uchiumi et al., 2006). Moreover the amount of YBX1 decrease gradually during aging and at old age it is only found in the liver (Eliseeva et al., 2011, Uchiumi et al., 2006). YBX1 stabilizes known oncogenes by binding to their 3´ untranslated region (UTR) area. Goodarzi et al. showed in 2015 that tRFs from $tRNA_{Glu}$ (tRNA molecule that binds L-glutamate), $tRNA_{Asp}$ (tRNA molecules that binds L-aspartate), $tRNA_{Gly}$ (tRNA molecule that binds glycine) and $tRNA_{Tyr}$ (tRNA molecule that binds L-tyrosine) bind YBX1 and a number of known oncogenic transcripts are displaced from YBX1. This results in transcript destabilization and because YBX1 is overexpressed in various cancer types it therefore suppresses tumor progression and metastasis (Goodarzi et al., 2015).

Common for all the YBX proteins are there distinct protein structure. They have an alanine/proline rich domain (N-terminal), a cold shock domain (CSD), and a long C-terminal domain with alternating positively and negatively charged amino acids (Eliseeva et al., 2011) (Figure 5). The CSD is a nucleic acid binding domain, consisting of two consensus sequences RNP-1 and RNP-2 (Landsman, 1992), that present RNA and ds/ss DNA binding to YBX proteins (Matsumoto and Bay, 2005). The C-terminal domain consists of alternating acidic and basic amino acids and is likely to hold YBX ability to associate with other proteins and RNA-binding. The N-terminal is associated with actin. The C- and N-terminals are less conserved than CSD (Matsumoto and Bay, 2005).

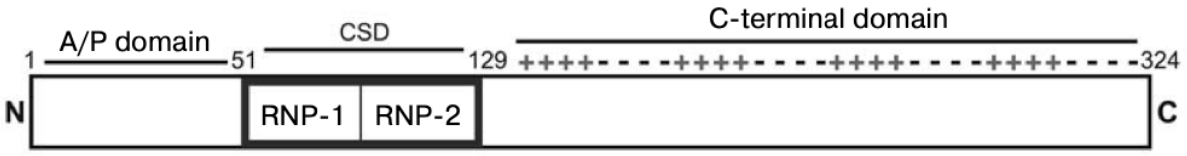

Figure 5. YBX1 protein domain organization. *Structural organization of human YBX1. YBX1 consist of A/P domain at the N-terminal, CDS with RNP-1 and RNP-2 consensus sequences and the C-terminal doimain. Adapted from (Eliseeva et al., 2011).*

1.3.3 IGF2BP1

IGF2BP1 belongs to a family of single-stranded RNA-binding proteins which includes the three proteins IGF2BP1-3. The expression of IGF2BP1 in adult tissues is limited, but it is broadly expressed in fetal tissues and in several cancer types (Huang et al., 2018). In the cytoplasm, IGF2BP1 controls translation, localization and the amount of some specific transcripts. It also has an important role in regulation of cell growth, migration and proliferation (Stöhr and Hüttelmaier, 2012). IGF2BP1 is composed of two RNA recognition motifs (RRMs) and four K homology (KH) domains, which forms six RNA binding motifs in total (Figure 6) (Wachter et al., 2013).

Figure 6. Protein domain structure of IGF2BP*. Domain structure of IGF2BP1. RNA-binding domains consist of two RRMs (blue) and four KH-domains (green). Adapted from (Huang et al., 2018).*

Subcellular localization of YBX, IGF2BP1 and Ro60

Ro60 is localized in cytoplasm and nucleus in unstressed cells, but after Ultra-violet (UV) irradiation it becomes strongly nuclear (Chen et al., 2003). In 2012 Sim *et al*. showed that IGF2BP1 was almost entirely cytoplasmic in unstressed cells, but 15 and 24 h after UV irradiation it was also detected in the nuclei (Sim et al., 2012). IGF2BP1 has been reported to accumulate in stress granules (SG´s) after arsenite or heat shock treatment in human osteosarcoma cells (Stöhr et al., 2006). However, upon UV irradiation, neither IGF2BP1 or GFP-IGF2BP1 accumulated strongly in SG´s (Sim et al., 2012).

SG´s are cytoplasmic assemblies that are formed as a response to certain stress factors. SG´s contain a range of RNAs and proteins, for example the poly-A-binding protein and translational initiation factors (Alberts et al., 2015). The purpose of SG formation is temporarily inhibition of translation of housekeeping genes and optimized translation of genes related to stress response. The aim of the SG´s is to raise the odds of cell survival (Kedersha et al., 2013).

YBX1 is distributed both in the nucleus and the cytoplasm, and has been reported to accumulate in nuclei after UV irradiation (Keike et al., 1997). YBX1 localizes to SGs, but its function in SGs biology is not known. In 2015 it was reported that YBX1 and the RNA-binding protein G3BP1 expression are correlated in SG´s in human sarcomas (Somasekharan et al., 2015).

Experiments done by Sim *et al.* showed that the fraction of IGF2BP1 associated with Ro60 increased four times after UV irradiation. This increase was specific to IGF2BP1, as the levels of YBX1 were unchanged. They also found that the interaction of Ro60 with IGF2BP1 is dependent on Y RNA3 (Sim et al., 2012). Co-localization in the cell supports possible interactions and common functions.

1.4 Endonuclease V

EndoV homologs are widespread in nature, found in all three domains of life and belongs to a family of highly conserved proteins (Fladeby et al., 2012). The bacterial homologs are active on both DNA and RNA, whereas the different mammalian variants only cleave RNA (Nawaz et al. 2016a). Endo V was, as the fifth (V) endonuclease, discovered in 1977 in *E. coli* by Gates and Linn. eEndoV was characterized as a deoxyribonuclease (DNase) with affinity to uracil which is the deamination product of cytosine (Gates and Linn, 1977). EndoV from the hyperthermophilic bacteria *Thermotoga maritima (Tma)*, has also been well characterised and is showing similar substrate preferences as eEndoV (Huang et al., 2002, Huang et al., 2001). EndoV characterization from the protozoan parasite *Trypansoma brucei* (TbEndoV), shows that TbEndoV prefers ssRNA oligonucleotides with inosine, but exhibit weak activity on DNA. It is believed that TbEndoV plays an important role in the RNA metabolism of the parasite. Parasites lacking TbEndoV are viable, but show growth defects in the insect stage of their life cycle (García-Caballero et al., 2017).

EndoV specifically recognize and cuts the second phosphodiesterbond 3´to inosine with Mg^{2+} as a cofactor generating 3´OH and 5´P-termini (Figure 7) (Yao et al., 1994, Dalhus et al., 2009). EndoV does not show exonuclease activity, meaning that other factors are required to remove the base after cleavage (Lee et al., 2010).

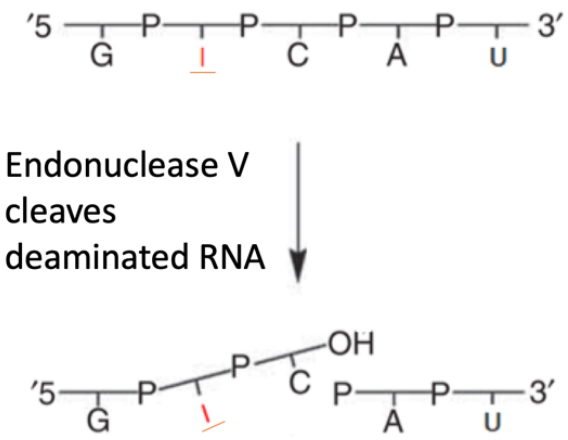

Figure 7. EndoV activity on deminated RNA. *EndoV cleaves the second phosphodiester bond 3´to inosine. Adapted from (Dalhus et al., 2009).*

EndoV is not an essential gene, and *E. coli* cells that are lacking EndoV have a normal spontaneous mutation frequency. However when exposed to nitrous acid, *nfi*$^{-}$ cells are hypermutators and an increase in AT→GC and GC→AT transition as well as GC→CG transversion mutations are shown (Schouten and Weiss, 1999). Mice lacking EndoV are viable with normal appearance. To further investigate the *in vivo* function of mEndoV both wild type and EndoV$^{-/-}$ mice were challenged with diethylnitrosamine (DEN) to induce hepatocellular carcinoma. Liver tumors were developed for both types, but were smaller and fewer for EndoV$^{-/-}$ (Kong et al., 2020).

1.4.1 Human Endonuclease V

The *hEndoV* gene is located on chromosome 17q25.3, it shares approximately 30% amino acid sequence identity with bacterial EndoV and encodes a transcript that holds 10 exons (Mi et al., 2012, Fladeby et al., 2012). Most hEndoV transcripts holds exon 5-8, but splicing of the 3´end increase transcriptomic diversity (Nawaz et al., 2016a).

In 2012 it was shown that by fusion of hEndoV with green fluorescent protein (GFP) that hEndoV is localized in the cytosol and nucleus in HeLa-cells (Fladeby et al., 2012). hEndoV relocalize to SG´s when exposed to stress, and it is suggested that this is as a strategy to create an environment low on adenosine triphosphate (ATP) to allow hEndoV activity. hEndoV is inhibited by normal intracellular ATP concentrations, and SG´s do not overlay with ATP stores. hEndoV activity seem to be regulated in cells (Nawaz et al., 2016a). Studies have

shown that when the cells are exposed to toxic agents such as arsenite and hydrogen peroxide, there is a significant drop in the intracellular ATP levels. A 70-80% reduction in ATP level diminish the hEndoV inhibition. These harmful agents are also known to introduce deamination damage to RNA, which is a substrate for hEndoV (Nawaz et al., 2016a).

The *in vitro* function of hEndoV was characterized in 2013 by Vik *et al.* and Morina *et.al.* Analysis of hEndo V DNA/RNA binding and nuclease activity showed that hEndoV strongly preferred inosine-containing single stranded RNA (ssRNA) substrates. As previously mentioned prokaryotic EndoV can cleave both DNA and RNA, an ability hEndoV seems to have lost as it can only cleave RNA (Morita et al., 2013, Vik et al., 2013). The biological role of RNA cleavage at inosines by hEndoV is not known (Nawaz et al., 2016a).

1.4.2 Structures of hEndoV

The 3D-structure of hEndoV consists of 8 β-folds and 6 α-helix structures and seems to be absolutely necessary for enzyme function. The main difference between prokaryotic and eukaryotic EndoV is found in residue 167-174 were hEndoV has an extra α-helix, while prokaryotic EndoV is 11 residues shorter (Figure 9). In addition hEndoV has a longer C-terminal (Nawaz et al., 2016b).

The crystal structure of the hEndoV apoenzyme has been described (Zhang et al., 2014). It was found that the enzyme maintains a general “RNase H-like” structure in the metal-binding site, wedge motif and inosine-binding pocket especially. In addition hEndoV also present various extra insertions and a characteristic four-cysteine motif (not shown in Figure) (Zhang et al., 2014).

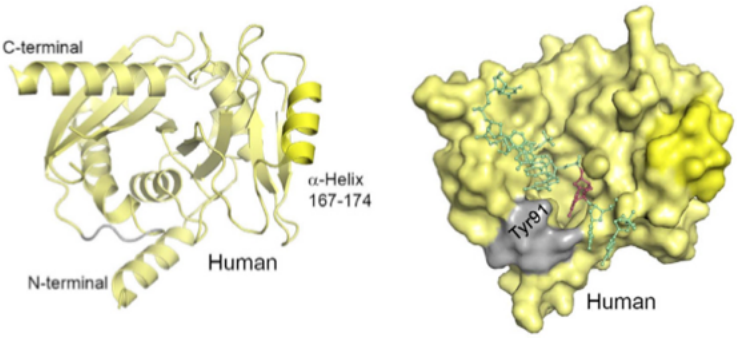

Figure 9. The structure of hEndoV. *The overall structure is shown to the left. The human version used in crystallization has been truncated (comprising amino acid residues 13-250). The indicated α-helix (residues 167-174) is only found in eukaryotic EndoV. Surface display of hEndoV is shown to the right. The DNA (coloured green and the inosine residue red) was taken drom the TmaEndoV-DNA co-crystallisation. Adapted from (Nawaz et al., 2016b).*

1.4.3 Splice variants of hEndoV

Splicing of precursor mRNA (pre-mRNA) is an important and critical step in the posttranscriptional regulation of gene expression and it provide diversity to the proteome. The average human gene is made up of eight exons and seven introns, which give rise to an average of three or more spliced mRNA isoforms (Lee and Rio, 2015). The alternative splicing may result in protein isoforms with separate biological properties that could play essential roles in many biological processes (Stastna and Eyk, 2013). It is therefore important to investigate the splicing of different isoforms to understand their function.

Expression of *hEndoV* mRNA varies among tissues and cells and are generally low (Fladeby et al., 2012). The sequence data available in public databases suggest that there is a high degree of alternative splicing of *hEndoV* transcripts which results in a large number of different isoforms. *hEndoV* with RefSeq identifier NP_775898 corresponds to a full-length mRNA transcript that contains 10 exons. Exon 3, which contains a segment encoding a β-strand and an α-helix, is what makes up the catalytical domain and is in fact absent in many of the transcripts. If translated, these are likely non-functional enzymes. The majority of the hEndoV transcripts available in the public databases is likely not to produce functional proteins (Fladeby et al., 2012, Berges et al., 2019).

Among the many hEndoV transcripts only two in addition to the full-length 282 contain all conserved exons 1-8, no extra exons in the core region and a common exon 9. The three isoforms differ in the length of exon 9 (coding part) and two have alternative 3´exons, exon 10a and 10b (NM_173627.40 = hEndoV 282, NM_001352761.1 = hEndoV 308 and NM_001352760.1 = hEndoV 309) (Figure 8). hEndoV 309 is the variant conserved in mammals, and the isoform used in the research in this thesis (amino acid sequence given in appendix A) (Berges et al., 2019). Berges et al. showed in 2019 that the isoform 282 that has been previously used in research have a significantly lower mRNA level than the two isoforms hEndoV 308 and 309 (Berges et al., 2019).

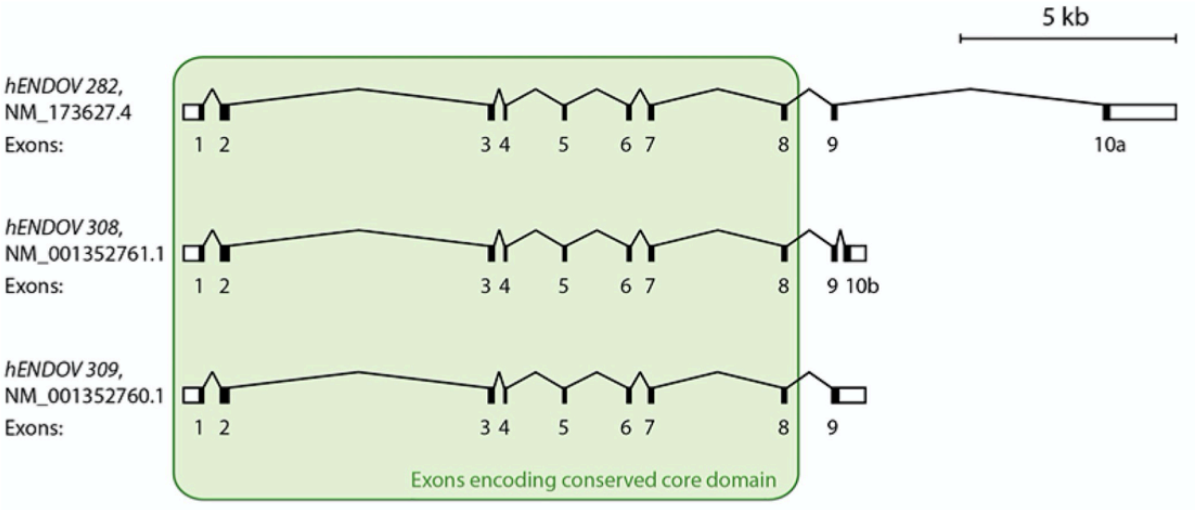

Figure 8. Transcript variants of hEndoV. *Only three of the around 40+ predicted transcripts of hEndoV (hEndoV 282, 308 and 309) are likely to produce functional proteins. These transcripts comprise all exons 1-8, have no extra exons in the core region and a common exon 9. All other proteins are lacking important catalytic core encoding exons or have additional exons encoding segments that disrupt the structure and thereby the functions of the protein. The white boxes (in exon 1 and the 3´exon) show the 5´UTR and 3´UTR. The exon length is not propotional correct. Adapted from (Berges et al., 2019).*

1.4.4 Relocation to stress granules

As mentioned earlier hEndoV is shown to relocate to SG´s when exposed to oxidative (arsenite) and nitrosative (sodium nitrite) stress and viral infections mimics (poly(I:C)). Also, hEndoV colocalize with another protein called PABPC1, which also functionally and physically interact with each other. The significance of this interaction is not known (Nawaz et al., 2016a).

1.5 Aims of this study

For several years our research group at Oslo University Hospital (OUH) has had interest in EndoV. In an attempt to identify which RNAs are targeted by EndoV inside the cells, an iCLIP was performed and it was found that both tRNA and Y RNA were bound to hEndoV. This was somehow unexpected, as the specific tRNA identified nor Y RNAs are known to contain inosines. The aim of this study is to have a closer look and confirm the findings made in the iCLIP analysis and in addition to study other possible protein partners. Novel finding here may shed light on the *in vivo* functions of hEndoV.

The hEndoV isoform 309 and the corresponding inactive mutant D52A will be expressed in *E. coli* and purified for *in vitro* analysis. In human cells endogenous hEndoV expression is generally below the detection limits of most assays, so human cell lines overexpressing both wild type and mutant hEndoV will be used for cellular analyses.

Mass spectrometry (MS) analysis performed earlier reported that hEndoV may interact with the two proteins YBX1 and IGF2BP1 (appendix B). We know that these also can be linked to Y RNA, and therefore Co-immunoprecipitation with hEndoV will be performed. It is a hypothesis that hEndoV might share some functions with the proteins it interacts with, and therefore this could be helpful in understanding the *in vivo* function of hEndoV.

2 Methods

All materials are given in appendix C.

All DNA, RNA and protein extracts were kept on ice during the experiments if not stated otherwise. DNA were stored at -20°C, while RNA and proteins were stored at -80°C.

2.1 Purification of hEndoV

hEndoV and the inactive mutant hEndoV D52A were expressed in *E. coli* and purified for downstream experiments. The protein expression can be achieved by transforming an expression plasmid with the gene of interest into a suitable host. Cell cultures are then grown, and proteins purified.

Protein purification was performed using a nickel-nitrilotriacetic (Ni-NTA) agarose column. The Ni-NTA Purification system is designed for purification of 6xHistidine (His)-tagged recombinant proteins. The protein of interest will bind to Ni-NTA resin with its 6xHis -Tag (at the C – or N-terminal), while other proteins pass through the column. Proteins can be purified under denaturing, native or hybrid conditions using the Ni-NTA agarose. Proteins bound to the resin are eluted with a buffer containing excessive imidazole that competes with the 6xHis-Tag for binding to the Ni-NTA resin (Novex, 2015).

2.1.1 Transformation

Electroporation was used to transform the expression construct into competent ER2566 (*rnfi*$^{-}$ *nhb*$^{-}$) cells. Electroporation is an efficient transformation technique which, briefly explained, involves the transportation of a plasmid into a competent cell by electric shock (Potter and Heller, 2003).

Of the plasmid constructs (pETM41-hEndoV and pETM41-hEndoV D52A; Plasmid map is given in appendix D), 50 ng was added to competent *E. coli* cells. The cells were then transferred to an electroporation cuvette and the electroporation was carried out at 1800 V. 950 µl SOC-media was immediately added to the cell-construct mixture and incubated at 37°C for at least 1 h. The transformants were streaked out on Luria-Bertani (LB)-kanamycin (50 µg kanamycin/ml) plates and incubated overnight (ON) at 37°C.

2.1.2 Expression of hEndoV

ON cultures were made by inoculating transformants in LB-medium (40 ml) containing 50 µg/ml kanamycin. The ON cultures were incubated at 37°C with strong shaking. 10 ml of ON culture was transferred to 1 l LB-sorbitol medium and incubated at 37°C on shaker until the OD_{600} had reached 0.4-0.6. The protein expression was induced by addition of IPTG to a final concentration of 0.5 mM, and the cells were further grown ON at 16°C. The cells were harvested by centrifugation at 4500 rpm for 15 min at 4°C and resuspended in 10 ml Imidazole buffer I per litre cell culture (4 l).

2.1.3 Protein purification of hEndoV with Ni-NTA column

The harvested cell suspension was sonicated for 3x30 sec with 60% amplitude, with a 30 second cooling period between each session. The cell suspension was centrifuged at 15,000 rpm for 30 min at 4°C to pellet the cell remains. The supernatant containing the proteins was transferred to a fresh tube and kept on ice. Ni-NTA resin was equilibrated by using 1 ml Ni-NTA agarose per litre cell culture, and added 10 ml Imidazole buffer I. The resin was settled by centrifugation at 3000 rpm for 3 min at 4°C, and the supernatant was removed. The supernatant containing the proteins of interest was added to the settled resin and incubated for 30 min at 4°C on a roller to keep the resin and supernatant resuspended. The resin was then settled by gravity, and the supernatant was allowed to flow through. The flow-through (FT) was kept at 4°C for gel analysis. The column was washed two times with 10 ml Imidazole buffer II, and the wash fractions were kept at 4°C for gel analysis. Bound proteins were eluted with Imidazole buffer III, and collected in seven fractions of 1.5 ml.
The purified proteins were analysed using gel analysis and aliquoted into fractions with 20% glycerol for storage at -80°C. The protein concentrations were determined with Bovine Serum Albumin (BSA) as the standard and BioRad Protein Assay.

To remove the fusion tag from the recombinant proteins, Tobacco Etch Virus (TEV) protease was used. The expression constructs have a TEV sequence encoding 7 amino acids which the TEV protease cleaves. For the TEV protease to work the proteins have to be dialyzed against a TEV-buffer. The protein fractions were added 1:100 with TEV protease and transferred to a Molecular porous membrane (MWCO 6-8,000 Da) and dialyzed in TEV buffer (0.5 l x 2) for 1 h at 4°C with rotation. Before further purification by a size exclusion chromatography

(Superdex 75) the proteins were dialyzed back to the original Imidazole buffer I for 30 min at 4°C with rotation and purified once more on a Ni-NTA column to remove the tag from the protein fraction. The proteins also have a maltose binding protein (MBP)-tag, which was removed together with the His-tag.

SDS polyacrylamide gel electrophoresis

Sodium dodecyl sulphate (SDS) polyacrylamide gel electrophoresis (SDS-PAGE) is a technique used to separate proteins according to their size in an electric field. Binding of SDS to the proteins cause all proteins to have the same ratio-to-mass upon which proteins are separated (Tymoczko et al., 2015). By using molecular markers with known molecular weight, the molecular weight of the protein(s) can be determined (Sambrook and Russell, 2006).

FT, wash fraction and the eluted proteins from section 2.1.3 were prepared for gel electrophoresis by mixing the following components; 5 µl 4xBOLT™ Sample Buffer, 1 µl DTT (1 M), 6 µl of the protein fractions and 8 µl MQ-water.

The samples were incubated for 5 min at 95°C and loaded at Bolt 10% Bis-Tris Plus gel in 1xNuPAGE® MOPS buffer. 7 µl SeeBlue®Plus2 was used as molecular marker (given in appendix E). The gel was run at 200 V for 50 min. After the electrophoresis, the gel was stained for 1 h with Coomassie Blue staining solution and destained for ~ 30 min in destaining solution.

2.1.4 Superdex 75 HR 10/30

Further purification of hEndoV was performed on a Superdex 75 HR 10/30 by a laboratory engineer. Superdex 75 is a column that separates proteins based on their size. Superdex 75 has an optimal separation range at 3000-70,000 Da (GE Healthcare, 2017).

2.2 Culturing and maintaining cell cultures

Cell cultures are tools often used in molecular and cell biology which represents biological models creating a system of the intended experiment. The mammalian cells have often undergone transformations allowing them to divide infinitely (Alberts et al., 2015).

The Flp-In™ T-REx™ System allows stable mammalian cell lines to exhibit tetracycline-inducible expression of a gene of interest from a specific genomic location. This is done in three major steps; Firstly, independent integration of a plasmid containing a Flp Recombination Target (FRT) site and a plasmid expressing the Tet repressor (repressor of the tetracycline resistance element) into the genome of a mammalian cell line to generate a Flp-In™ T-REx™ host cell line. Secondly, introduction of an expression vector containing the gene of interest. This is done under control of a tetracycline-inducible promoter via a Flp recombinase-mediated DNA recombination at the FRT site into the genome. Thirdly, induction of the gene of interest by the addition of tetracycline/doxycycline (Invitrogen, 2012). The Flp-In™ T-REx™ System was used for overexpression of hEndoV and hEndoV D52A in this thesis.

A humidified atmosphere with 5.0% CO_2 and 37°C was used for all incubations. To secure exponential growth, the cells were regularly monitored in microscope and passaged when confluent. The different cell lines used, required different culture media (see appendix D). Phosphate buffered saline (PBS), Trypsin-EDTA(1x) and culture medium should be kept at 25-37°C when added to the cells and otherwise kept at 4°C. All cell lines used are adherent, meaning they attach to the flask or plate.

2.2.1 Cell culture from freezing stock initiation

The cell cultures were kept in a nitrogen tank. Cell cultures were initiated by immediately thawing cells at 37°C and mixing with 1 ml culture medium. The solution was then centrifuged at 1200 x g for 4 min. Supernatant was removed and the cell-pellet resuspended in 1 ml culture medium by mixing gently. The cell suspension was transferred to a Nunclon™ flask, either 75 cm^2 (T-75) or 175 cm^2 (T-175) and added 15 ml (T-75) or 20 ml (T-175) culture medium. The cells were examined on the microscope and incubated at 37°C until the cell confluency had reached 70-80%.

2.2.2 Passaging of cells

When the cells had reached a confluency of 70-80%, the culture medium was removed. Because of the adherence the cells remained attached to the flask. The cells were washed with PBS to remove any remaining culture medium. To detach the cells, Trypsin-EDTA (1x)

(trypsin) was added, just enough to cover the cell surface, and incubated for 1-5 min at 37°C and 5% CO_2. By adding 10-20 ml culture medium (1:9 trypsin/culture medium final volume), trypsin was inactivated by trypsin inhibitors present in Fetal Bovine Serum (FBS). The medium was added vigorously to make sure the cells were detached, and cells observed under the microscope. The cell suspension was split and diluted with culture medium up to 10 ml (T75) or 20 ml (T175). Passaging of cells were performed every 2-5 days depending on the confluency and incubated at 37°C and 5% CO_2. For experiments where the number of cells used is important, the cells were counted using Trypan Blue Solution 0.4 % and Invitrogen™ Countess™ Automated Cell Counter.

2.3 Co-immunoprecipitation

Protein-protein interactions occur in well-defined contexts and are involved in most cellular processes. Co-immunoprecipitation is a widely used technique to detect such protein-protein interactions, and can be used to examine interactions in a variety of environments, tissues or cell-types (Zhu et al., 2017). Protein complexes are isolated from a solution, in this case a lysate, by utilizing an antibody specific for one of the proteins in the complex. The antibody is bound to a solid substrate, often magnetic beads, that allows the proteins to be precipitated from the solution. Proteins tightly bound to the antibody-specific protein will then be co-precipitated in the assay (Iqbal et al., 2018). Bound proteins can be detected using western blotting (Section 2.3.3). Co-immunoprecipitation was performed with Flp-in T-REx 293, and Flp-in T-REx 293 Flag hEndoV cells.

2.3.1 Preparation of cell lysate for co-immunoprecipitation

Cell lysate was made from three confluent 15 cm petri dishes giving approximately 3-5 mg protein using the NETN lysate buffer with the following protocol. 24 h before harvesting the cells were added 1 µg/ml doxycycline to promote protein expression. If treated by arsenite, 0.5 mM was added directly to the cells 2 h prior to harvesting.

Culture media was removed, and the cells were washed in 5-8 ml ice cold PBS. Harvesting of the cells was done by scraping them off the dish with 5 ml ice cold PBS. The cell suspension was transferred to a 50 ml falcon tube and centrifuged at 1500 x g for 5 min at 4°C. The supernatant was removed, and the cell pellet resolved in 1 ml ice cold PBS and transferred to

an Eppendorf tube. The tube was centrifuged for another 5 min at 1500 x g at 4°C before the supernatant again was removed and added 1-1.5 ml NETN lysis buffer depending on the volume of the pellet. The cells were lysed for 30 min on a roller at 4°C followed by centrifugation at 13,000 rpm for 10 min. The supernatant containing the proteins of interest was transferred to a fresh Eppendorf tube and the concentration was measured using the BioRad Protein Assay. The lysate was used directly or aliquoted and kept at -80°C.

2.3.2 Co-immunoprecipitation

Flag is a small tag of 25 amino acids that is a widely used tag for immunoprecipitation of proteins. Anti-Flag M2 antibody recognizes and binds Flag-tagged proteins. The Flag sequence is located at the N-, Met-N- or C-terminis of the proteins (Gerace and Moazed, 2015). 4% magnetic agarose beads bound with the Anti-Flag M2 antibody made it possible to separate the proteins bound to the antibody, from the lysate remains using a magnetic rack. All cell lines used in this experiment express Flag-tagged proteins.

For each sample 10 µl of Anti-Flag® M2 Magnetic Beads were used. Before addition of protein lysate the beads were washed twice in 1 ml NT2 equilibration buffer (eq.buffer) and resuspended in 500 µl NT2 eq.buffer, 1 µl DTT and 40 µl EDTA. For samples that were not going to be added RNAse, 2 µl VRC and 2.5 µl RNaseOUT was also added. Then 1.5 mg of protein lysates were added to the tubes, and the samples were incubated ON at 4°C on rotation. The lysate was removed, and the beads washed four times with 1 ml NT2 wash buffer. Samples to be RNAse treated, were resuspended in 1 ml NT2 eq.buffer and added 100 ng RNaseA and incubated for 15 min at 37°C before washing. NT2 buffers were made freshly before each experiment. The samples were added 20 µl 2x Laemmeli Sample Buffer with DTT (1 M) and boiled at 95°C for 5 min. The samples were separated on a 10% Bis-Tris gel for 40 min at 140 V in 1xNuPAGE® MOPS buffer and the gel was further used in Western blot analysis. SeeBlue® Plus2 Prestained Standard was used as the molecular marker. Input samples using 40 µg lysate was also included, as positive control.

2.3.3 Western blot

Western blot makes it possible to identify specific proteins from a complex mixture of proteins extracted from cells or tissues. Proteins are separated based on molecular weight through gel electrophoresis and transferred to a membrane producing a band for each protein

(Mahmood and Yang, 2012). Membrane with transferred proteins is blocked to prevent unspecific binding, before being incubated with a primary antibody specific for the target protein. A secondary antibody with a chromogenic/fluorescent enzyme attached, binds to the primary antibody allowing visualization of the proteins of interest (Tymoczko et al., 2015).

Proteins separated by gel electrophoresis were transferred to a nitrocellulose membrane using Trans-Blot® Transfer System at 25 V for 7 min. Post-transfer the membrane was washed in PBS for 2 min and blocked in PBS with 5% skim-milk on a shaker for 1 h at room temperature (RT) or at 4°C ON. PBS with 0.05% Tween was used to wash the membrane 3 times for 5-8 min on a shaker, before the membrane was incubated with primary antibody in PBS with 5% skim milk for at least 1 h at RT or ON at 4°C on a shaker. An overview of the dilutions of antibodies employed are found in appendix C. Before incubation with the secondary antibody the same wash as above was performed. A secondary antibody, anti-rabbit IgG horseradish peroxidase antibody (1:1000 dilution) was added, and the membrane incubated for 30-60 min at RT on a shaker. The membrane was washed as above. SuperSignal^{R} West Femto Maximum Sensitivity Substrate from Thermo scientific was used according to the manufacturer´s instructions, and the membrane was immediately visualized in a BioRad Molecular Imager.

If more than one protein was being detected on the same membrane the antibodies could be removed by stripping. Both the primary and secondary antibodies were removed, and the membranes re-incubated with an antibody specific for another protein of interest.
The membrane was incubated with a stripping buffer with SDS two times for 10 min on rotation. After incubation with stripping buffer, washing, blocking and incubation with primary and secondary antibodies was performed as described above before visualization of the proteins.

2.4 Immunocytochemistry for Flp-in T-REx GFP-hEndoV

ICC is a powerful method in search for the localization of cell antigens ranging from amino acids and proteins to specific cellular populations. The method can be divided in two phases. 1. Preparation of the cells and stages involved for the reaction, 2. Quantification and interpretation of the acquired expression. ICC is based on the employment of specific primary

antibodies that can be visualized through staining with fluorescent secondary antibodies (Matos et al., 2010). ICC was performed with Flp-in T-REx 293 GFP-hEndoV cells.

To a Nunclon™ Dish 24-well, sterile 12 mm coverslips were added and covered in 20 µg/ml fibronectin in sterile water. The coverslips were incubated at 37°C for 30 min. After incubation the fibronectin was removed and coverslips dried in RT. Cells were seeded in each well (0.15 x 10^6 cells/well) in culture medium with 1 µg/ml doxycycline for protein expression and incubated for 24 h. Cells were fixated to the coverslips with 4% PFA in PBS for 15 min. Cells treated with arsenite were added 0.5 mM 2 h prior to fixation and cells treated with UV irradiation was treated with 120 mJ/cm^2 in a UV-1800 UV-VIS spectrophotometer 12 h prior to the fixation. After fixation cells were washed twice in PBS.

To prepare the cells for immunostaining they were quenched with 100 mM glycine in PBS for 10 min at RT, permabilized with 0.1 % Triton in PBS for 10 min at RT and blocked with 0.5% BSA in PBS for 30 min at RT. Primary antibodies were diluted in 0.5 % BSA in PBS and incubated with the cells for 1 h at RT (30 µl dilution per well). After incubation the cells were washed 3 times in PBS. Secondary antibodies were diluted in 0.5 % BSA in PBS and incubated as with primary antibodies (all antibodies with correct dilution listed in appendix C). Then the cells were washed as above. The coverslips with treated cells were mounted on to microscope slides with Vectashield Hardset Antifade Mounting Medium with dapi and dried in RT ON.

Images were attained on Leica TCS Sp8 gSTED microscopy (Leica Microsystems) using a 40x oil immersion objective, set with Leica LAX software. Images were processed with brightness/contrast levels in the Fiji Software. All cells with the same antibody staining/GFP were imaged with the same acquisition parameters.

2.5 Biochemical activity assays

To detect, quantify and study the activity of an enzyme, *in vitro* biochemical activity assay is a well-known analytical method (Tu and Cohen, 1980). Biochemical activity assays were performed with recombinant hEndoV, MH-hEndoV and MH-hEndoV D52A purified enzymes.

Activity assay was performed in two ways; with [^{32}P]-5´-labeled RNA substrates and northern blot. When working with radioactive substances, the appropriate protection was used.

2.5.1 Labelling probes for Northern Blot

The oligonucleotides were end-labeled using T4 polynucleotide kinase (PNK) and [γ-^{32} P]ATP. To label the probes a mixture of 20 µl was prepared by mixing the following components: 2 µl 10 x PNK buffer, 1 µl T4 PNK, 3.5 pmol oligonucleotide, 1 µl [γ-^{32}]-ATP and 15 µl MQ-water.

The sample was incubated at 37°C for 30 min prior to 85°C for 5 min. The labeled probes were stored at -20°C or used directly.

2.5.2 Isolation of small RNA using RNAzol®

Small RNA used as substrates in activity assay and affinity analysis were isolated from HAP C665 cells using the RNAzol® method. The method is based on the interaction of phenol and guanidine with cellular components for separation of RNA from other molecules (RNAzolRT Brochure, 2009).

The cells were washed in PBS and lysed by addition of 1 ml RNAzol®RT. Vigorous pipetting ensured homogenization. 0.4 ml RNAse free water was added per 1 ml of homogenate. The homogenate was shaken vigorously for 15 sec and stored for 5-15 min in RT. Next, the sample were centrifuged for 15 min at 12,000 x g. After centrifugation RNA remains in the supernatant which were transferred to a fresh tube. 0.4 ml of 75% ethanol was added to the sample and incubated at RT for 5-20 min followed by centrifugation at 12,000 x g for 5-8 min. Small RNA present in the supernatant was transferred to a fresh tube. The sample was added 0.8 volume of isopropanol and incubated at 4°C for 30 min. The precipitated small RNA was sedimented at 12,000 x g for 15 min at RT. The RNA pellets were washed twice by mixing with 70% isopropanol followed by centrifugation at 12,000 g for 15 min. Small RNA was dissolved in RNAse free water and RNA concentration was measured on NanoDrop™ One/One^{C} Microvolume UV-Vis.

2.5.3 Activity assay performed with [^{32}P]-5´-labeled RNA substrates

Activity assay with [^{32}P]-5´-labeled RNA substrates are based on radioactively labelling the nucleic acid in one end and incubated with an enzyme of interest to study it´s activity. The enzymatic reaction is stopped, and samples are separated on a denaturing polyacrylamide gel (Alberts et al., 2015). The radioactive products can be visualized by phosphorimaging by exposure of the gel to a phosphor imager screen, and quantified based on the proportion of emitted light to the amount of radioactivity in the samples. By the size of the labelled substrate a possible break in the nucleic acid strand can be determined (Alberts et al., 2015, GE Life Sciences, 2018). The [^{32}P]-5´-labeled single stranded IIUI (ssIIUI) RNA substrate used was a 20-nucleotide long RNA nucleotide containing 3 inosines (sequences given in appendix C). The double stranded IIUI (dsIIUI) was the same ssIIUI annealed to the complementary strand.

A reaction buffer was prepared by adding the following components to a tube: 1.3, 6.5 or 25 nM enzyme, 2 µl 5 x Reaction buffer (Rb), 2 µl ^{32}P-labeled substrate and 5 µl MQ-water. The reaction samples were incubated at 37°C for 15 min. To stop the reactions an equal volume of formamide loading dye was added. The samples were then denatured for 3 min at 52°C and separated on a 20% polyacrylamide gel at 200 V for 60 min in 1x taurine buffer. Of each sample, 6 µl was applied to the gel.

The gel was dried for 30 min at 80°C under vacuum and exposed to a phosphorimager screen ON. The radiolabelled product on the gel was visualized by using a Typhoon PhosphorImager scanner and quantified using the ImageQuant TL software.

2.5.4 Activity assays performed with small endogenous RNA in northern blot

Activity assays were also performed with small endogenous RNA in a Northern blot analysis. Northern blot analysis refers to a hybridization that uses DNA as a probe and RNA as the target molecule to detect a specific RNA molecule among a sample of RNAs (Clark and Pazdernik, 2013). RNA is firstly separated by size on a denaturing gel. The RNA is then transferred to a nylon membrane and fixed to the membrane, often by UV-light. Next, the membrane is treated with labelled probes complementary to a particular RNA sequence in the sample, the probe will then hybridize or bind to a specific RNA fragment on the membrane

(He, 2013). The probes were labelled with [γ-^{32} P]ATP as described in 2.5.1 and the membrane exposed to a phosphor screen and visualized as described in 2.5.3.

A reaction mixture was prepared by adding the following components to a tube: 0.8 or 1.6 µM enzyme, 2 µl 5 x Rb (Mg^{2+}), 8 pmol (500 ng/µl) small RNA and 6.5 µl MQ-water.

The mixed reaction samples were then incubated at 37°C for 20 min. To stop the reactions an equal volume of formamide loading dye was added. The samples were then denatured for 3 min at 52°C. Samples were separated on a 15% denaturing polyacrylamide gel at 200 V for 60 min in 1x taurine buffer. About 16 µl of each sample was applied to the gel.

Blotting and incubating membranes

The samples, now separated by size, were transferred to a charged nylon membrane in a semi-dry blot system for 60 min at 200 mA and 20 V in RT. After blotting the membranes were crosslinked with UV irradiation at 120 mJ/cm^2 in a UV-1800 UV-VIS spectrophotometer.

Membranes were pre-hybridized in 5-8 ml ULTRAhyb™-Oligo Hybridization buffer for at least 30 min rotating at 37°C. The labelled probes as described under section 2.3.1 were then added directly to the solution and incubation continued with rotation at 37°C for 3 h. The membranes were washed in 5 ml low stringency buffer 2x5 min rotating at RT. Following, the membranes were washed in 5 ml high stringency buffer for 5 min rotating at 37°C. The membranes were visualized and quantified as above.

2.6 Electrophoretic mobility shift assay

EMSA is a fast and sensitive method to detect interactions between proteins and nucleic acids. The method is based on the observation that the electrophoretic mobility of a free nucleic acid is more than that of a protein-nucleic acid complex. A solution of protein and nucleic acid are mixed and subjected to electrophoresis under native conditions using an agarose or polyacrylamide gel. After electrophoresis, the migration of complexes containing nucleic acids are determined. The nucleic acids are often ^{32}-P labeled or the gel is transferred to a membrane in a northern blot. Normally, protein-nucleic acid complexes migrate slower

through the gel than free nucleic acids, and interactions can be detected (Hellmann and Fried, 2007).

EMSA was performed with recombinant hEndoV on [^{32}P]-5´-labeled RNA substrates and recombinant hEndoV, MH-hEndoV and MH-hEndoV D52A in northern blot. EMSA was performed as activity assays, with a few alterations stated in the protocols.

2.6.1 Electrophoretic mobility shift assay performed on [^{32}P]-5´-labeled RNA substrates

EMSA was performed using RNA oligonucleotides corresponding to different structural parts of Y RNA4: 5´stem: bulge, 5´stem: complementary, Hairpin and ds-control RNA (dsCTR RNA). In addition, ssIIUI and dsIIUI were included.

A reaction mixture was prepared by adding the following components to a tube: 100, 200 or 400 nM enzyme, 2 µl 5 x Rb T/A, 1 µl ^{32}P-labelled substrate, 1 µl $CaCl_2$ and 5 µl MQ water.

The reaction samples were incubated on ice for 15 min under UV irradiation to optimize binding between the substrates and the proteins. The reactions were stopped by adding 1 µl DNA loading buffer, and 4-6 µl was applied on a 10% native gel. The gel was run at 100 V in 1x taurine buffer for 60 min. The gel was dried and exposed as explained in section 2.5.3.

2.6.2 Electrophoretic mobility shift assay with endogenous small RNAs in northern blot

Small RNA from HAP C665 wt cells were isolated as described in section 2.5.2 and used in this experiment.

A reaction mixture was prepared by adding the following components to a tube: 0.8 or 1.6 µM enzyme, 2 µl 5 x Rb T/A, 8 pmol (500 ng/µl) small RNA, 2 µl $CaCl_2$ and 4.5 µl MQ-water.

The reaction samples were incubated on ice for 20 min, before being added 2 µl DNA Loading buffer. Then 8 µl of the samples were loaded and separated on a 10% polyacrylamide gel for 60 min at 100 V in 1x taurine buffer. When finished the gel was blotted on a membrane and probed as described in section 2.5.4.

2.7 *Y RNA* gene expression

2.7.1 Quantitative reverse transcription Polymerase Chain Reaction

RT-qPCR is a method for detection and expression analysis of genes in real time and are based on the original PCR invented in 1984 (Deepak et al., 2007). The goal with RT-qPCR is to precisely measure and distinguish specific nucleic acids in a sample. PCR is a cyclic process of three steps; denaturation of DNA, annealing of primers to the DNA template strand and polymerization. In PCR the product is only detected at the end of the reaction, while in qPCR the products are measured as they are generated. This provides a fast and accurate quantification of DNA and RNA (Valasek and Repa, 2005).

A limitation with PCR is that DNA generally must be used as template. This is because the DNA polymerase cannot amplify RNA. Therefore, complementary DNA (cDNA) must be generated from an RNA template which is done by the enzyme reverse transcriptase (RT). The cDNA is amplified in RT-qPCR and detected by addition of fluorescent probes that bind to the DNA. Binding to cDNA increase the intensity of the fluorescence proportionally making it possible to confirm the amount of target RNA (Valasek and Repa, 2005).

Isolation of RNA from cells were done using RNeasy Mini Kit from Qiagen according to manufacturer's protocol. Cells grown in culture media was added doxycyclin and treated with either arsenite, poly I:C or UV irradiation. cDNA synthesis was performed with 2 µg RNA using an rtStar™ tRNA-optimized First-Strand cDNA Synthesis Kit from Arrystar INC according to manufacturer's protocol.

Treatment of cells

Three different treatments were used to investigate any impact on the expression of Y RNA. UV irradiation was performed at 120 mJ/cm^2 in a UV-1800 UV-VIS spectrophotometer. Arsenite treatment was performed 2 h prior to harvesting cells by adding 0.5 mM arsenite directly to the cells. Poly I:C mimics a virus infection in the cell. Poly I:C was added by mixing 1.6 µg poly I:C with 10 µl Lipofectamine™ RNAiMAX both resuspended in 500 µl OPTI-MEM® I Reduced Serum Medium. The mixture was incubated for 5 min at RT before transferred directly to the cells and incubated with 5.0% CO_2 and 37°C for 7 h.

Preparing for qPCR-analysis

Of cDNA, 50 ng/µl was used for each reaction. The primers used in this thesis amplified *Y RNA1* and *Y RNA4,* and as a control glyceraldehyde 3-phosphate dehydrogenase (*GAPDH)* primers were used. The following reaction mixture was prepared for each of the primer pairs, and all reactions were prepared in duplicates; 1 µl (50 ng) cDNA, 0.1 µl forward primer (10 pmol), 0.1 µl reverse primer (10 pmol), 5 µl PowerTrack SYBR Green Master Mix and 3.8 µl MQ-water.

RT-qPCR was performed using the following program: Comparative method of relative quantification in StepOne™ v2.1 Software, provided by Applied Biosystems. The results were analyzed using the Comparative C_T Method ($\Delta\Delta C_T$ Method).

3 Results

To gain a better understanding of the biological role of hEndoV and to confirm the finds in the iCLIP analysis, protein extracts from mammalian cells and recombinant hEndoV have been used.

3.1 Purification of hEndoV Proteins

The proteins hEndoV and hEndoV D52A, expressed in *E. coli nfi⁻ rnhb⁻* cells using PETM41 constructs, were affinity purified using Ni-NTA columns. Analyses by SDS-PAGE® revealed the induction of proteins of 64 kDa corresponding to the expected size of MBP-His hEndoV fusion protein. The MBP-His tag attached to the proteins was removed with cleavage by TEV-protease, which was successful for hEndoV, but not for hEndoV D52A. It was therefore decided to continue with the tagged versions of both proteins (MBP-His-(MH)-hEndoV and MBP-His-(MH)-hEndoV D52A as well as a TEV-cleaved version of the wild type hEndoV (hEndoV). The proteins were further purified by size exclusion chromatography. The purest and most concentrated protein fractions were used for enzyme characterization and are shown in Figure 3.1. The protein concentration was determined to 350 ng/µl for hEndoV, 590 ng/µl for MH-hEndoV and 600 ng/µl for MH-hEndoV D52A for the purified fractions.

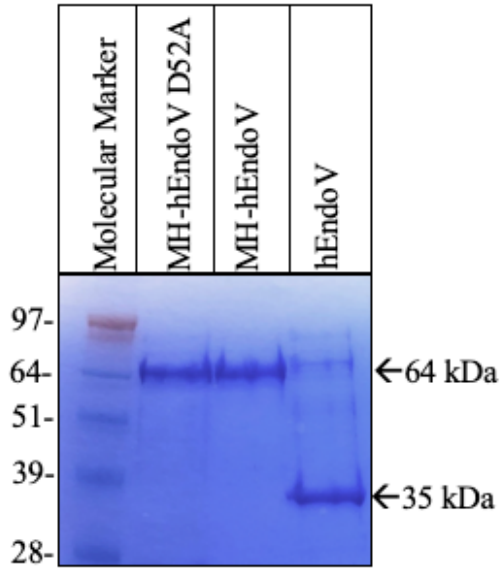

Figure 3.1. Purification of hEndoV recombinant proteins. *hEndoV and D52A proteins were purified after overexpression in E. coli. SDS-PAGE® and Comassie Blue staining revelaed bands of expected sizes. The arrows indicate the presence of hEndoV and hEndoV D52A with expected molecularweigth of 64 kDa for fusionproteins and 34 kDa for the cleaved protein. SeeBlue® Plus2 Prestained Standard (1x) was used as molecular marker (given in kDa).*

3.2 Cleaving activity of recombinant hEndoV

The inosine-affinity of hEndoV is well described. However, the iCLIP-analyses suggest that hEndoV also can bind RNA without inosine. Interestingly, this is also the conclusion in a study of EndoV from mouse (Kong et al., 2020). It could be that these RNAs (certain tRNAs and Y RNA) have other properties or signatures that hEndoV recognizes. Therefore, the activity and affinity of hEndoV for some of these substrates were tested.

Recombinant hEndoV, MH-hEndoV and MH-hEndoV D52A were used in biochemical activity assay to better understand their cleaving activity with different RNA substrates.

3.2.1 Cleaving activity of hEndoV on ssIIUI and dsIIUI RNA fragments

To test whether the purified enzymes had the expected activity, assays using RNA substrates containing inosine were performed (full sequence given in appendix C). hEndoV and MH-hEndoV showed a clear cleaving activity for both substrates (Figure 3.2). MH-hEndoV with the ssIIUI substrate showed an initial cleaving activity of 24% with 1.3 nM of enzyme, which increased to 66% and 85% with increased amount of enzyme (6.5 and 25 nM). For the dsIIUI substrate, MH-hEndoV showed an initial cleaving activity of 50% with 1.3 nM of enzyme which increased to 64% and 80% with increased amount of enzyme. hEndoV showed almost full cleavage for both the ssIIUI (84%) and the dsIIUI (87%) substrate already at the lowest enzyme concentration. It thus appears that hEndoV which is without the purification tag, has a higher cleaving activity.

MH-hEndoV D52A is an inactive mutant and therefore cleavage of the substrates is not expected. However, the activity assay showed that MH-hEndoV D52A had some rest activity (25% for ssIIUI and 50% for dsIIUI) indicating that the enzyme is not completely “dead” (Figure 3.2). Cleavage did not increase with increasing amount of enzyme and the activity was far less than for the wild type enzymes. These results show that the purified hEndoV wild type enzymes have the expected activity, whereas MH-hEndoV D52A is close to inactive. hEndoV and MH-hEndoV is the same enzyme except from the MH-tag. The difference in the cleaving activity may therefore indicate that the tag plays a role and prevents access to the RNA substrate.

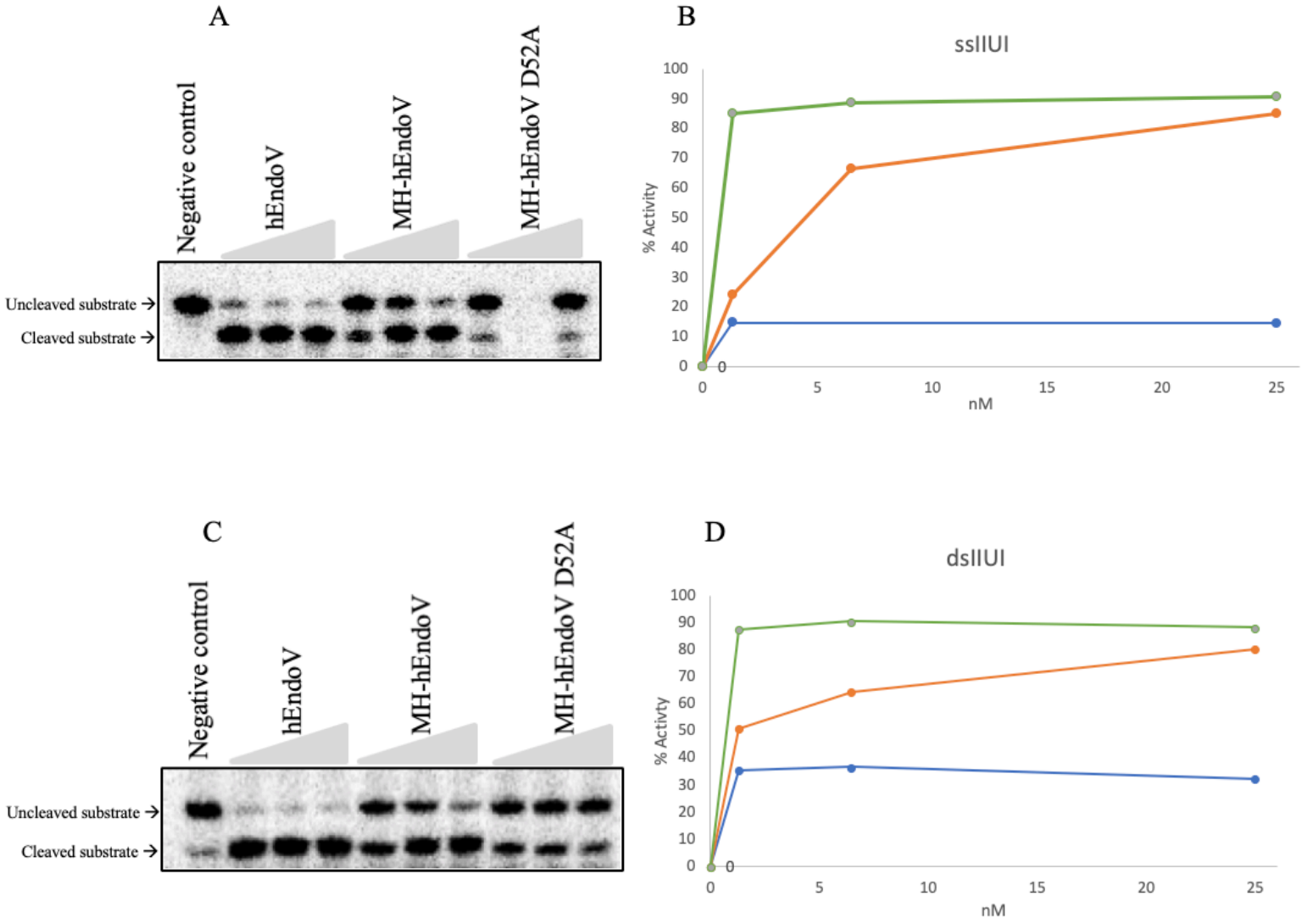

Figure 3.2 Activity of hEndoV proteins upon ^{32}P-labeled ssIIUI and dsIIUI RNA. A and C. *Different amounts of recombinant protein (1.3 nM, 6.5 nM and 25 nM) were incubated with ssIIUI(A) and dsIIUI (C) substrates containing inosine for 15 min at 37℃. Cleaved RNA fragments were separated from intact substrate on a 20% denaturing polyacrylamide gel and visualized by phoshporimaging. A sample without enzyme was used as negative control.* ***B and D.*** *The cleavage products were quantified using ImageQuant TL.*

3.2.2 hEndoV cleaving activity on endogenous small RNA

To investigate the cleaving activity of hEndoV on endogenous small RNA molecules, northern blot analyses were performed. Previous research has shown that hEndoV cleave inosine containing RNAs *in vitro* and here also the activity towards RNAs without inosine was investigated. Of particular interest was Y RNA and tRNA for glutamic acid (GluCTC) as both were found bound to hEndoV in the iCLIP analyses performed previously. Small RNA isolated from human haploid cell line HAP1 C665 cells, was used as substrates. After incubation with the various hEndoV proteins, samples were separated by denaturing gel electrophoresis. RNA was transferred to a membrane that was hybridized with labelled oligonucleotide probes recognizing Y RNA1/4 or the tRNAs alanine (AlaAGC), GluCTC or valanine (ValAAC) transcripts (full sequences given in appendix C). Y RNA1/4 is a mix of two oligoes, Y RNA 1 and Y RNA 4. AlaAGC and ValAAC have both inosine in the wobble position, whereas GluCTC does not. Cleavage by hEndoV and fragmentation of tRNA is therefore expected only for the two first.

Using probes binding to AlaAGC and ValAAC, clear cleavage products were detected for hEndoV and MH-hEndoV, but not MH-hEndoV D52A (Figure 3.3 and 3.4). For AlaAGC the activity of hEndoV and MH-hEndoV was roughly the same at 30% with 0.8 μM of enzyme. With an increase in enzyme to 1.6 μM the cleavage increased to 40% for hEndoV, while no increase was seen for MH-hEndoV. For ValAAC the cleaving activity was respectively 15% for MH-hEndoV and 17% for hEndoV (0.8 μM for each). Double amount of hEndoV resulted in cleavage of 17% for MH-hEndoV, and 33% for hEndoV. Thus, the increase in amount of enzyme in each sample, does not directly reflect increase in enzyme activity for MH-hEndoV.

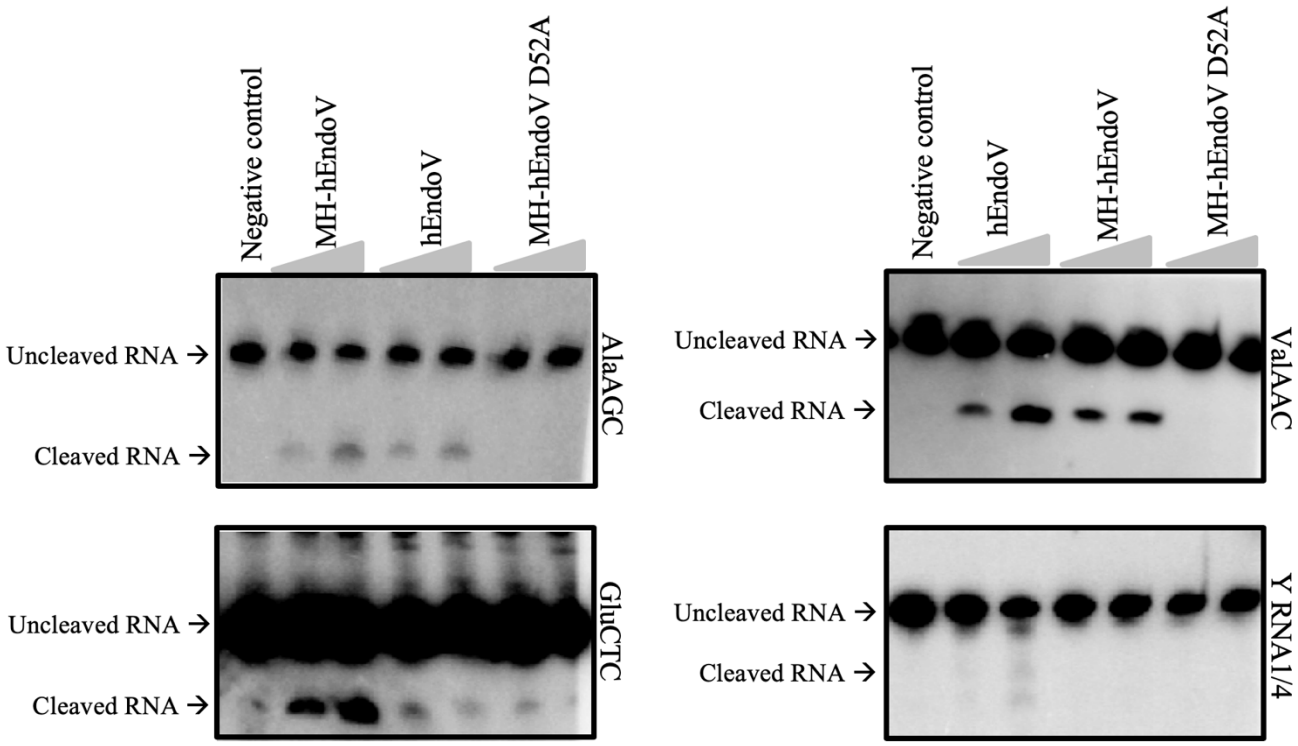

***Figure 3.3**. **Northern blot analyses of small RNA incubated with hEndoV, MH-hEndoV and MH-hEndoV D52A.** hEndoV enzymes were investigated for activity towards endogenous small tRNA, using probes for AlaAGC, ValAAC, GluCTC and Y RNA1/4. Increasing amounts of protein were added (0.8* μM and 1.6 μM). *The protein-RNA mixtures were incubated for 20 min at 37℃. Cleaved RNA fragments were separated on a 15% denaturing polyacrylamide gel and visualized by phoshporimaging. A sample without enzyme was used as negative control. The cleavage products were quantified using ImageQuant TL.*

For GluCTC a clear cleavage by hEndoV was seen, as well as some cleavage by MH-hEndoV and MH-hEndoV D52A (Figure 3.3). 0.8 μM of hEndoV cleaved 8% of GluCTC which increased to 12% with 1.6 μM enzyme. For MH-hEndoV the initial cleaving activity was 3% which increased to 5.3% by with 1.6 μM enzyme (Figure 3.4). The activity assay showed that MH-hEndoV D52A had some rest activity of 3% indicating that the enzyme is not completely "dead", as described above. A faint band was also detected for the negative control for GluCTC, suggesting that there might be some unspecific cleavage (Figure 3.3).

For Y RNA1/4 weak cleavage was detected for hEndoV, but not for MH-hEndoV and MH-hEndoV D52A (Figure 3.3). The initial activity of hEndoV was 3.2% (0.8 μM) which increased to 11% when the amount of enzyme was doubled (1.6 μM) (Figure 3.4).

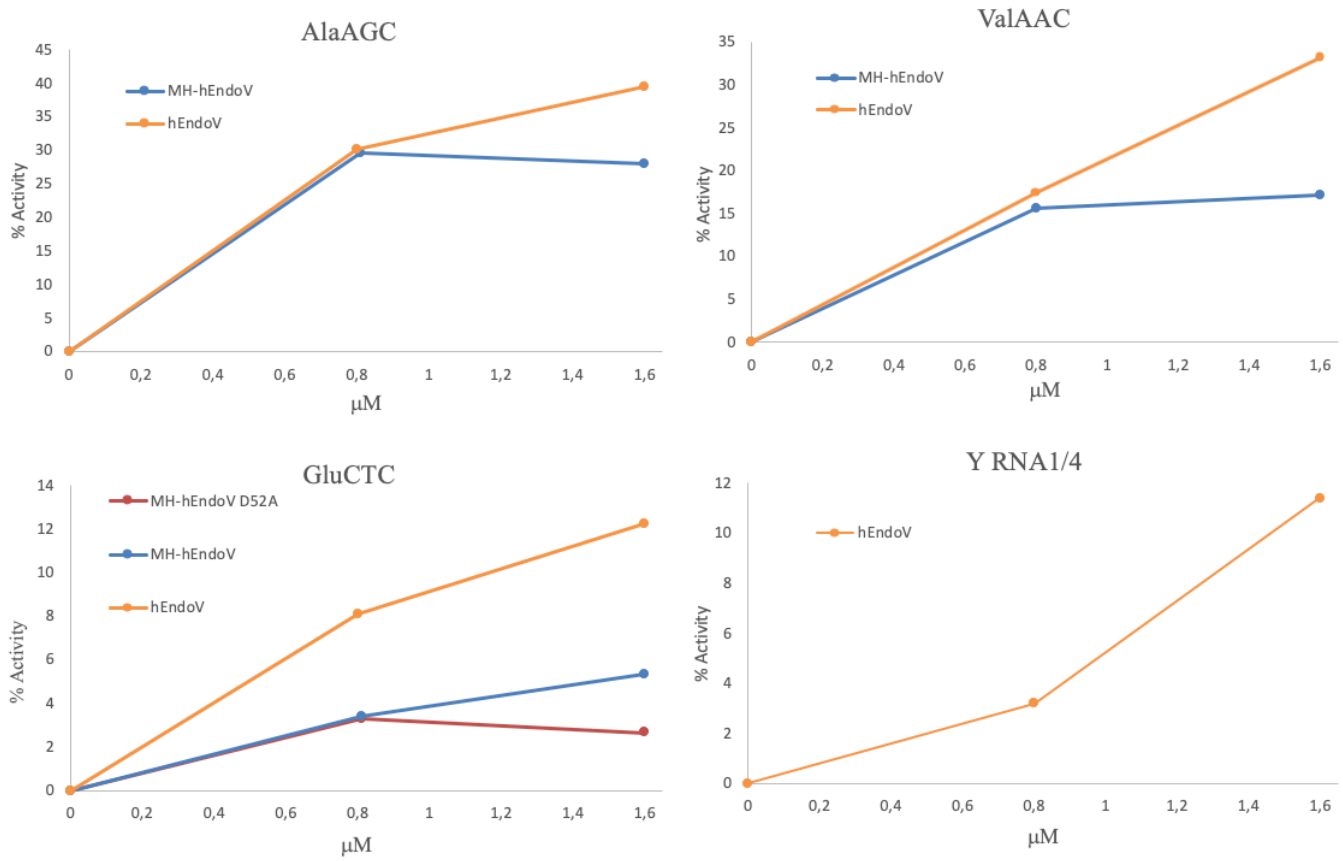

Figure 3.4 Quantifiaction of hEndoV products from northern blot analysis by ImageQuant TL. *Each graph shows the percentage increase of the cleaving of each protein hEndoV/MH-hEndoV/hEndoV D52A per µM. The amount of enzyme was increased from 0.8 nM to 1.6 nM.*

In sum, various small RNAs isolated from human cells are cleaved by hEndoV. As previously reported, tRNAs containing inosines (AlaAGC and ValAAC) are the best substrates, however, some cleavage is also seen for those without (GluCTC and Y RNA1/4).

3.3 Affinity of recombinant hEndoV

3.3.1 Affinity of hEndoV to Y RNA4 derived fragments

Y RNA4 was the most abundant RNA found in the iCLIP-analyses of hEndoV. To test whether this affinity can be reproduced *in vitro*, EMSA were performed using RNA oligonucleotides corresponding to different structural parts of Y RNA4: 5´stem: bulge, 5´stem: complementary, Hairpin and dsCTR RNA. 5´stem: bulge and Hairpin are bulged/loop structures whereas 5´stem: complementary and dsCTR RNA have a simpler structure (Figure

3.5). In addition, ssIIUI and dsIIUI were included as positive controls. The band shift assay was performed with increasing amount of hEndoV, 100, 200 and 400 nM.

hEndoV showed affinity for all six substrates tested (Figure 3.5 and 3.6). The strongest shifts were seen when using the inosine-containing ss- and ds-RNA substrates (ssIIUI and dsIIUI), where the best were ssIIUI. For both substrates the affinity increased with increasing amount of hEndoV. By using 100 nM of hEndoV, 55 % of ssIIUI was bound and binding increased to 75 % and 78 % with 200 and 400 nM enzyme, respectively. For dsIIUI 100 nM enzyme led to 23 % of substrate being bound, which increased to 28 % and 44 % with increased amount of enzyme.

Both the Hairpin and 5´stem bulge substrates have regions of double - and single stranded character (Figure 3.5). hEndoV show stronger affinity for 5´stem bulge with an initial shift at 15%, which increased to 24 % and 30 % with increasing amount of hEndoV. For the Hairpin substrate, hEndoV had an initial affinity of 7%, which increased to 12.5 % and 15 % with increasing amount of hEndoV (Figure 3.6).

Two of the substrates were ordinary double stranded RNAs without any distortions. hEndoV has the least affinity for these two (5´stem complementary and dsCTR RNA). For dsCTR RNA hEndoV had an initial affinity of 1.3 %, which barely showed any increase with 200 and 400 nM enzyme. For 5´stem complimentary, hEndoV had an initial affinity of 1.2 %, no increase in activity was seen (Figure 3.6).

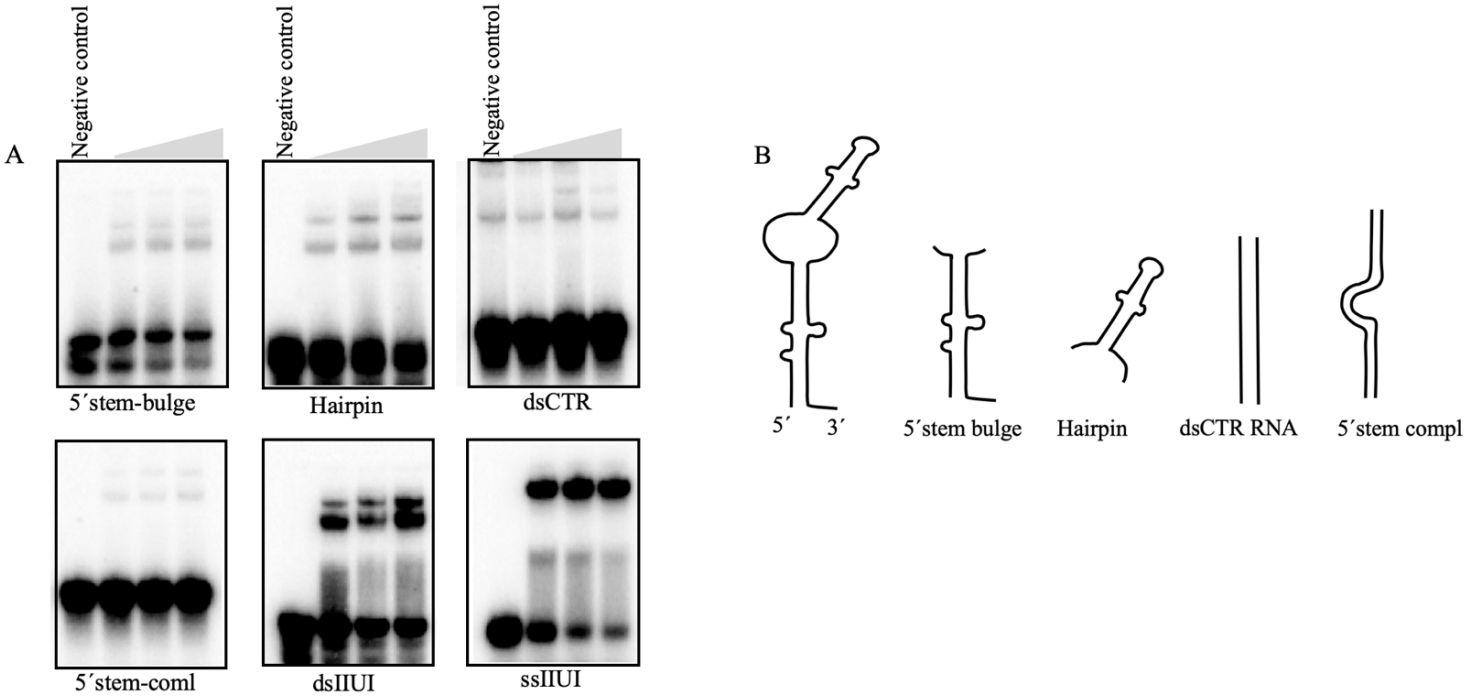

Figure 3.5 Electrophoretic mobility shift assay with hEndoV and Y RNA 4 substartes. A *hEndoV (100, 200 or 400 nM) and six substrates 5´stem complementary, Hairpin, dsCTR, 5´stem bulge, dsIIUI and ssIIUI. Reactions were incubated on ice under UV irradiation prior to separation of protein-substrate complexes from unbound substrate on a 10 % native polyacrylamide gel.* ***B.*** *Four regions of Y RNA4 were ^{32}P-labelled and used as substrates for electrophoretic mobility shift assay; 5´stem complimentary, 5´stem bulge, Hairpin and dsCTR RNA.*

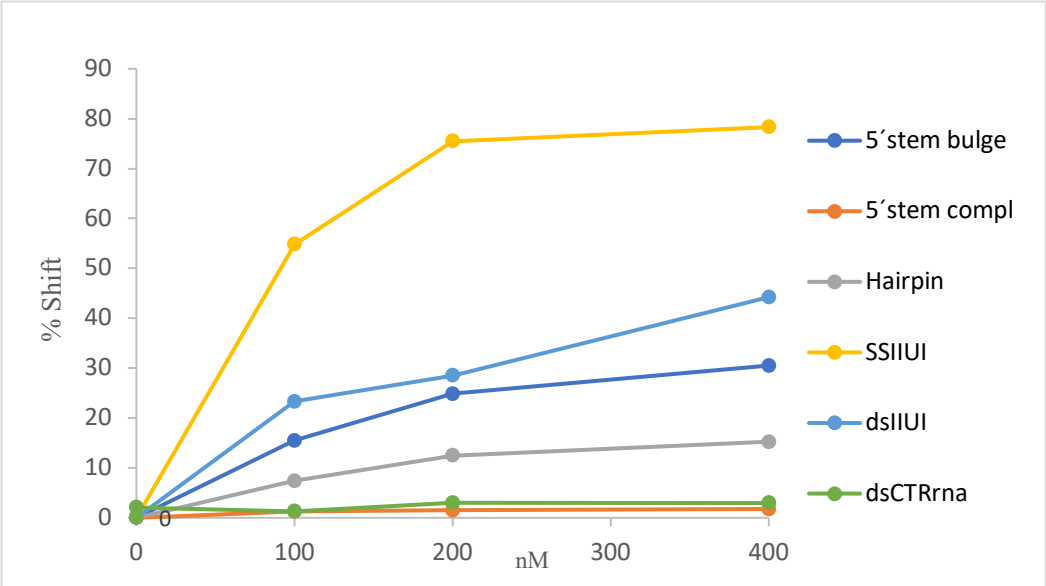

Figure 3.6 Quantification of EMSA. *Quantification of band shifts by ImageQuant TL software. The quantifications showed how much of hEndoV that was bound in a protein-RNA complex. Increasing amounts of hEndoV was used, 100, 200 abd 400 nM.*

hEndoV has the highest affinity for RNA substrates containing inosine, thereafter the bulge/loop structured substrates, and the least affinity for RNA without branched structure.

3.3.2 Affinity of hEndoV for endogenous small RNAs

To determine the affinity of hEndoV to endogenous small RNAs, EMSA and detection by northern blot analyses were performed. Five different hybridizations were done using probes that detects Y RNA1/4, and the tRNAs GluCTC (5´and 3´termini), glycine (GlyACC, 5´and 3´termini), arginine (ArgACG, 5´end) and ValAAC (5´end). For GluCTC, GlyACC and Y RNA1/4 two oligos were used in the same hybridisation, for GluCTC and GlyACC these are named as mix whereas for Y RNA1/4, 1/4 indicates the two oligos. GluCTC and GlyACC does not contain inosine, while ArgACG and ValAAC have inosine in wobble position. As with the EMSA with hEndoV and Y RNA4 fragments, an interaction between RNA and protein can be seen as a shift when samples are separated on a native gel.

hEndoV and MH-hEndoV D52A showed shifts for all small RNAs tested (Figure 3.7). In general, hEndoV showed stronger shifts than MH-hEndoV D52A, whereas MH-hEndoV did not bind any of the RNAs (Figure 3.7). Of the RNAs tested, strongest shifts were seen with ArgACG. hEndoV showed a shift increasing from 15% to 25 % and MH-hEndoV D52A showed a shift increasing from 15% to 22 % using 0.8 and 1.6 μM of enzyme, respectively (Figure 3.7). For the other four RNAs the shifts were weaker, all under 11 % for hEndoV and under 5 % for MH-hEndoV D52A. For both proteins, weakest affinity was seen for GlyACC.

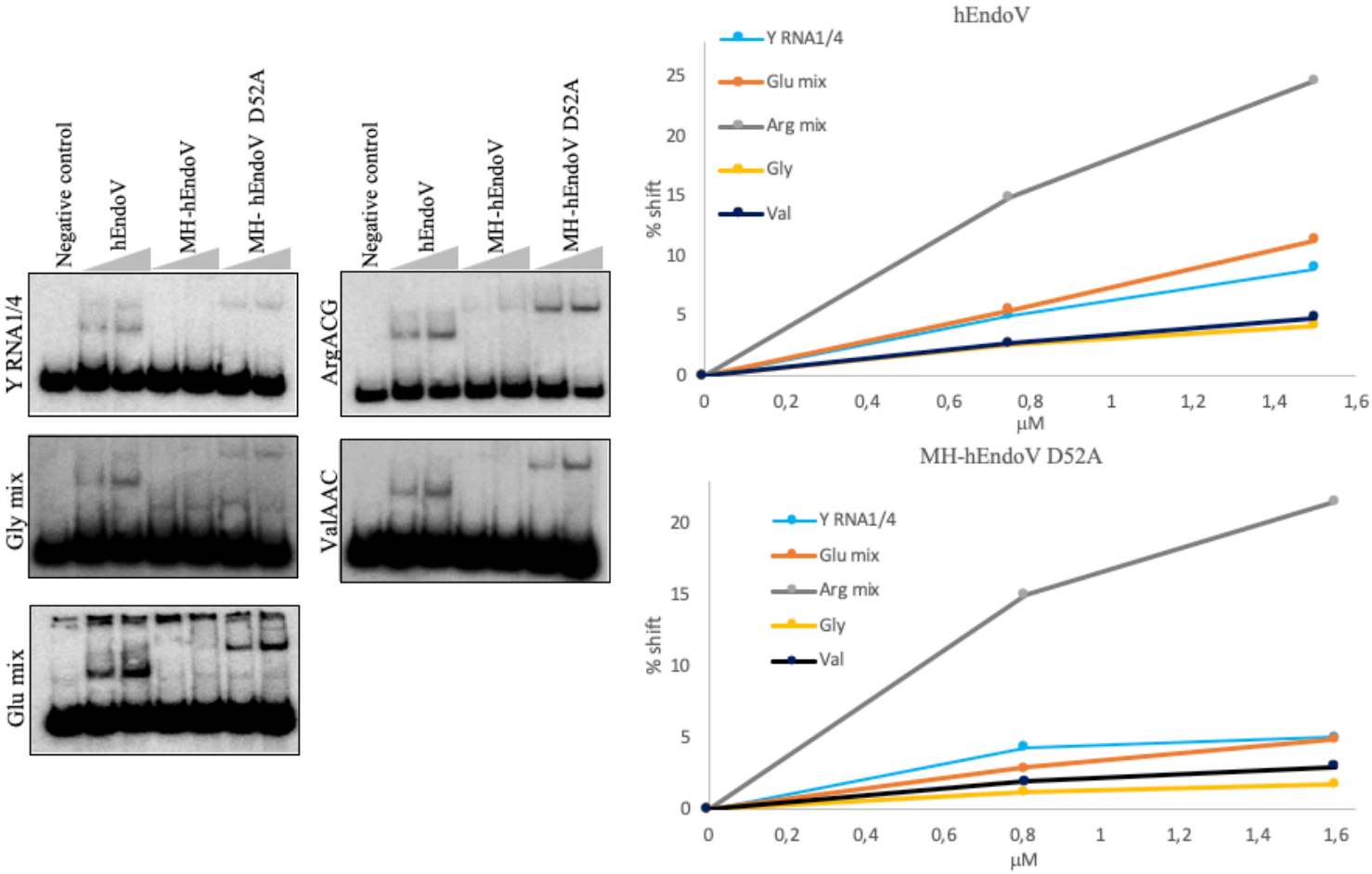

Figure 3.7. Electrophoretic mobility shift assay using hEndoV and small RNAs. A. *hEndoV (0.8-1.6 μM) and five RNA probes Y RNA1/4, GlyACC mix, GluCTC mix, ArgACG, and ValAAC. Reactions were incubated on ice prior to separation of protein-RNA complexes from unbound RNA on a native polyacrylamide gel and treated with labelled RNA probes.* ***B.*** *Quantification of band shifts by ImageQuant TL software. The quantifications showed how much of the protein bound in a protein-RNA complex.*

These results show that hEndoV has highest affinity for tRNA ArgACG, whereas the affinity for tRNAs GlyACC and ValAAC was the lowest. Interstingly, ValAAC contains inosine, but not GlyACC, nevertheless the binding of these two tRNAs by hEndoV was almost the same under the given conditions. The affinity for GluCTC and Y RNA1/4 was in the middle.

3.4 Identification of hEndoV protein partners by co-immunoprecipitation

Co-immunoprecipitation is a technique for detection of possible protein-protein interactions. Co-precipitated proteins are identified using western blotting with specific antibodies for the proteins of interest.

Co-immunoprecipitation were performed with magnetic anti-Flag® M2 magnetic beads, and lysates from mammalian cell lines Flp-in T-REx 293. The cells were treated with 0.5 mM arsenite. Different amounts of protein lysate were tested for optimization of co-immunoprecipitation, but it was concluded that 1.5 mg gave the best results.

3.4.1 Co-immunoprecipitation of YBX1

The RNA-binding protein YBX1 was one of the interacting proteins identified by MS after co-immunoprecipitation of Flag-hEndoV D52A. Using the same Flp-in T-REx 293 cells overexpressing Flag-hEndoV and Flag hEndoV D52A, co-immunoprecipitation of hEndoV and YBX1 was reproduced (Figure 3.8). For the Flp-in T-REx 293 cells not overexpressing hEndoV only a faint background band is visible meaning that the YBX1 interaction with hEndoV D52A is specific. YBX1 has a predicted size of 36 kDa but migrates by SDS-PAGE at 50 kDa. For all results presented, also additional bands are detected, especially in the input samples. Whether they represent unspecific binding of the antibody or recognition of alternative YBX1 splice variants with different sizes is not known.

To test whether the interaction between hEndoV and YBX1 is affected by stress, cells were treated with arsenite prior to co-immunoprecipitation (only Flp-in T-REx 293 and Flp-in T-REx 293 Flag-hEndoV D52A was tested). Exposing the cells to oxidative stress did not change the amount of YBX1 bound to hEndoV. The samples treated with or without arsenite had approximately the same intensity of the YBX1 band (Figure 3.8).

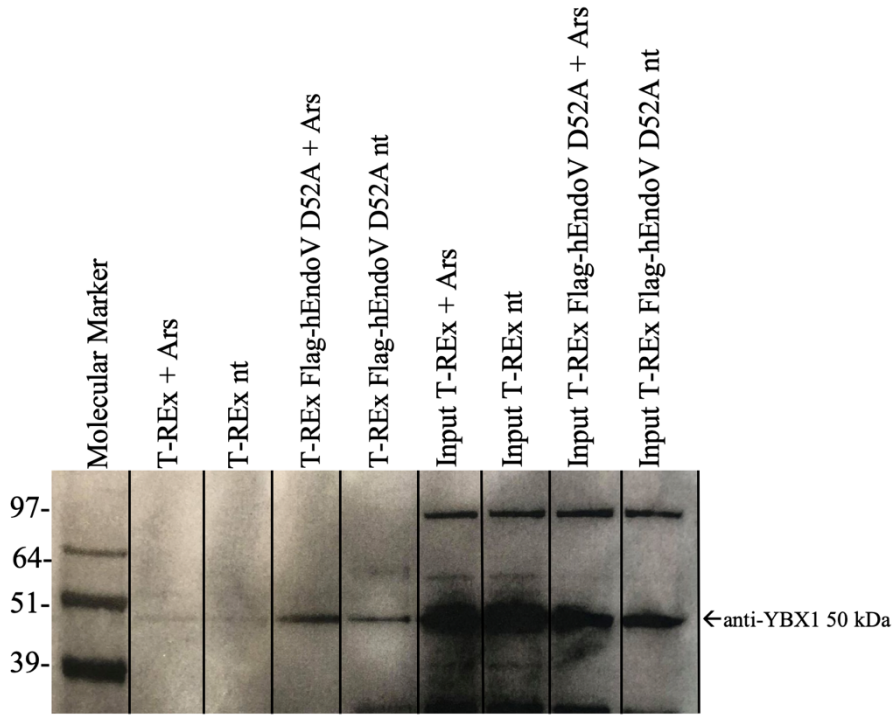

Figure 3.8 Co-immunoprecipitation with YBX1. *Western blot of co-immunoprecipitation with magnetic anti-Flag® M2 beads. The samples were added 1.5 mg protein lysate and separated on a NuPAGE® Bis-Tris gel. Input samples were added 40 µg lysate. The membrane was probed with YBX1 antibody. SeeBlue® Plus2 Prestained Standard (1x) was used as the molecular marker (given in kDa).*

An experiment was also performed to investigate whether RNA is required for the interaction. Samples were treated with RNAse A, an enzyme that degrades RNA. The interaction between hEndoV and YBX1 was lost when treated with RNAse A (Figure 3.9), suggesting that hEndoV and YBX1 are not directly interacting but that the complex is held together via an RNA molecule.

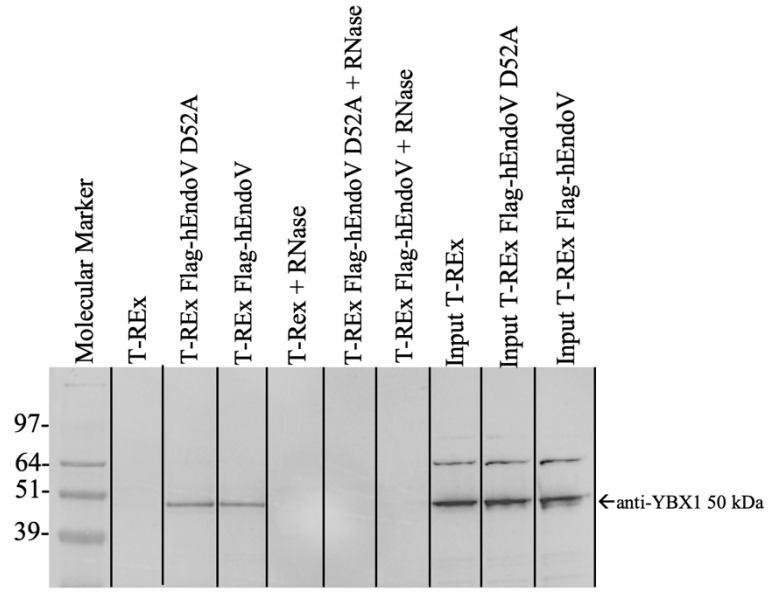

Figure 3.9 Co-immunoprecipitation with YBX1. *Western blot of co-immunoprecipitation with magnetic anti-Flag® M2 beads. The samples were added 1.5 mg protein lysate. RNAse A treated samples were added 100 ng RNase. The membrane is probed with YBX1 antibody. Input samples were added 40 µg lysate. Samples were separated on a NuPAGE® Bis-Tris gel, and the molecular marker was SeeBlue® Plus2 Prestained Standard (1x) (given in kDa).*

To control that the binding of YBX1 was specific to hEndoV, the membrane in Figure 3.9 were reprobed with hEndoV antibody (Figure 3.10).

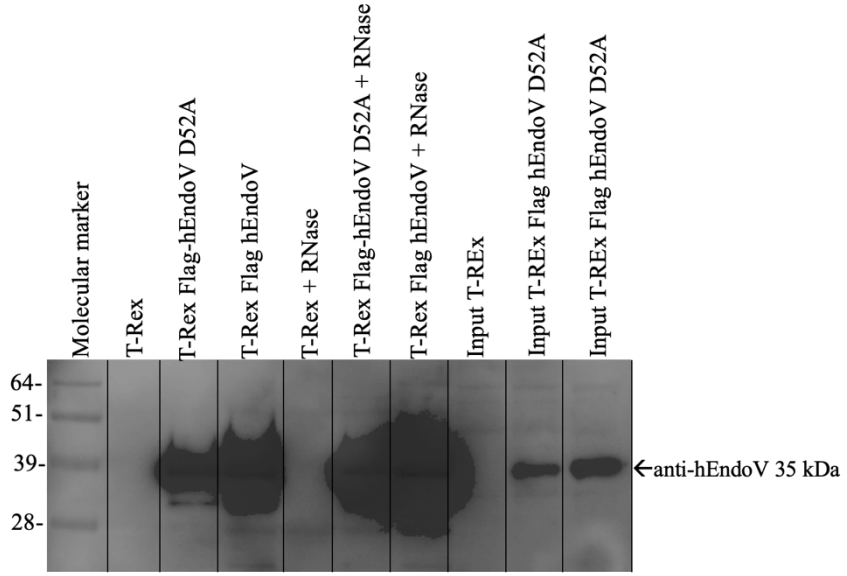

Figure 3.10 Membrane reprobed with hEndoV. *Western blot of co-immunoprecipitation with magnetic anti-Flag® M2 beads. The samples were added 1.5 mg protein lysate. RNAse A treated samples were added 100 ng RNase. The membrane is probed with hEndoV antibody. Input samples were added 40 µg lysate. Samples were separated on a NuPAGE® Bis-Tris gel was, and the molecular marker was SeeBlue® Plus2 Prestained Standard (1x) (given in kDa).*

3.4.2 Co-immunoprecipitation of IGF2BP1

The single stranded RNA binding protein IGF2BP1 belongs to a family of single-stranded RNA-binding proteins that is broadly expressed in fetal tissues and in several cancer types (Huang et al., 2018). IGF2BP1 was also identified by MS as a protein co-immunoprecipitated of Flag-hEndoV D52A. To reproduce this result, co-immunoprecipitation for IGF2BP1 was performed as for YBX1. Experiments showed that hEndoV and IGF2BP1 co-precipitated under the given conditions (Figure 3.11). Further, experiments showed that treatment with arsenite did not have any impact on the co-precipitation between the two proteins (data not shown). For the T-REx cells not overexpressing hEndoV D52A, no band corresponding to IGF2BP1 was detected, confirming that the interaction is specific. IGF2BP1 has a predicted band size of 65 kDa.

The dependence of RNA was tested as for YBX1. Treatment with RNAse A did not have an impact on the interaction between hEndoV and IGF2BP1, as equal bond intensities were shown for both samples (Figure 3.11). This suggests that the interaction between hEndoV D52A and IGF2BP1 is direct and not via RNA.

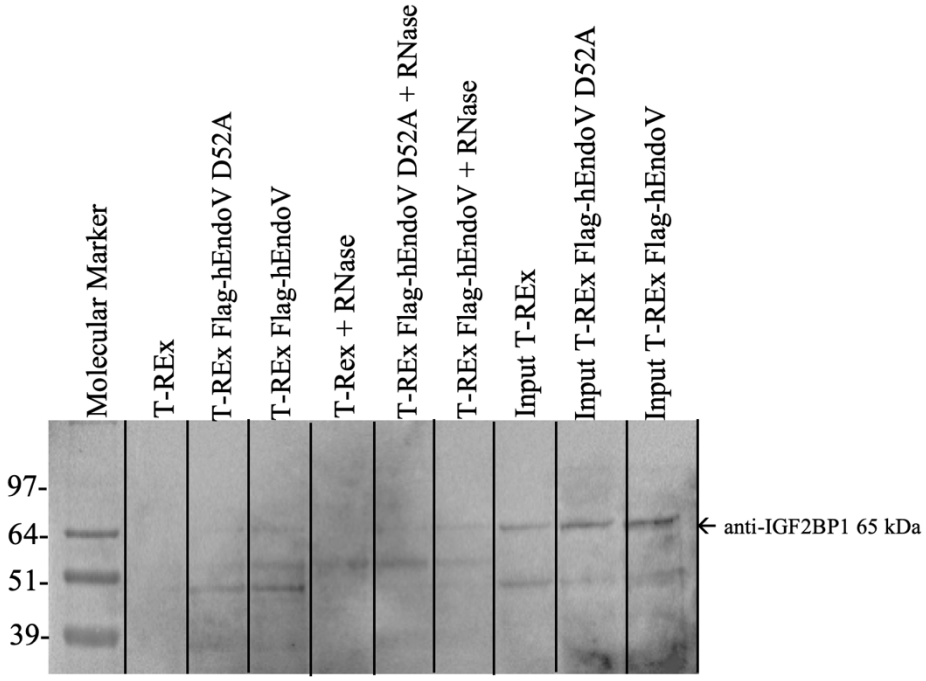

Figure 3.11 Co-immunoprecipitation with IGF2BP1. *Western blot of co-immunoprecipitation with magnetic anti-Flag® M2 beads. The samples were added 1.5 mg protein lysate. The membrane is probed with YBX1 antibody. Input samples were added 40 µg lysate. Samples were separated on a NuPAGE® Bis-Tris gel was used, and the molecular marker was SeeBlue® Plus2 Prestained Standard (1x). all samples arsenite treated (given in kDa).*

To control that the binding of IGF2BP1 was specific to hEndoV, the membrane in figure 3.11 was reprobed with hEndoV antibody (Figure 3.10).

3.5 ICC for localization of hEndoV, YBX1, IGF2BP1 and Ro60

hEndoV is known to localize mostly in the cytoplasm but has been shown to relocate to SG´s when exposed to stress (Nawaz et al., 2016a). To check for a possible colocalization of hEndoV with IGF2BP1 and/or YBX1 whether in SG´s or other positions, a series of ICC experiments were performed with Flp-in T-REx 293 cells stably overexpressing hEndoV fused to green fluorescent protein (GFP). Also, Ro60 was included in this analysis. The cells were treated with both arsenite and UV irradiation.

GFP-hEndoV, IGF2BP1 and Ro60 were all found in the cytoplasm in the unstressed cells (Figure 3.12). YBX1 in the non-treated cells were difficult to interpret due to a lot of background staining, but the images indicate that YBX1 is mostly found in the cytoplasm. GFP-hEndoV relocated to what is thought to be SG´s (a SG indicator was not included) in most cells treated with both arsenite and UV irradiation, and is best seen in the panels with IGF2BP1 and Ro60 (Figure 3.12). Arsenite treatment seemed to relocate YBX1 to structures around the nucleus. The same localization in these structures were not detected after UV-irradiation. After UV-irradiation IGF2BP1 seemed to locate mostly around nucleus in what may resemble the structures observed for YBX1. Arsenite treatment gave weaker signals of IGF2BP1 in these structures, but they were still detectable. Ro60 was in addition to cytoplasmic localization seen in some accumulated cytoplasmic structures.

Except from in the cytoplasm, hEndoV does not show any signs of colocalization with YBX1 or IGF2BP1 in stressed cells (Figure 3.12).

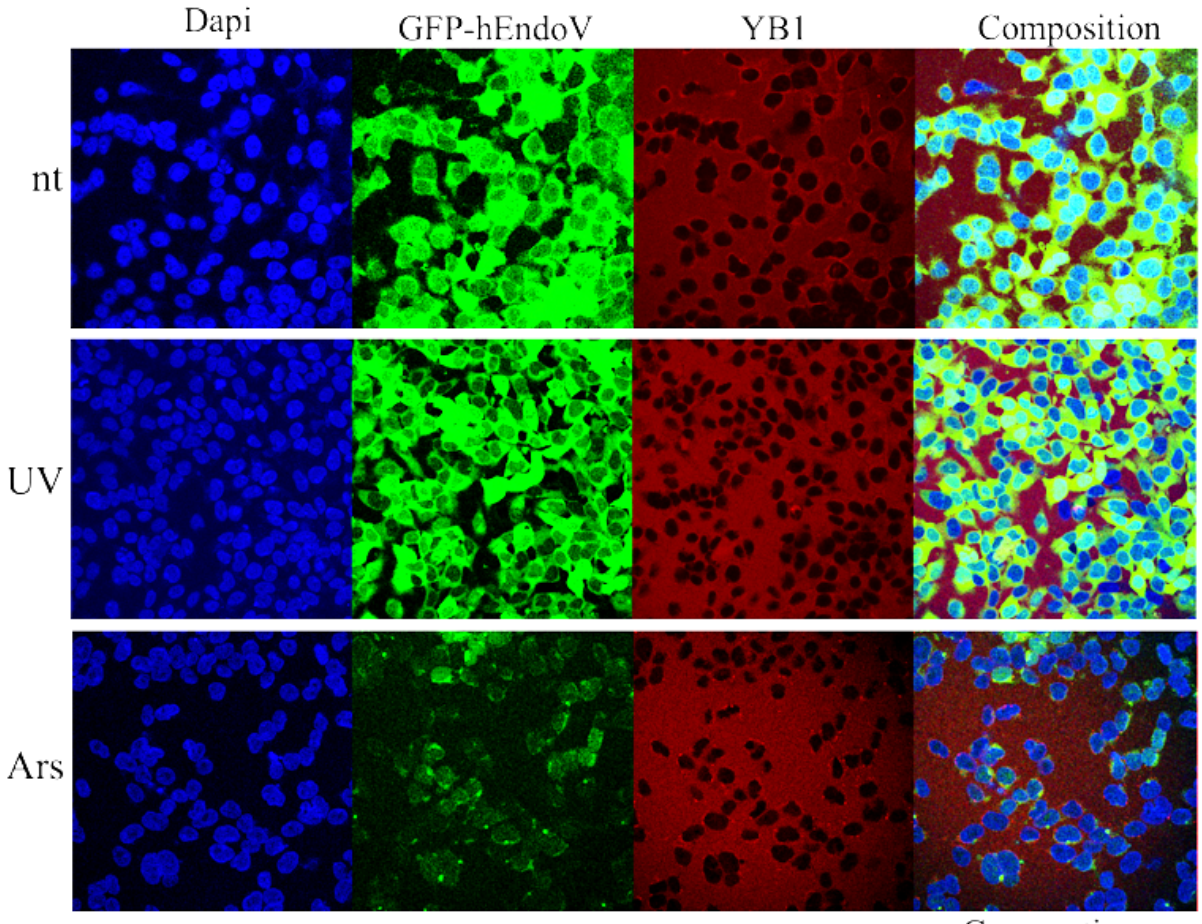
Dapi
GFP-hEndoV
YB1
Composition
nt
UV
Ars

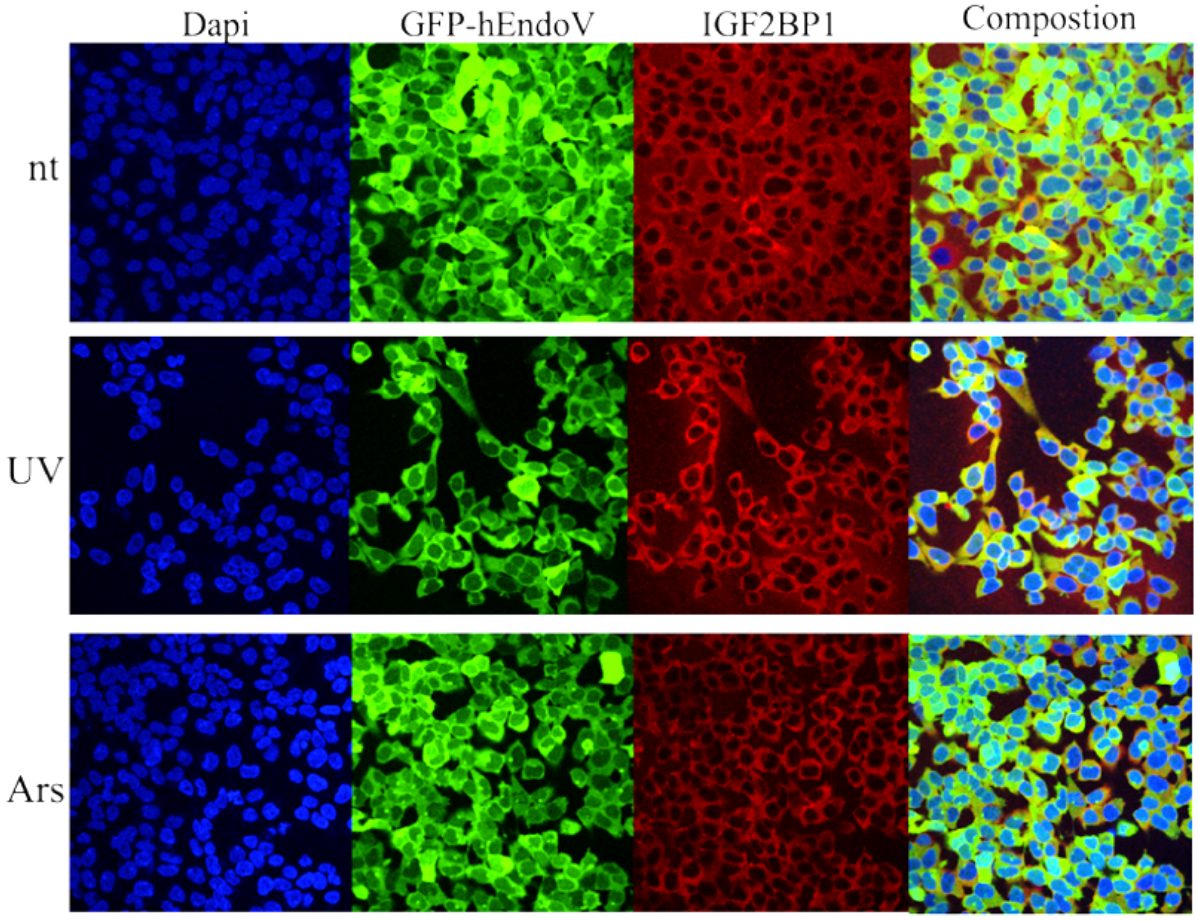
Dapi
GFP-hEndoV
IGF2BP1
Compostion
nt
UV
Ars

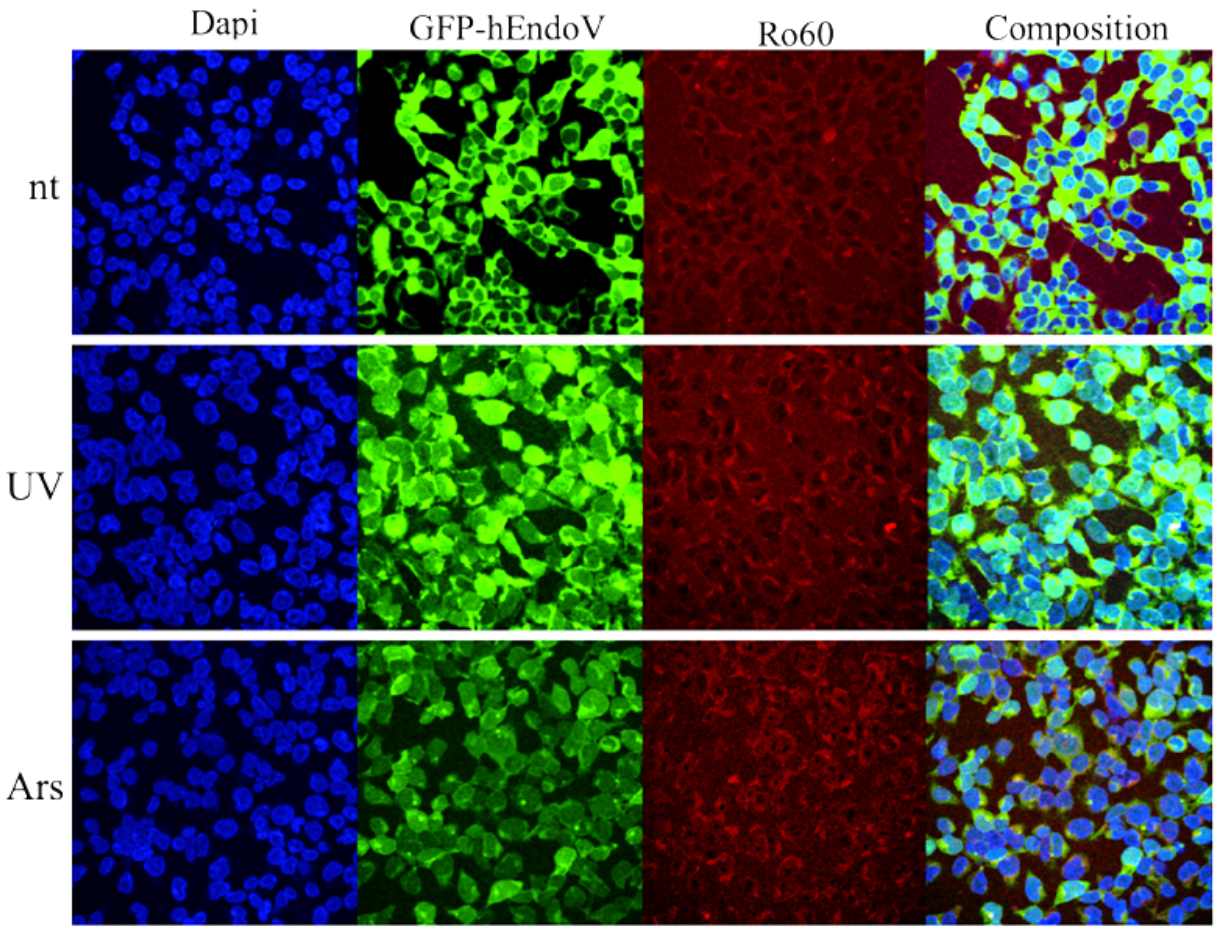

Figure 3.12. ICC of hEndoV and partners. *ICC was performed with T-REx HEK 293 cells overexpressing GFP-hEndoV. Cells were stressed with either UV-irradiation or arsenite. Unstressed cells are referred to as nt. Nucleus was stained with dapi, and YBX1, IGF2BP1 and Ro60 was probed with antibodies with red fluorescent. Composition image is Dapi, GFP-hEndoV and protein of interest together. Images was aquired on Leica TCS Sp8 gSTED microscopy, with a 40X oil immersion objective. Images were processed with Fiji Software.*

3.6 Regulation of Y RNA levels by hEndoV

hEndoV has affinity for Y RNA *in vitro*, but the biological role of this is not known. One possibility is degradation of the Y RNA transcript as hEndoV is a ribonuclease. Alternatively, as supported by a recent publication from the group (Kong et al., 2020), binding yields protection of transcripts by inhibiting attack by other nucleases. Anyway, one may expect that the level of hEndoV in cells, influences the amount of Y RNA transcripts present. To check this, small RNA was isolated from Flp-in T-REx 293 and Flp-in T-REx 293 Flag-hEndoV

cells and converted to cDNA by reverse transcriptase. Y RNA1 and Y RNA4 were chosen for the analysis of gene regulation as they were most abundant in the iCLIP-analysis. The gene *GAPDH* was chosen as the reference for normalization as it is stably and constitutively expressed in most tissues and cells (primer sequences given in appendix C).

The cells were treated with three different stress factors to investigate whether they impact Y RNA levels; poly I:C, arsenite and UV irradiation. These factors simulate viral infection, oxidative stress and damage to genetic material and proteins. The method was optimized regarding the amount of cDNA applied, where 50 ng/µl gave the best results.

The analysis showed that both Y RNA1 and Y RNA4 are present in all cell types (Figure 3.13). Y RNA1 transcripts were more abundant (C_T-values of 14-17) than Y RNA4 transcripts (C_T-values of 23-27). The C_T value is defined as the number of amplifications cycles needed to reach a fixed signal threshold. The level of Y RNA1 in untreated cells were set to 1 for both Y RNA1 and YRNA4 and the other samples were related to this. The levels of Y RNA1 and Y RNA4 transcripts did not change in response to any of the stress with endogenous levels of hEndoV (in Flp-in T-REx 293 cells; Figure 3.13). However, when hEndoV was overexpressed and cells treated with poly I:C, the level of Y RNA1 increased 4 times and the level of Y RNA increased 2 times. Contrary, under UV irradiation and hEndoV overexpression, Y RNA1 and Y RNA4 levels were reduced to 0.6 and 0.15 respectively, of non-treated cells. Y RNA levels were not changed in response to arsenite treatment.

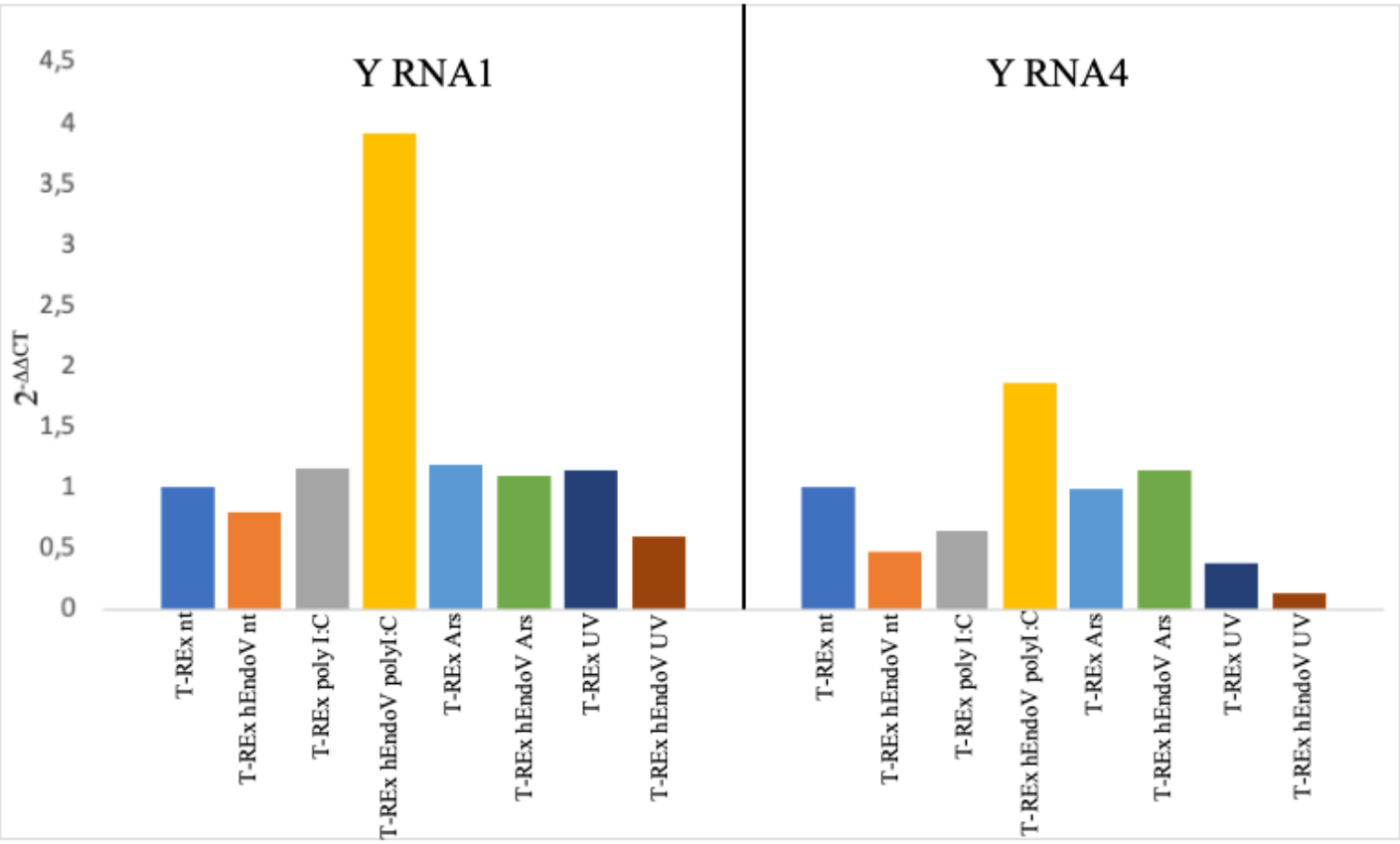

Figure 3.13 Expression of Y RNA. *Transcript level of Y RNA1 and Y RNA4 were measured by RT-qPCR in Flp-in T-REx 293 Flag and Flp-in T-REx 293 Flag-hEndoV cells treated with or without poly I:C, arsenite and UV irradiation. Values relative to GAPDH were calculated using the Comparative C_T Method.*

Caution must be taken when concidering this experiment, as it was done only once. *GAPDH* was chosen as the reference for normalization and small variations will have major consequences. The level of *GAPDH* varied more for the poly I:C treated samples of T-REx hEndoV cells, which adds even more uncertainty to the high levels observed. It was not possible to do statistical tests due to too few samples.

4 Discussion

4.1 Properties of recombinant hEndoV on RNA with inosine

hEndoV was purified for further use in recombinant activity and affinity assays. The purification on the Ni-NTA column was successful after optimization with the amount of agarose and IPTG used. The MH-tag was successfully removed from hEndoV, but not from hEndoV D52A. Several attempts were made with different amounts of TEV-protease and incubation time. The nucleotide sequence provided from the manufacturer was verified, and presence of a TEV site was confirmed. A possible reason for why the removal was unsuccessful could be introduction of a spontaneous mutation in the expression construct disrupting the TEV site. This could prevent the TEV protease from removing the MH-tag. Because of the time limitations, MH-hEndoV D52A was used in further experiments together with hEndoV and MH-hEndoV.

To confirm the activity and affinity of the purified recombinant proteins, activity assay and EMSA was performed. The cleaving activity and affinity of recombinant hEndoV was demonstrated upon ^{32}P-labelled substrates ssIIUI and dsIIUI and endogenous small RNA.

Results presented revealed that MH-hEndoV and hEndoV were active upon both ds and ss RNA substrate containing inosine, however MH-hEndoV had a lower cleaving percentage than hEndoV without the MH-tag (Figure 3.2). This suggests that the MH-tag impact how MH-hEndoV interacts with the RNA substrates maybe by inhibiting binding and thereby lowering the activity. Cleaving activity by the inactive mutant MH-hEndoV D52A was expected to be significantly reduced. A 100% inactive protein is not likely, as some of the residue may still be active. Compared to the wildtype enzyme, the activity of D52A was noticeably reduced.

Affinity of recombinant hEndoV for ssIIUI and dsIIUI was shown for hEndoV in an EMSA. Together with the finds in the biochemical activity assay it is clear that hEndoV both has affinity for and cleaving activity upon ssIIUI and dsIIUI, which is expected after what is already known about hEndoV´s role upon inosine.

4.2 Properties of recombinant hEndoV on endogenous tRNA

In a northern blot analysis hEndoV activity upon and affinity for endogenous small RNA was detected. Endogenous small RNA both with and without inosine was used.

Previous research has reported that hEndoV cleave inosine containing RNAs *in vitro (Vik et al., 2013, Morita et al., 2013).* Here, the cleaving activity upon both inosine-containing tRNA AlaAGC and ValAAC for hEndoV and MH-hEndoV was confirmed (Figure 3.3 and 3.4). The inactive mutant D52A did not show any activity, demonstrating that the cleavage of the two tRNAs indeed is performed by hEndoV. Also here, MH-hEndoV had lower cleaving activity than hEndoV and the difference was even more pronounced. As the MH-tag is relatively large (~ 30 kDa), it could mean that it physically hinders the access of full length tRNA to the active site, whereas the RNA oligos are smaller and can more easily reach the active sites of the enzyme. A similar inhibiting effect of the tag was also seen in the EMSAs (Figure 3.7). Despite the tag, the MH-hEndoV D52A variant still shows binding. Previously also stronger binding with the D52A than the wild type enzyme has been seen (Nawaz et al., 2016a)

tRNA GluCTC was of special interest as it was detected in the iCLIP-analysis as a possible substrate for hEndoV. GluCTC does not contain wobble inosine, but fragmentation is still observed when incubating with hEndoV (Figure 3.3 and 3.4). Compared to tRNAs containing inosine, the cleaving activity of hEndoV is reduced for GluCTC. Faint fragmentation was also seen in the negative control which was subtracted during quantification. As tRNA fragmentation occurs in cells, some background signals are expected in this particular type of experiments. The EMSA revealed binding of hEndoV to tRNA GluCTC, and to lesser extend GlyACC and ValAAC. Of these GlyACC is without inosine, but not ValAAC (Figure 3.7).

As hEndoV *in vitro* is an inosine-specific nuclease, these results are not easily interpreted. Fragmentation of tRNA GluCTC suggests that hEndoV does not require inosine to cleave in the anticodon loop. On the other hand, in these experiments, large amount of enzyme is used compared to what exists in the cells, which may force enzymatic effects that normally are not seen. Also, one may speculate whether *in vivo* conditions unfavor cleavage by hEndoV, but instead allow binding to tRNA and interactions with other proteins. In a northern blot analysis it was reported that samples lacking EndoV had more tRNA halves than the wildtype (Kong et al., 2020). These observations suggest that hEndoV is not active under normal conditions *in vivo,* but rather bind to and protect tRNAs from cleavage by other nucleases. Experiments

performed in mice showed that tRNA fragmentation was dysregulated in EndoV$^{-/-}$ livers and was apparently inosine-independent. Cleaved tRNAs are important signalling molecules in cells affecting important vital processes (Kong et al., 2020). These results suggest that EndoV by regulating the levels of tRNA fragments, can impact gene expression and cellular metabolism.

In 2012 it was reported that EndoV have affinity for structural DNA (Fladeby et al., 2012). tRNA GluCTC has a branched secondary structure and maybe hEndoV has the same affinity for branched RNA as seen for DNA. The 3-dimentional structure of tRNA molecules have numerous branches and may have corresponding structural areas to hEndoV (Kong et al., 2020).

4.3 tRNA fragmentation in human cells

As previously stated, the exact biological role of hEndoV is not known and we investigated whether hEndoV expressed in human cells is involved in fragmentation of tRNA (data not shown). Arsenite is a chemical compound that has been found to produce tRFs when added to cells and can lead to various types of disease or death if inhaled or absorbed through the skin (Liu et al., 2018). The induction of tRF molecules are highly mediated by ribonucleases. The ribonuclease Ang has been shown to be responsible for stress induced cleavage of tRNA in the anticodon loop to produce tRFs, and this inhibits protein translation (Yamasaki et al., 2009). It was expected that a cleavage by Ang should be detectable as shown in earlier research, but this was not observed in our experiments. It was also anticipated to see some fragmentation by endogenous/overexpressed hEndoV, but this was also not the case. The same conditions as published were used, but the cell lines were diffrerent. Ang fragmentation of tRF5-AlaCGC, demonstrated by Liu et al., suggests that the fragmentation is modest and that perhaps a larger amount of tRNA is needed to allow detection (Liu et al., 2018).

4.4 Y RNA and the role of hEndoV

In the iCLIP analysis mentioned earlier Y RNA1 and Y RNA4 were abundant targets for hEndoV, and this analysis indicated that at least overexpressed hEndoV could bind Y RNA1/4 inside the cells. The *in vitro* cleaving activity of recombinant hEndoV and affinity upon Y RNA was therefore investigated. To our knowledge, there are no reports showing that Y RNA contains inosines.

Some cleavage of Y RNA1/4 was observed for hEndoV, however the activity was weak compared to small RNAs containing inosine. Also, the binding affinity of hEndoV upon endogenous Y RNA as demonstrated by EMSA, was weaker than for inosine-containing tRNA, but at the level of tRNA GluCTC. These results suggest that the hEndoV affinity upon endogenous RNA is not inosine dependent. Also, the shifts shown for Y RNA1/4 is stronger than for the inosine containing tRNA ValAAC.

To analyse which regions of Y RNA4 hEndoV binds, substrates corresponding to the different part were made and used in EMSAs.
hEndoV showed shifts for all four substrates, but the strongest shifts were seen by the 5´stem bulge and Hairpin structures (Figure 3.5 and 3.6). 5´stem bulge and Hairpin both have branched structures (Figure 3.5). As discussed above, hEndoV seems to have a higher affinity for structural RNA, which is supported by the findings in this assay. Biochemical activity assay has also been performed on the same substrate, but no visible fragmentation was detected. This might be interpreted as short RNA oligos must have inosine to be cleaved by, but not for binding to hEndoV. This suggest that the structure of a RNA molecule is sufficient for binding by hEndoV, but inosine is preferred for cleavage to occure.

The results suggest that affinity between hEndoV and Y RNA is of some importance, but the significance is not known. The ribonuclease RNase L has been described as a nuclease that cleave tRNA in response to dsRNA, but it has also been reported to be able to cleave Y RNA (except Y RNA4) (Donovan et al., 2017). It cannot be excluded that the fragmentation of Y RNA by hEndoV is not specific, but that it rather facilitates or inhibits cleavage of Y RNAs from either RNase L or other nucleases, as discussed above. The binding of hEndoV to Y RNA might play a similar role.

Y RNAs; expression, protein that binds and chemical modifications

Y RNA forms an RNP complex consisting primarily of Y RNA and Ro60 (RoRNP). Ro60 is related to the autoimmune rheumatic disease's systemic lupus erythematosus and Sjögren´s syndrome (Kowalski and Krude, 2015), and the RNP complexes are implicated in RNA processing and quality control. The loop domain of Y RNA has been reported to bind to several other proteins, but the roles of these interactions is not known. It has been suggested

that the interactions could modulate the localization of Ro60, and also alter cellular functions by binding to Y RNA (Kowalski and Krude, 2015, Sim and wolin, 2011). Binding of hEndoV to Y RNA could therefore have an impact on the function of Ro60, and the autoimmune functions in the cell.

Ro60 is bound at the lower stem domain of Y RNA in the RoRNP complex. The 5´stem bulge which hEndoV showed strong shifts towards is also located in the lower stem domain. It is possible that hEndoV competes with Ro60 for binding to Y RNA and might therefore hold some of the same functions. Double-stranded RNA can bind to RNA receptors in the cell and trigger immune responses, which can be prevented by Ro60 and La proteins. hEndoV outcompeting Ro60 could possibly alter the autoimmune function.

A co-immunoprecipitation experiment with hEndoV and Ro60 was attempted, but no interactions were detected. This suggests that they don't interact directly, but may still have some of the same functions and interacting partners. Both Ro60 and hEndoV have been found to interact with the proteins YBX1 and IGF2BP1 as well as Y RNA, and the relevance of this will be discussed in a later section.

tRNA is the most modified RNA, with an average of 13 modifications per molecule (Pan, 2018). Modifications of Y RNA have not been reported, however Y RNA resembles tRNA in structure and it is therefore conceivable that some of the enzymes modifying tRNA could also act on Y RNA. Modifications could be of special importance for proper function and stabilisation of the tertiary structure of Y RNA. For example ADAR catalyze adenosine to inosine editing of RNA that possesses double-stranded RNA (George et al., 2011). The secondary structure of Y RNA has as previously described, areas with double strands. This suggests that Y RNA can be a possible substrate for ADAR, which in turn can lead to ds RNA destabilization.

The number of methyl modifications in RNA is several times greater than what is found in DNA, and the role of RNA methylation has in recent years been reported in numerous fundamental and disease-associated cellular processes (Mongan et al., 2019). Methylation of tRNA, mRNA and rRNA are normal modifications, and methylation of Y RNA is therefore not unlikely. The presence of methyl groups can influence for example the reverse transcriptases either by blocking the enzyme or by inducing misincorporation in the cDNA

opposite the modification (Ovcharenko and Rentmeister, 2018). RT-qPCR was performed with hEndoV and Y RNA1/4 to investigate if the level of hEndoV in cells influences the amount of Y RNA transcripts present. In this experiment cDNA was generated from an RNA template, which was done by reverse transcriptase. If Y RNA at any point was methylated, this could have prevented the generation of cDNA and affected the result of the RT-qPCR analysis.

The RT-qPCR analysis showed that both Y RNA1 and Y RNA 4 are present in the cells under all tried conditions (Figure 3.13). An effect of overexpressing hEndoV was seen for two stressors; poly I:C and UV irradiation. Poly I:C treatment resulted in higher levels of Y RNA1 and Y RNA4 when hEndoV also was present, whereas the opposite effect was seen for UV radiation. Poly I:C is a synthetic analogue of dsRNA, mimics molecular pattern associated with viral infections. This pattern is known to trigger the production of inflammatory cytokines and chemokines (InvivoGen, n.d). Viral infections might also induce SG´s, which hEndoV is known to relocate to (Nawaz et al., 2016a). How hEndoV influences the Y RNA levels under stress is not known. Maybe hEndoV offers protection of the Y RNA transcripts during poly I:C treatment as already discussed. However, after UV irrradiation other mechanisms seems to apply. It should be mentioned, that it is not known whether Y RNA expression is increased or if degradation is reduced.

4.5 hEndoV and interacting partners

It is unlikely that hEndoV carries out its functions by itself, and through a series of experiments it was found that hEndoV interacts with several other proteins. YBX1 and IGF2BP1 were two of the proteins identified as the top 25 interaction partners by MS after co-immunoprecipitation of hEndoV D52A (Nawaz et al., 2016a). The results in this thesis suggest that the interactions with both YBX1 and IGF2BP1 are specific (Figure 3.8, 3.9 and 3.11).

It is known that oxidative stress can alter the localization of the proteins in cells (Nawaz et al., 2016a). It was therefore investigated whether the interaction of the proteins changed when exposed to arsenite. Arsenite treatment of the cells did not affect amount of YBX1 bound to hEndoV (Figure 3.8). This suggest that the proteins either relocate together, or that the amount of protein relocated is too small to be detected in co-immunoprecipitation.

To test whether RNA is required for the interaction between YBX1 and hEndoV, samples were treated with RNase. The results showed that the interaction between hEndoV and YBX1 was lost, suggesting that hEndoV and YBX1 are not directly interacting, but that the complex is held together via an RNA molecule (Figure 3.9). This is interesting considering that YBX1 interacting with Ro60 is RNA dependent, and that both Ro60 and hEndoV show interactions with Y RNA. Perhaps a "super complex" of proteins and Y RNA is formed, influencing or contributing to cellular processes.

Also, the interaction between hEndoV and IGF2BP1 was confirmed (Figure 3.11). IGF2BP1 showed weaker bonds for both samples and input compared to YBX1, suggesting that the amount of IGF2BP1 in the cells is lower. As for YBX1, experiments showed that treatment with arsenite did not have any impact on the co-precipitation between the two proteins. Contrary to YBX1, RNAse treatment did not destroy the binding between IGF2BP1 and hEndoV (Figure 3.11). This suggests that this interaction is direct and not via RNA.

4.5.1 Colocalization in the cell

For proteins to interact, they must exist at the same location in the cells. As previously stated, hEndoV is found mostly in the cytoplasm, but show relocalization to SG´s when exposed to arsenite (Nawaz et al., 2016a). YBX1 and IGF2BP1 have also been reported to localize in SG´s when exposed to stress. It has also been shown that YBX1 is involved in the formation of SG´s in cells (Sim et al., 2012, Stöhr and Hüttelmaier, 2012). To check for a possible colocalization of these three proteins, a series of ICC experiments was performed. Also, Ro60 was included in this analysis.

As expected GFP-hEndoV, IGF2BP1 and Ro60 were all found in the cytoplasm in the unstressed cells. YBX1 in the non-treated cells was difficult to interpret due to a lot of background staining, but the images indicate that YBX1 is mostly found in the cytoplasm (Figure 3.12)

A SG indicator was not included, but GFP-hEndoV relocated to what is thought to be SG´s It is not known how much of the hEndoV that relocalize to the SG´s, but these results suggest that it varies widely. UV irradiation is not a good inducer of SG´s. Arsenite treatment seemed

to relocate YBX1 to structures around the nucleus. These structures did not overlap with the assumed SG´s as seen for GFP-hEndov, and therefore it is not believed that they are SG´s (Figure 3.12). It has been reported that YBX1 is required for sorting into exosomes (Shurtleff et al., 2017), and the observed structures might be related to this function.

Ro60 is localized in cytoplasm and nucleus in unstressed cells, but is reported to become strongly nuclear after UV irradiation (Chen et al., 2003). Nuclear localization of Ro60 after UV-irradiation was not detected in this experiment, but some cytoplasmic structures with accumulations of Ro60 were seen (Figure 3.12). A possible reason for Ro60 not being detected in nucleus is that the antibodies might have had difficulties entering the nucleus.

hEndoV was only found to colocalize with YBX and IGF2BP1 in the cytoplasm, both in stressed and unstressed cells. Some colocalization between hEndoV and Ro60 is maybe seen in the stressed cells (Figure 3.12).

4.5.2 The role of hEndoV and its relating partners

Both YBX1 and IGF2BP1 have important cellular functions (Stöhr and Hüttelmaier, 2012, Matsumoto and Bay, 2005). Results presented here suggested that hEndoV interacts with both; the binding of YBX1 was indirect and RNA-dependent whereas the binding of IGF2BP1 was direct and RNA-independent. The nature of the RNA molecule in this experiment is not known, and it is possible that it is YRNA. It is shown that Ro60 can bind to the internal loop of Y RNA and promote degradation. EMSA and activity assay suggest that hEndoV has affinity for and cleaving activity upon Y RNA. Ro60 has also been shown to interact whit YBX1 and IGF2BP1 in an RNA-dependant manner (Jønson et al., 2007, Sim et al., 2012). There are several finding that indicate a possible complex of hEndoV, YBX1, IGF2BP1, Ro60 and Y RNA. If not all of them interacting at the same time, there is a possibility of different compositions, with different functions.

In 2017 Shurtleff et al., reported that YBX1 plays a role in the sorting of abundant small ncRNAs species, including Y RNA into exosomes. Exosomes are defined as 30-100 nm vesicles originated from multivesicular bodies (MVB) which contains late endosomal markers (Shurtleff et al., 2017). Exosomes are shed by all cell types under normal – and patho-physiological conditions and are found in abundance in body fluids (blood, urine, milk, semen etc.). They are important factors in inter-cellular communications and are capable of

modulating the cell behaviour by cell signalling (Patel et al., 2019). A theory is that hEndoV contributes to the sorting of Y RNAs into exosomes and in this way regulate the content. If hEndoV has a role in the distribution of Y RNA in exosomes it could also have an effect on the immune response, not just by competing with Ro60 as previously suggested, but by controlling RoRNP complexes.

Mice lacking EndoV appear, act and breeds normally suggesting that EndoV is not critical under normal unstressed conditions (Kong et al., 2020). Interestingly, when these mice are given diethylnitrosamine (DEN) to induce liver cancer (hepatocellular carcinoma), they had fewer and smaller tumors compared to the wild type (Kong et al., 2020). It could be that hEndoV has a specific role in regulation of selected transcripts in HCC, maybe through exosome controlling, or that hEndoV itself is secreted via exosomes.

5 Conclusion

In this thesis the main goal was to gain a better understanding of the roles of hEndoV, by identifying which RNAs are targeted by hEndoV and confirm possible interacting proteins.

EMSA analysis revealed that MH-hEndoV and MH-hEndoV D52A have affinity for all endogenous small RNA tested, in addition to the known inosine containing RNA substrates. MH-hEndoV had reduced cleaving activity and did not show any band shifts, which could be explained by the presence of the purification MH-tag that may physically hinder the binding. These results suggested that hEndoV can cleave and bind to both oligonucleotide substrates and endogenous small RNA with or without inosine, nevertheless with preference for inosine.

It was shown that hEndoV can cleave endogenous Y RNA and that it has affinity for both endogenous Y RNA and substrates that corresponds to structural part of Y RNA 4. The results suggested that hEndoV have a higher affinity for structural RNA than ordinary RNA duplexes, which is also supported by the affinity of hEndoV for endogenous small RNAs. Y RNA1/4 was showed to be expressed in T-REx and T-REx Flag hEndoV cells, and hEndoV affected the levels of Y RNA after poly I:C and UV treatment.

Co-immunoprecipitation showed that both YBX1 and IGF2BP1 bind specifically to hEndoV. Whereas the binding of YBX1 is RNA-dependent, the hEndoV- IGF2BP1 is direct and RNA-independent. Treatment with oxidative stress did not alter the interactions. For proteins to bind they must exist at the same localization in the cell. All proteins were found in the cytoplasm, but only hEndoV was found to relocalize to SG´s when exposed to stress.

Future aspects

One of the main goals with this thesis was to identify the *in vivo* substrates of hEndoV and confirm the finding of the iCLIP analysis. This thesis confirms that hEndoV can cleave and bind to Y RNAs *in vitro*, but a lot can be done to contribute further in the field of Y RNA. The validation of Y RNA as a substrate for hEndoV will be a central part of the future work.

To get a better understanding of Y RNA levels of hEndoV it would be interesting to reproduce the RT-qPCR analysis and investigate the influence of viral infections. Treatment with AlkB could reverse possible methylations of Y RNA with the potential to prevent

reverse transcriptase. To learn more about the function of Y RNA biotinylated DNA probes have been designed to specifically isolate Y RNAs, using both wt and EndoV$^{-/-}$ cells to check for differences and the impact of hEndoV. Some of the known enzymes to cleave Y RNA are Ang and RNaseL and it would be interesting to explore the possibility of an interaction between hEndoV and these enzymes. As nothing is known about modifications of Y RNA, it would also be interesting to analyze RNA modifications by MS.

To continue the research with hEndoV protein partners it would be interesting to improve the colocalization assay and study the field of exosomes. A clear colocalization of hEndoV with YBX1 and IGF2BP1 was not seen even though in theory they should colocalize. To study localization of the proteins, fluorescent fusionproteins can be used for YBX1/IGF2BP1/Ro60 as with hEndoV. Probing with antibodies has its limitations, when it comes to penetrating all parts of the cell, and therefore fusionproteins could be a good alternative. The possible role of hEndoV impact on exosomes needs further investigation. Exosomes can be isolated from small amounts of biological fluids, and their cargo can be investigated. Their cargo serves as disease-specific biomarkers, which can give deep insight into how the components interact. The classical way to isolate exosomes is through ultracentrifugation, but several commercial kits exist (Patel et al., 2019). By isolating exosomes from T-REx HEK Flag-hEndoV cells a possible sorting of hEndoV into exosomes can be revealed.

6 Reference list

ALBERTS, B., JOHNSON, A., LEWIS, J., MORGAN, D., RAFF, M., ROBERTS, K. & WALTER, P. 2015. Molecular Biology of The Cell. 6 ed. USA: Garland Science.

ALSETH, I., DALHUS, B. & BJØRÅS, M. 2014. Inosine in DNA and RNA. *Current Opinion in Genetics & Development,* 26**,** 116-123.

BERGES, N., NAWAZ, M. S., DAHL, T. B., HAGEN, L., BJØRÅS, M., LAERDAHL, J. K. & ALSETH, I. 2019. Complex alternative splicing of human Endonuclease V mRNA, but evidence for only a single protein isoform. *PloS ONE,* 14 (11): e0225081.

BOCCALETTO, P., MACHNICKA, M. A., PURTA, E., PIATKOWSKI, P., BAGINSKI, B., WIRECKI, T. K., CRECY-LAGARD, V. D., ROSS, R., LIMBACH, P. A., KOTTER, A., HELM, M. & BUJNICKI, J. M. 2018. MODOMICS: a database of RNA modification pathways. 2017 update. *Nucleic Acids Research,* 46 (D1): D303-D307.

BOCCITTO, M. & WOLIN, S. L. 2019. Ro60 and Y RNAs: structure, function, and roles in autoimmunity. *Critical Reviews in Biochemistry and Molecular Biology,* 54 (2): 133-152.

CAO, W. 2013. Endonuclease V: an unusual enzyme for repair of DNA deamination. *Cellular and Molecular Life Sciences,* 70 (17): 3145-3156.

CHEN, X., SMITH, J. D., SHI, H., YANG, D. D., FLAVELL, R. A. & WOLIN, S. L. 2003. The Ro Autoantigen Binds Misfolded U2 Small Nuclear RNAs and Assists Mammalian Cell Survival after UV Irradiation. *Current Biology,* 13 (24): 2206-2211.

CLARK, D. P. & PAZDERNIK, N. J. 2013. Molecular Biology. *Academic Cell.* Second ed. Oxford: Elsevier Academic Press.

CRICK, F. H. 1968. The origin of the genetic code. *Journal of Molecular Biology,* 38 (3): 367-379.

DALHUS, B., ARVAI, A. S., ROSNES, I., OLSEN, Ø. E., BACKE, P. H., ALSETH, I., GAO, H., CAO, W., TAINER, J. A. & BJØRÅS, M. 2009. Structure of Endonuclease V with DNA Reveal Initiation of Deaminated Adenine Repair. *Nature structural & molecular biology,* 16 (2): 138-143.

DEDON, P. C., BARTH, M., CHEN, B., MOTT, M. D., DENDROULAKIS, V., DONG, M., KALINGA, S., ELMQUIST, E., MARGOLIN, Y., PANG, B. & ZHOU, X. 2006. Chapter 2 Diverse Mechanisms of Endogenous Nucleobase Deamination in DNA and RNA. *Advances in Molecular Toxicology,* 1:25-63.

DEEPAK, S., KOTTAPALLI, K., OROS, G., RANGAPPA, K., IWAHSHI, H., MASUO, Y. & AGRAWAL, G. 2007. Real-Time PCR: Recolutionizing Detection and Expression Analysis of Genes. *Current Genomics,* 8 (4): 234-251.

DHAHBI, J. M., SPINDLER, S. R., ATAMNA, H., BOFFELLI, D. & MARTIN, D. I. 2014. Deep Sequencing of Serum Small RNAs Identifies Patterns of 5′ tRNA Half and YRNA Fragment Expression Assciated with Breast Cancer. *Biomark Cancer,* 6: 37-47.

DONOVAN, J., RATH, S., KOLET-MANDRIKOV, D. & KORENNYKH, A. 2017. Rapid RNase L-driven Arrest of Protein Synthesis in the sdRNA Response Withouth Degradation of Translation Machinery. *RNA,* 23(11): 1660-1671.

ELISEEVA, I. A., KIM, E. R., GURYANOV, S. G., OVCHINNIKOV, L. P. & LYABIN, D. N. 2011. Y-Box-Binding Protein 1 (YB-1) and Its Functions. *Biochemistry (Moscow),* 76 (13): 1402-1433.

EMARA, M. M., IVANOV, P., HICKMAN, T., DAWRA, N., TISDALE, S., KEDERSHA, N., HU, G.-F. & ANDERSON, P. 2010. Angiogenin-induced tRNA-derived Stress-

induced RNAs Promotes Stress-induced Stress Granule Assembly. *The Journal of Biological Chemistry,* 285 (14): 10959-10968.
EMBL. 2016. European Molecular Biology laboratory. Available: https://www.embl.de/pepcore/pepcore_services/cloning/choice_vector/ecoli/embl/popup_emblvectors/.
FLADEBY, C., VIK, E. S., LAERDAHL, J. K., NEURAUTER, C. G., HEGGELUND, J. E., THORGAARD, E., STRØM-ANDERSEN, P., BJØRÅS, M., DALHUS, B. & ALSETH, I. 2012. The Human Homolog of Escherichia coli Endonuclease V Is a Nucleolar Protein with Affinity for Branched DNA Structures. *PLoS one,* 7 (11): e47466.
FU, Y., LEE, I., LEE, Y. S. & BAO, X. 2015. Small Non-coding Transfer RNA-Derived RNA Fragments (tRFs): Their Biogenesis, Function and Implication in Human Diseases. *Genomics Inform,* 13 (4): 94-101.
GARCÍA-CABALLERO, D., PÉREZ-MORENO, G., ESTÉVEZ, A. M., RUÍZ-PÉREZ, L. M., VIDAL, A. E. & GONZÁLEZ-PACANOWSKA, D. 2017. Insights into the role of endonuclease V in RNA metabolism in *Trypanosoma brucei. Scientific Reports,* 7 (1): 8505.
GATES, F. T. & LINN, S. 1977. Endonuclease V of Escherichia coli. *The Journal of Biological Chemistry,* 252 (5): 1647-1653.
GE HEALTHCARE. 2017. Superdex 75 HR 10/30. Available: https://www.gelifesciences.co.jp/tech_support/manual/pdf/71603100af.pdf.
GE LIFE SCIENCES. 2018. Storage Phosphor Screen BAS-IP. Available: https://cdn.gelifesciences.com/dmm3bwsv3/AssetStream.aspx?mediaformatid=10061&destinationid=10016&assetid=16330.
GELDER, C. W. G. V., THIJSSEN, J. P. H. M., KLAASSEN, E. C. J., STURCHLER, C., KROL, A., VENROOIJ, W. J. V. & PRUIJN, G. J. M. 1994. Common structural features of the Ro RNP associated hY1 and hY5 RNAs. *Nucleic Acids Research,* 22 (13): 2498-2506.
GEORGE, C. X., GAN, Z., LIU, Y. & SAMUEL, C. E. 2011. Adenosine Deaminases Acting on RNA, RNA editing, and Interferon Action. *Journal of Interferon & cytokine research : the official journal of the International Society of Interferon and Cytokine Research,* 31 (1): 99-117.
GERACE, E. & MOAZED, D. 2015. Affinity Pull-Down of Proteins Using Anti-FLAG M2 Agarose Beads. *Methods in enzymology,* 559: 99-110.
GOODARZI, H., LIU, X., NGUYEN, H. C. B., ZHANG, S., FISH, L. & TAVAZOIE, S. F. 2015. Endogenous tRNA Derived Fragments Suppresses Breast Cancer Progression via YBX1 Displacement. *CellPress,* 161 (4): 790-802.
GRAY, M. W. 2012. Evolutionary Origin of RNA Editing. *Biochemistry,* 51(26): 5235-5242.
HAUSSECKER, D., HUANG, Y., LAU, A., PARAMESWARAN, P., FIRE, Z. & KAY, M. A. 2010. Human tRNA-derived small RNAs in the global regulation of RNA silencing. *Rna,* 16 (4): 673-695.
HE, S. L. 2013. Northen blot. *Methods in enzymology,* 530: 75-87.
HELLMANN, L. M. & FRIED, M. G. 2007. Electrophoretic Mobility Shoft Assay (EMSA) for Detecting Protein-Nucleic Acid Interactions. *Nature Protocols,* 2 (8): 1849-1861.
HILL-PERKINS, M., JONES, M. D. & KARRAN, P. 1986. Site-specific Mutagenesis *in Vivo* by Single Methylated or Deaminated Purine Bases. *Mutation Reasearch,* 162 (2): 153-163.
HOPPER, A. K., PAI, D. A. & ENGELKE, D. R. 2011. Cellular dynamics of tRNAs and their genes. *National Institutes of Health,* 584 (2): 310.

HUANG, J., LU, J., BARANY, F. & CAO, W. 2001. Multiple Cleavage Activities of Endonuclease V from *Thermotoga maritima:* Recognition and Strand Nicking Mechanisms. *Biochemistry,* 40 (30): 8738-8748.
HUANG, J., LU, J., BARANY, F. & CAO, W. 2002. Mutational Analysis of Endonuclease V from *Themotoga maritima. Biochemistry,* 41 (26): 8343-8350.
HUANG, X., ZHANG, H., GUO, X., ZHU, Z., CAI, H. & KONG, X. 2018. Insulin-like growth factor 2 mRNA-binsing protein 1 (IGF2BP1) in cancer. *Journal of Hematology & Oncology,* 11: 88.
IBBA, M. & SÖLL, D. 2000. Aminoacyl-tRNA Synthesis. *Annual Review of Biochemistry,* 69 (1): 617-650.
INVITROGEN. 2012. Flp-in T-REx Core Kit. Available: https://www.thermofisher.com/document-connect/document-connect.html?url=https%3A%2F%2Fassets.thermofisher.com%2FTFS-Assets%2FLSG%2Fmanuals%2Fflpintrex_man.pdf&title=RmxwLUluIFQtUkV4IENvcmUgS2l0.
INVIVOGEN. n.d. Poly (I:C) HMW. Available: https://www.invivogen.com/polyic-hmw.
IQBAL, H., AKINS, D. R. & KENEDY, M. R. 2018. Co-immunoprecipitation for Identifying Protein-Protein Interactions in *Borrelia burgdorferi*. *Methods in molecular biology,* 1690: 47-55, .
ISHITANI, R., NUREKI, O., NAMEKI, N., OKADA, N., NISHIMURA, S. & YOKOYAMA, S. 2003. Alternative Tertiary Structure of tRNA for Recognition by a Posttransriptional Modification Enzyme. *Cell Press,* 113: 383-394.
IVANOV, P., EMARA, M. M., VILLEN, J., GYGI, S. P. & ANDERSON, P. 2011. Angiogenin-Induced tRNA Fragments Inhibit Translation Initiation. *Molecular Cell,* 43 (4): 613-623.
JØNSON, L., VIKESAA, J., KROGH, A., NIELSEN, L., HANSEN, T., BORUP, R., JOHNSEN, A., CHRISTIANSEN, J. & NIELSEN, F. 2007. Molecular composition of IMP1 ribonucleoprotein granules. *Mol Cell Proteomics,* 6 (5): 798-811.
KEAM, S. P. & HUTVAGNER, G. 2015. tRNA-Derived Fragments (tRFs): Emerging New Roles for an Ancient RNA in the Regulation of Gene Expression. *Life,* 5 (4): 1638-1651.
KEDERSHA, N., IVANOV, P. & ANDERSON, P. 2013. Stress granules and cell signaling: more than just a passing phase?. *Trends Biochemical Science,* 38 (10): 4394-506.
KEIKE, K., UCHIUMI, T., OHGA, T., TOH, S., WADA, M., KOHNO, K. & KUWANO, M. 1997. Nuclear translocation of the Y-box binding protein by ultraviolet irradiation. . *FEBS Lett,* 417(3): 390-394.
KONG, X. Y., VIK, E. S., NAWAZ, M. S., BERGES, N., DAHL, T. B., VÅGBØ, C., SUGANTHAN, R., SEGERS, F., HOLM, S., QUILES-JIMÉNEZ, A., GREGERSEN, I., FLADEBY, C., AUKRUST, P., BJØRÅS, M., KLUNGLAND, A., HALVORSEN, B. & ALSETH, I. 2020. Deletion of Endonuclease V suppresses chemically induced hepatocellular carcinoma. *Nucleic Acids Research,* 48 (8): 4463-4479.
KOWALSKI, M. P. & KRUDE, T. 2015. Functional roles of non-coding Y RNAs. *The International Journey of Biochemistry & Cell Biology,* 66:20-29.
KRISHNA, S., YIM, D. G., VAIRAVAN, LAKSHMANAN, TIRUMALAI, V., KOH, J. L., PARK, J. E., CHEONG, J. K., LOW, J. L., LIM, M. J., SZE, S. K., SHIVAPRASAD, P., GULYANI, A., RAGHAVAN, S., PALAKODETI, D. & DASGUPTA, R. 2019. Dynamic expression of tRNA-derived small RNAs define cellular states. *EMBO reports,* 20 (7): e47789.
LANDSMAN, D. 1992. RNP-1, an RNA-binding motif is concerved in the DNA-bidning cold shock domain. *Oxford University Press,* 20 (11): 2861-2864.

LEE, C., YANG, Y.-C., GOODMAN, S. D., YU, Y.-H., LIN, S.-B., KAO, J.-T., TSAI, K.-S. & FANG, W.-H. 2010. Enonuclease V-mediated deoxyinosine excision repair in vitro. *DNA Repair,* 9 (10): 1073-1079.
LEE, Y. & RIO, D. C. 2015. Mechanisms and Regulation of Alternative Pre-mRNA Splicing. *Annual Review of Biochemistry,* 84: 291-323.
LEE, Y. S., SHIBATA, Y., MALHOTRA, A. & DUTTA, A. 2015. A novel class of small RNAs: tRNA-derived RNA fragments (tRFs). *Genes & Develpoment,* 23 (22): 2639-2649.
LERNER, M. R., BOYLE, J. A., HARDIN, J. A. & STEITZ, J. A. 1981. Two Novel Classes of Small Ribonucleoproteins Detected by Antibodies Assoiciated with Lupus Erythematosus. *Science,* 211 (4480): 400-402.
LI, S. & HU, G.-F. 2012. Emerging role of angiogenin in stress response and cell survival under adverse conditions. *Jornal of Cellular Physiology,* 227 (7): 2822-2826.
LIU, S., CHEN, Y., REN, Y., ZHOU, J., REN, J., LEE, I. & BAO, X. 2018. A tRNA-derived RNA Fragment Plays an Important Role in the Mechanism of Arsenite-induced Cellular Responses. *Scientific Reports,* 8: 16838.
LORENZ, C., LÜNSE, C. E. & MÖRL, M. 2017. tRNA Modifications: Impact on Structure and Thermal Adaptation. *Biomolecules,* 7 (2): 35.
MAHMOOD, T. & YANG, P.-C. 2012. Western Blot: Technique, Theory, and Trouble Shoot. *North American journal of medical sciences,* 4 (9): 429-434.
MARAIA, R., SAKULICH, A. L., BRINKMANN, E. & GREEN, E. D. 1996. Gene encoding human Ro-associated autoantigen Y5 RNA. *Nucleic Acids Research,* 24 (18): 3552-3559.
MATOS, L. L. D., TRUFELLI, D. C., MATOS, M. G. L. D. & PRINCHAL, M. A. D. S. 2010. Immunohistochemistry as an Important Tool in Biomarkers Detection and Clinical Practice. *Biomark Insights,* 5: 9-20.
MATSUMOTO, K. & BAY, B.-H. 2005. Significance of the Y-box proteins in human cancers. *Journal of Molecular and Genetic Medicine,* 1 (1): 11-17.
MI, R., ALFORD-ZAPPALA, M., KOW, Y. W., CUNNINGHAM, R. P. & CAO, W. 2012. Human Endonuclease V as a Repair Enzyme for DNA Deamination. *Mutation Reasearch,* 735 (1-2): 12-18.
MONGAN, N. P., EMES, R. D. & ARCHER, N. 2019. Detection and analysis of RNA methylation. *F1000Research,* 8: F1000 Faculty Rev-559.
MORITA, Y., SHIBUTANI, T., NAKANISHI, N., NISHIKURA, K., IWAI, S. & KURAOKA, I. 2013. Human endonuclease V is a ribonuclease specific for inosine-containing RNA. *Nature Communications,* 4: 2273.
MOSIG, A., GUOFENG, M., STADLER, B. M. R. & STADLER, P. F. 2007. Evolution of the Vertebrate Y RNA Cluster. *Theory in Biosciences,* 129: 9-14.
NAWAZ, M. S., VIK, E. S., BERGES, N., FLADEBY, C., BJØRÅS, M., DALHUS, B. & ALSETH, I. 2016a. Regulation of Human Endonuclease V Activity and Relocalization to Cytoplasmic Stress Granules. *The Journal of Biological Chemistry,* 291 (41): 21786-21801.
NAWAZ, M. S., VIK, E. S., RONANDER, M. E., SOLVOLL, A. M., BLICHER, P., BJØRÅS, M., ALSETH, I. & DALHUS, B. 2016b. Crystal structure and MD simulation of mouse EndoV reveal wedge motif plasticity in this inosine-specfic endnuclease. *Scientific Reports,* 6: 24979-24979.
NOVEX. 2015. Ni-NTA Purification System. *Life Technologies* [Online]. Available: http://tools.thermofisher.com/content/sfs/manuals/ninta_system_man.pdf.
OVCHARENKO, A. & RENTMEISTER, A. 2018. Emerging approaches for detection of methylation sites in RNA. *Open Biology,* 8: 180121.

PAN, T. 2018. Modifications and functional genomics of human transfer RNA. *Cell Research,* 28: 1-10.
PATEL, G. K., KHAN, M. A., ZUBAIR, H., SRIVASTAVA, S. K., KHUSMAN, M. D., SINGH, S. & SINGH, A. P. 2019. Comparative analysis of exosome isolation methods using culture supernatant for optimum yield, purity and downstream applications. *Scientific Reports,* 9: 5335.
PERREAULT, J., PERREAULT, J.-P. & BOIRE, G. 2007. Ro-Associated Y RNAs in Metazoans: Evolution and Diversification. *Molecular Biology and Evolution,* 24 (8): 1678-1689.
POTTER, H. & HELLER, R. 2003. Transfection by Electroporation. *Current Protocols in molecular biology,* Unit 9-3.
PRABHU, L., HARTLEY, A.-V., MARTIN, M., WARSAME, F., SUN, E. & LU, T. 2015. Role of post-translational modifications of the Y box binding protein 1 in human cancers. *Genes & Diseases,* 2 (3): 240-246.
RNAZOLRT BROCHURE 2009. *Molecular Research Center, Inc. Cincinnati, OH*.
ROBERTSON, H. D., ALTMAN, S. & SMITH, J. D. 1972. Purification and Properties of a Spesific Escherichia coli Ribonuclease which Cleaves a Tyrosine Transfer Ribonucleic Acid Precursor. *The Journal of Biological Chemistry,* 247 (16): 5243-5251.
ROBINSON, P. K. 2015. Enzymes: principles and biotechnological applications. *Essays in biochemistry,* 59: 1-41.
SAMBROOK, J. & RUSSELL, D. W. 2006. SDS-Polyacrylamide Gel Electrophoresis of Proteins. *CSH Protocols,* 2006 (4): pdb.prot4540.
SCHIFFER, S., RÖSCH, S. & MARCHFELDER, A. 2002. Assigning a function to a conserved group of proteins: the tRna 3´-processing enzymes. *The EMBO journal,* 21 (11): 2769-2777.
SCHOUTEN, K. A. & WEISS, B. 1999. Endonuclease V protects Escherichia coli against specific mutations caused by nitrous acid. *Mutation Research,* 435 (3): 245-254.
SHEN, Y., YU, X., ZU, L., LI, T., YAN, Z. & GUO, J. 2018. Transfer RNA-derived fragments and tRNA halves: biogenesis, biological functions and their role in diseaes. *J Mol Med (Berl),* 96 (11): 1167-1176.
SHURTLEFF, M. J., YAO, J., QIN, Y., NOTTINGHAM, R. M., TEMOCHE-DIAZ, M. M., SCHEKMAN, R. & LAMBOWITZ, A. M. 2017. Broad role of YBX1 in defining the small noncoding RNA composition of exosomes. *Proceedings of the National Academy of Sciences USA,* 114 (43): E8987-E8995.
SIM, S. & WOLIN, S. L. 2011. Emerging roles for the Ro 60-kDa autoantigen in noncoding RNA metabolism. *Wiley Interdiciplinary Reviews RNA,* 2 (5): 686-699.
SIM, S., YAO, J., WEINBERG, D. E., NIESSEN, S., III, J. R. Y. & WOLIN, S. L. 2012. The zipcode-binding protein ZBP1 influences the subcellular location of the Ro 60-kDa autoantigen and the noncoding Y3 RNA. *Cold Spring Harbor Laboratory Press,* 18 (1): 100-110.
SOBALA, A. & HUTVANGER, G. 2011. Transfer RNA-derived fragments: origins, processing, and functions. *Wiley Interdisiplinary Review RNA,* 2 (6): 853-862.
SOMASEKHARAN, S. P., EL-NAGGAR, A., LEPRIVIER, G., CHENG, H., HAJEE, S., GRUNEWALD, T. G. P., ZHANG, F., NG, T., DELATTRE, O., EVDOKIMOVA, V., WANG, Y., GLEAVE, M. & SORENSEN, P. H. 2015. YB-1 regulates stress gtanule formation and tumor progresson bt translationally activating G3BP1. *Journal of Cell Biology,* 208 (7): 913-929.
STASTNA, M. & EYK, J. E. V. 2013. Analysis of protein isoforms: can we do it better? *Proteomics,* 12 (0): 2937-2948.

STÖHR, N. & HÜTTELMAIER, S. 2012. IGF2BP1, A post-transcriptional «driver» of tumor cell migration. *Cell Adhesion & Migration* 6 (4): 312-318.
STÖHR, N., LEDERER, M., REINKE, C., MEYER, S., HATZFELD, M., SINGER, R. H. & HÜTTELMAIER, S. 2006. ZBP1 regulates mRNA stability during cellular stress. *The Journal of Cell Biology,* 175 (4): 527-534.
TEUNISSEN, S. W. M., KRUITHOF, M. J. M., FARRIS, A. D., HARLEY, J. B., VENROOIJ, W. J. V. & PRUIJN, G. J. M. 2000. Conserved features of Y RNAs: a comparison of experimentally derived secondary structures. *Nucleic Acids Research,* 28 (2): 610-619.
THERMO FISHER SCIENTIFIC. n-d. SeeBlue™ Plus2 Pre-stained Protein Standard. Available: https://www.thermofisher.com/order/catalog/product/LC5925#/LC5925.
TU, C. P. & COHEN, S. N. 1980. 3'-end labeling of DNA with [alpha-32P]cordycepin-5'-triphosphate. *Gene,* 10 (2): 177-183.
TUCK, A. C. & TOLLERVEY, D. 2011. RNA in pieces. *Trends in Genetics,* 27 (10): 422-432.
TYMOCZKO, J. L., BERG, J. M. & STRYER, L. 2015. Biochemistry. A Short Course. 3 ed. New York: W.H Freeman & Company.
UCHIUMI, T., FOTOVATI, A., SASAGURI, T., SHIBAHARA, K., SHIMADA, T., FUKUDA, T., NAKAMURA, T., IZUMI, H., TSUZUKI, T., KUWANO, M. & KOHNO, K. 2006. YB-1 Is Important for an Early Stage Embryonic Development. *Neural Tube Formation And Cell Proliferation,* 281 (52): 40440-40449.
VALASEK, M. A. & REPA, J. J. 2005. The power of real-time PCR. *Advances in Physiology Education,* 29 (3): 151-159.
VIK, E. S., NAWAZ, M. S., ANDERSEN, P. S., FLADEBY, C., BJØRÅS, M., DALHUS, B. & ALSETH, I. 2013. Endonuclease V cleaves at inosines in RNA. *Nature Communications,* 4:2271.
WACHTER, K., KOHN, M., STOHR, N. & HUTTELMAIER, S. 2013. Subcellualr localization and RNP formatioin of IGF2BPs (IGF2 mRNA-binding proteins) is modulated by distinct RNA binding domains. *Journal of Biological Chemistry,* 394 (8): 1077-1090.
YAMASAKI, S., IVANOV, P., HU, G.-F. & ANDERSON, P. 2009. Angiogenin cleaves tRNA and promotes stress-induced translational repression. *Journal of Cell Biology,* 185 (1): 35-42.
YANG, W. 2011. Nucleases: Diversity of Structure, Function and Mechanism. *Quarterly reviews of biophysics,* 44 (1): 1-93.
YAO, M., HATAHET, Z., MELAMEDE, R. J. & KOW, Y. W. 1994. Purification and Characterization of a Novel Deoxyinosine-specific Enzyme, Deoxyinosine 3´Endonuclease, from Escherichia coli. *The Journal of Biological Chemistry,* 269 (23): 16260-16268.
YOSHIOKA, N., WANG, L., KISHIMOTO, K., TSUJI, T. & HU, G.-F. 2006. A therapeutic target for prostate cancer based on angiogenin-stimulated angiogenesis. *Proceedings of the National Academy of Sciences USA,* 103 (39): 14519-14524.
ZHANG, Z., HAO, Z., WANG, Z., LI, Q. & XIE, W. 2014. Structure of human endonuclease V as an inosine-specific ribonuclease. *Acta Crystallographica D Biol Crystallogr,* 70 (Pt 9): 2286-2294.
ZHU, L., GE, J., LI, T., SHEN, Y. & GUO, J. 2019. tRNA-derived fragments and tRNA halves: The new players in cancers. *Cancer Letters,* 452: 31-37.
ZHU, X., ZELMER, A. & WELLMANN, S. 2017. Visualization of Protein-protein Interaction in Nuclear and Cytoplasmic Fractions by Co-immunoprecipitation and In Situ Proximity Lifation Assay. *Journal of Visualized Experiments,* (119): 55218

Appendix A. Amino acid sequence of hEndoV 309

Translation (309 aa):

MALEAAGGPPEETLSLWKREQARLKAHVVDRDTEAWQRDPAFSGLQRVGGVDVSFVKGDSVRACASLVVL
SFPELEVVYEESRMVSLTAPYVSGFLAFREVPFLLELVQQLREKEPGLMPQVLLVDGNGVLHHRGFGVAC
HLGVLTDLPCVGVAKKLLQVDGLENNALHKEKIRLLQTRGDSFPLLGDSGTVLGMALRSHDRSTRPLYIS
VGHRMSLEAAVRLTCCCCRFRIPEPVRQADICSREHIRKSLGLPGPPTPRSPKAQRPVACPKGDSGESSG
EGQPPQDHSPGPRTAPRPGSQEQAGKDWQ

Appendix B. Top 25 proteins identified as possible protein partners for hEndoV with MS after Co-IP.

TABLE 1

25 top proteins identified by MS after co-IP with FLAG-hEndoV(D52A)

Ribosomal proteins are omitted from the list.

T test *p* value	*T* test difference	Protein name	Gene name	Peptide counts (all)
2.52E-05	3.70734	Endonuclease V	ENDOV	21;17;17;14;11;8;8;7;6;6;6;6;6;5;4;2;2;1
5.26E-06	3.00836	X-box-binding protein 1	XBP1	1;1;1;1
4.0E-06	2.98271	Insulin-like growth factor 2 mRNA-binding protein 1	IGF2BP1	15;11
2.30E-05	2.30214	Polyadenylate-binding protein 1; polyadenylate-binding protein 3	PABPC1;PABPC3	22;21;21;21;11;11;7;6;6;6;5;5;5;4;4;4;4; 3;3;3;2;1;1;1;1;1
0.000628637	2.10569	Insulin-like growth factor 2 mRNA-binding protein 3	IGF2BP3	6;2;1
0.000185407	1.90331	Nuclease-sensitive element-binding protein 1	YBX1	8;7;4;2
0.000237113	1.77645	Insulin-like growth factor 2 mRNA-binding protein 2	IGF2BP2	4;4;4;3;3;3;3
0.0430461	1.75115	Mesencephalic astrocyte-derived neurotrophic factor	MANF	1;1
0.00680958	1.74702	Polyadenylate-binding protein 4	PABPC4	16;16;16;16;12;7;4;3;3;2;2;2;2
0.0270908	1.65183	La-related protein 1	LARP1	9;8;6;3;3;2;1;1;1;1;1;1
0.016685	1.59752	Histone H3; histone H3.3C; histone H3.2; histone H3.1t; histone H3.3; histone H3.1	H3F3B;H3F3A;H3F3C;HIST2H3A; HIST3H3;HIST1H3A	2;2;2;2;2;2;2;2;2;2
0.000384325	1.54604	Guanine nucleotide-binding protein subunit β2-like 1	GNB2L1	1;1;1;1;1;1;1;1;1;1;1;1
0.000118816	1.5447	Y-box-binding protein 3	YBX3	7;6;6;2
0.0150847	1.5411	Double-stranded RNA-binding protein Staufen homolog 1	STAU1	7;7;7;6;2;1
5.38E-06	1.49226	La-related protein 7	LARP7	5;5;4;3;2;2
0.00318245	1.48783	Protein mago nashi homolog;Protein mago nashi homolog 2	MAGOHB;MAGOH	1;1;1;1;1
0.00348873	1.48094	Eukaryotic translation initiation factor 6	EIF6	2;1
0.000175999	1.36854	Uncharacterized protein C7orf50	C7orf50	1;1
0.000544839	1.34037	Putative helicase MOV-10	MOV10	4;4;2
0.000166308	1.23335	tRNA (cytosine(34)-C(5))-methyltransferase	NSUN2	14;12;8;6
0.00509954	1.23131	7SK snRNA methylphosphate capping enzyme	MEPCE	6;4
0.000423126	1.2146	Nuclear cap-binding protein subunit 1	NCBP1	2
0.00378886	1.18884	Protein BUD31 homolog	BUD31	3;2;1;1
0.00114663	1.17908	FACT complex subunit SPT16	SUPT16H	5
0.0128086	1.14924	Hepatoma-derived growth factor-related protein 3	HDGFRP3	3;2

Figure A1. 25 Top protein partners for hEndoV. *Proteins identified as possible protein partners of hEndoV by MS-analysis and Co-IP. YBX1 and IGF2BP1 is marked in red (Nawaz et al., 2016a)*

.

Appendix C. Materials

Bacterial strains

Strain	Characteristics	Genotype/Manufacturer
ER2566 *nfi⁻ rnhb⁻* (Nawaz et al., 2016a)	*E. coli*	F⁻λ-*fhuA2 [lon] ompT LacZ:: T7 gene1 sulA11 Δ (mcrC-mrr) 114:: ISI0*/ New England BioLabs

Plasmids

ER2566 *nfi⁻ rnhb⁻* was used as production organism.

Plasmid	Manufacturer
pETM-41-309	GeneScript

Enzymes

Enzyme	Manufacturer
TEV protease	Purified at Department of Microbiology, OUH.

Cell types

Cell type	Description
HAP1 C665 wt	Human cell line derived from male chronic myelogenous leukaemia
Flp-in T-REx 293 Flag	Human cell line stably expressing tetracycline repressor protein
Flp-in T-REx 293 Flag-hEndoV D52A	Human cell line stably expressing tetracycline repressor protein. Overexpressing Flag-hEndoV D52A
Flp-in T-REx 293 Flag-hEndoV	Human cell line stably expressing tetracycline repressor protein. Overexpressing Flag-hEndoV
Flp-in T-REx 293 GFP-hEndoV	Human cell line stably expressing tetracycline repressor protein. Overexpressing GFP-hEndoV

Antibodies

Antibody	Host	Dilutions	Manufacturer
Anti-YBX antibody (ab12148)	Rabbit	1 µg/ml	Abcam
Anti-IGF2BP1 (ab82968)	Rabbit	1:1000	Abcam
Anti-Rabbit IgG, Horseraddish	Rabbit	1:1000	Invitrogen
hEndoV-monoclonal IgG	Rabbit	1:10000	Santa Cruz Biotechnology
Goat anti-Rabbit IgG (H+L) Cross-adsorbed Secondary Antibody, Alexa Fluor 594 (A32794).	Rabbit	1:1000	Life technologies

^{32}P-labeled substrates

Substrate	Sequence 5´→3´
ssIIUI	ACUGGACA**[rI][rI]**U**[rI]**CUCCGAGG
dsIIUI	ACUGGACA[**rI**][**rI**]U[**rI**]CUCCGAGG + CCUCGGAGU[**rI**]UUUGUCCAGU
dsCtrRNA	GGCUGGUCCGAUGGUAGUGGG + CCCACUGCUAAAUUUGACUGGCUU
5´stem: bulge	GGCUGGUCCGAUGGUAGUGGG
5´stem: complimentary	GGCUGGUCCGAUGGUAGUGGG + CCCACUACCAUCGGACCAGCC
Hairpin	AUUAACAUUAGUGUCACUAAAGUUGGUAUACAACCC

Primers for northern blot

Primer	Description	Sequence
AlaAGC	5´termini	5´CAAGCGCTCTACCACTTGAGCTAATTCCCC
ArgACG	5´termini	5´ACGCGTTATCCATTGCGCCCACTGGCCC
GluCTC	5´termini	5´GCCGAATCCTAACCACTAGACCACCAGGGA
	3´termini	3´TTCCCTGACCGGGAATCGAACCCG
GlyACC	5´termini	5´GAGAATTCTACCACTGAACCACCAATGC
	3´termini	3´TGCATTGGCCGGGAATTGAACCCGG
ValAAC	5´termini	5´GGCGAACGTGATAACCACTACACTACGGAAAC
Y RNA1	5´termini	5´AATCAATTGAGATAACTACTACCTTCGGACCAGCC
Y RNA4	5´termini	5´AAAGCCAGTCAATTTAGCAGT

Primers for qPCR

Primer	Description	Sequence
Y RNA1	Forward	GGCTGGTCCGAAGGTAGTGAG
	Reversed	GGGGGAAAGAGTAGAACAAGG
Y RNA4	Forward	TCCGATGGTAGTGGGTTATCA
	Reversed	AAAGCCAGTCAAATTTAGCAGT
GAPDH	Forward	CCACATCGCTCAGACACCAT
	Reversed	GCGCCCAATACGACCAAAT

Gels

Gel	Manufacturer	Section
Bolt™ 10% Bis-Tris Plus	Invitrogen by Thermo Fisher Scientific	2.1.5 2.3.3
15% denaturing gel	-	2.4.4
20% denaturing gel	-	2.4.3
10% native denaturing gel	-	2.5.1, 2.5.2

Isotope

Isotope	Description	Specific Activity	Concentration	Manufacturer
[γ-^{32}P]ATP	Adenosine triphosphate	3000Ci(111TBq)/mmol	10 mCi/ml	Perkin Elmer

Molecular markers

Standard	Manufacturer
SeeBlue® Plus2 Prestained Standard (1x)	Invitrogen

Softwares

Software	Source	Section
Image Lab	Biorad	3.3.3
Typhoon Scanner control	Amersham Biosciences	2.4.3, 2.4.4, 2.5.1, 2.5.2
ImageQuant TL	Amersham Biosciences	2.4.3, 2.4.4, 2.5.1, 2.5.2
Fiji Image J	Image J	2.4, 3.5

Kits

Kit	Section	Manufacturer
miRNeasy® mini kit	2.6.1	Qiagen
rtStar™ First-Strand cDNA Synthesis kit	2.6.1	Go Beyond RNA ARRAYSTAR INC
SuperSignal^{R} West Femto Maximum Sensitivity Substrate	2.3.3	ThermoFisher scientific

Chemicals

Chemicals	Manufacturer	Concentration/Purity
4 x BOLT™ Sample Buffer B0007	Thermo Fisher Scientific	4 X
6 x DNA Loading Buffer/Dye R0611	Thermo Scientific	-
β-mercaptoethanol M3148-25ML	Sigma Aldrich	>99 %
Acetic acid	Merck	100 %
Ammoniumpersulphate (APS)	-	10 %
Blasticidin R210-01	Life Technologies	100 %
BioRad Protein Assay 5000006	BioRad	5x
Bolt™ LDS Sample Buffer B0008	Invitrogen	4x
Bovine Serum Albumin (BSA)	BioLabs® Inc.	10 mg/ml
Chloroform ($CHCl_3$) 288306	Sigma Aldrich	>99 %
Comassie Blue (s) B0770	Sigma Aldrich	-
Difco Luria Bertani (LB)-Broth	Miller	-
Dulbecco´s Modified Eagle medium with 4.5 g/l Glucos (DMEM)	Gibco	-
Dithiothreitol (DTT)	-	-
Doxycycline hyclate D9891-1G	Sigma	1 µg/µl
Ethanol 60068	antibac	100 %

Ethylenediaminetetraacetic acid (EDTA)	OUH	0.5 M
Fetal Bovine Serum (FBS) F7524	Sigma	-
Fibronectin bovine plasma F1141	Sigma Aldrich	1 mg
Formamide 11814320001	Sigma Aldrich	>99 %
Glycerol	OUH	60 %
Hygromycin B 10687010	Invitrogen	50 mg/ml
Imidazole (s)	Sigma Aldrich	>99 %
Iscove´s Modified Dulbecco´s Medium (IMDM) I6529-500ML	Sigma Life Science	
IPEGAL® CA-630 I8898	Sigma Aldrich	0.08 mM
Isopropanol 67-63-0	Merck	99.8 %
Isopropyl β-D-1-thiogalactopyranoside (IPTG)	OUH	1 M
Kanamycin	OUH	50 mg/ml
Laemmli Sample Buffer 1610747	BioRad	4x
Lipofectamine™ RNAiMAX	Invitrogen	-
Long Ranger™ Gel Solution	Lonza	-
Magnesium chloride ($MgCl_2$)	OUH	-
Methanol	VWR	98.5 %
3-(N-morpholino) propanesylfonic acid (MOPS)	Sigma Aldrich	> 99.5 %
N,N,N´,N´-tetramethylerhylenediamine (TEMED)	Sigma Aldrich	99 %
NuPAGE® MOPS SDS Running Buffer NP000102	Invitrogen	20x
Opti-MEM™ I Reduced Serum Medium 31985070	Gibco	-
Paraformaldehyde 158127-500G	Sigma Aldrich	95 %
Penicillin-streptomycin Glutamine 10378016	Gibco	100 x
Phenyl methane sulfonyl fluoride (PMSF)	Applichem	-
Phosphate buffered saline (PBS)	OUH	1x
Poly I:C	-	100 ng
PowerUp™ SYBR™ Green Master Mix A25742	Thermo Fisher	-
Protease Inhibitor cocktail P8340	Sigma Life sciences	-
Protino® Ni-NTA agarose (s) 745400	Macherey-Nagel	50 %
RNase A	OUH	10 mg/ml
RNaseOUT™ Recombinant Ribonuclease Inhibitor 10777019	Thermo Fisher	5,000 U
RNAzol® RT RN190	Molecular Research Center, Inc	-
Saline-sodium citrate	-	2x
Skim milk Powder 70166	Sigma Aldrich	-
Sodium arsenite solution ($Na_3ASO_{3)}$ 35000	Fluka Analytical	0.05 M
Sodium chloride (NaCl)	OUH	5 M
Sodium dodecyl sulphate (SDS)	OUH	20 %
Sorbitol (s)	VWR	-

T4 Polynucleotide Kinase M0201S	BioLabs®Inc	10,000 units/ml
T4 Polynucleotide Kinase Reaction Buffer B0201S	BioLabs®Inc	10 x
Taurine	OUH	20 x
Tris-HCl pH 7.4	OUH	1 M
Tris-HCl pH 8.0	OUH	1 M
Triton™ T8787	Sigma Aldrich	100 %
Trypan Blue Stain 15250061	Thermo Fisher	0.4 %
Trypsin-EDTA 25300-054	Gibco	0.05 %
Tween®20 P2287-500ML	Sigma Aldrich	
ULTRAhyb® Ultrasensitive Hybridization Buffer AM8670	Ambion	-
Urea 57-13-6	Merck	60.06 g/mol
Vanadyl ribonucleoside complex (VRC)	-	-
Vectashield HardSet Antifade Mounting Medium with Dapi	Vector Laboratorities, Inc.	-
Zeocin R25001	Invitrogen	100mg/ml

¨(s)=Solid

Recipes for buffers and solutions

Buffer/Solution	Recipe
Purification of proteins	
LB-kanamycin	25 g/l Difco LB Broth, 50 mg/l kanamycin
LB-sorbitol medium	25 g Difco LB Broth, 91 g sorbitol, in 1 l MQ
LB-kanamycin plates	25 g/l Difco LB Broth, 20 g/l agar, 50 mg/l kanamycin
Imidazole buffer I	50 mM Tris-HCl pH8, 300 mM NaCl, 10 mM Imidazole, 10 mM β-mercaptoethanol
Imidazole buffer II	50 mM Tris-Hcl pH8, 300 mM NaCl, 50 mM Imidazole, 10 mM β-mercaptoethanol
Imidazole buffer III	50 mM Tris-Hcl pH8, 300 mM NaCl, 300 mM Imidazole, 10 mM β-mercaptoethanol
Superdex 2000 buffer	50 mM Tris-HCl pH 8, 300 mM NaCl, 10 mM β-mercaptoethanol
TEV-buffer	50 mM Tris-HCl pH 8, 0.5 mM EDTA, 1 mM DTT
Solutions needed for culturing and maintaining cells:	
Culture medium for HAP CC665	Iscove´s Modified Dulbecco´s medium (IMDM) with sodium bicarbonate and L-glutamine, 10 % fetal bovine serum (FBS) and 1 % penicillin-streptomycin (P/S)
Culture medium for Flp-in T-REx 293	Dulbecco´s Modified Eagle medium (DMEM) containing 4.5 g/l glucose, 10 % FBS, 1 % P/S, 0.03 % blasticidin and 0.02 % zeocin

Culture medium for Flp-in T-REx 293 Flag-hEndoV	Dulbecco´s Modified Eagle medium (DMEM) containing 4.5 g/l glucose, 10 % FBS, 1 % P/S, 0.03 % blasticidin and 0.08 % hygromycin
NETN lysis buffer	100 mM NaCl, 30 mM Tris-HCl pH 8, 0,5% IGEPAL CA-630
Solutions needed for SDS PAGE	
Comassie Blue staining solution	40 % methanol, 10 % acetic acid, 0.1 % Coomassie Blue
Destaining solution	40 % methanol, 10 % acetic acid, 4 % Glycerol
Solutions needed for Western blot	
PBS/Tween buffer	1xPBS, 0.05 % Tween®20
PBS/Drymilk blocking buffer	1xPBS with 5 % Skim Milk Powder
Stripping buffer	20 ml 10 % SDS, 12.5 ml 0.5 M Tris-HCl pH 6.8, 0.8 ml β-mercaptoethanol, 67.5 ml MQ
Solutions needed during activity assay and EMSA	
10% native denaturing gel	0.25 ml 20x taurine buffer, 1 ml Long Ranger™ Gel Solution, 0.17 ml 60 % glycerol, 3.6 ml MQ, 35 µl 10 % APS, 3.5 µl TEMED
15% denaturing gel	7 M Urea (2.1 g), 0.25 ml 20xtaurine buffer, 1.5 ml Long Ranger™ Gel Solution, 1.55 ml MQ, 25 µl 10 % APS, 2.5 µl TEMED
Formamide loading dye	5% Bromophenol Blue, 5 % Xylene Cyanol, 10 mM EDTA in formamide
High Stringency buffer	2x Saline-Sodium Citrate (SSC), 0.1 % SDS
Low Stringency buffer	0.1 % SSC, 0.1 % SDS
Solutions needed for Co-IP	
NT2 equilibration buffer	50 mM Tris-HCl pH 7.4, 150 mM NaCl, 1 mM $MgCl_2$, 0.5 % IGEPAL CA-630
NT2 washing buffer	50 mM Tris-HCl pH 7.4, 300 mM NaCl, 1 mM $MgCl_2$, 0.5 % IGEPAL CA-630

Instruments

Type	Manufacturer
Spectrophotometer:	
NanoDrop™ One/One^C Microvolume UV-Vis	Thermo Fisher Scientific
UV-1800 UV-VISspectrophotometer	Shimadzu
Centrifuges:	
Sorvall LYNX 6000 Superspeed Centrifuge	Thermo Scientific
Capsulefuge PMC-860	TOMY
Spectrafuge mini	Labnet
Avanti™ J-25 Centrifuge	Beckman
Microplate Centrifuge, PCR Plate Spinner	VWR™

Mega Star 1.6R	VWR™
Megafuge 1.0R	Heraeus Instruments
5417R Refrigerated Centrifuge	Eppendorf
Incubator:	
Innova 4230 Refrigerated Incubator Shaker	New Brunswick Scientific
Innova 4000 Incubator Shaker	New Brunswick Scientific
Forma Steri-cycle CO_2	Thermo Scientific
Shake ´n´stack	Hybaid
Gel electrophoresis:	
Electrophoresis power supply EPS 60	Amersham pharmacia biotech
Mini Gel tank	Invotrogen
Mini-PROTEAN® II Electrophoresis	Bio-Rad
Sterile Hood	
Zafe 82 1200	Zystm A/S
Safe 2020, Class II Biological Safety Cabinet	Thermo scientific
RT-PCR:	
StepOnePlus Real-time PCR	Applied biosystems
Various:	
3 MM Chromotography paper	Whatman®
AT261 Delta Range weighing scale	Mettler Toledo
BioRad Molecular Imager	BioRad
BP 4100 weighing scale	Sartorius
CKX53 Inverted Microscope	Olympus
CL-1000 Ultraviolet Crosslinker	UVP
CoolCell™ LX Cell Freezing Container	Sigma
Countess™ Automated Cell Counter	Invitrogen
DynaMag™-2 Magnet	Thermo Fisher Scientific
Electroporator: MicroPulser	Bio-Rad
Electroporation cuvette 0.1 cm	Bio-Rad
Heat Block: QBT1	Grant
Image Eraser Light Box 410A	Molecular Dynamics
Microscope Cover Slips 12 mm	VWR
Mini-PROTEAN® Short Plates 0.75 mm 1653308	Bio-Rad
Molecular Imager® Gel doc™ XR system	Bio-Rad
Nitrogen tank: Cryo biological storage system	Thermolyne
Nunclon™ 75 cm^2 Treated flask, blue filter cap	Thermo Scientific
Nunclon™ 175 cm^2 Treated flask, blue filter cap	Thermo Scientific
Nunclon™ Dish 24-well	Thermo Scientific
PhosphorImager Screen	Amersham BioScienses

Protino® Ni-NTA Column	Macherey-Nagel
PTC-200 Peltier Thermal Cycler	MJ research
RNase-Free 1.5 ml Microfuge Tubes	Ambion
Spectra/Por®1 Dialysis Membrane	Spectrum Laboratories, Inc.
Stuart™ gyro-rocker, SSL3	Merck
Superfrost® Plus Microscope slides	Thermo Scientific
TCS Sp8 gSTED microscopy	Leica
Tissue Culture Dish 100 x 20 mm	Falcon®
Tissue Culture Dish with 20 mm Grid	Falcon®
Trans-Blot® SD Semi-Dry Transfer Cell	Bio-Rad
Trans-Blot® Turbo™ Transfer System	Bio-Rad
Typhoon 940 Variable Mode PhosphorImager	Amersham Biosciences
Vibra Cell™	Sonics and Materials Inc.

Appendix D. Plasmid map of vector pETM41

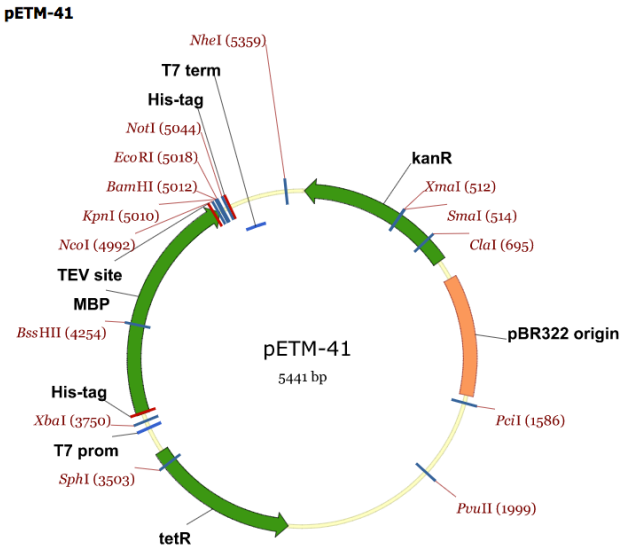

Figure A2. Plasmid map for pETM41. *pETM41contains a gene for kanamycin resistance (EMBL, 2016).*

Appendix E. Molecular marker

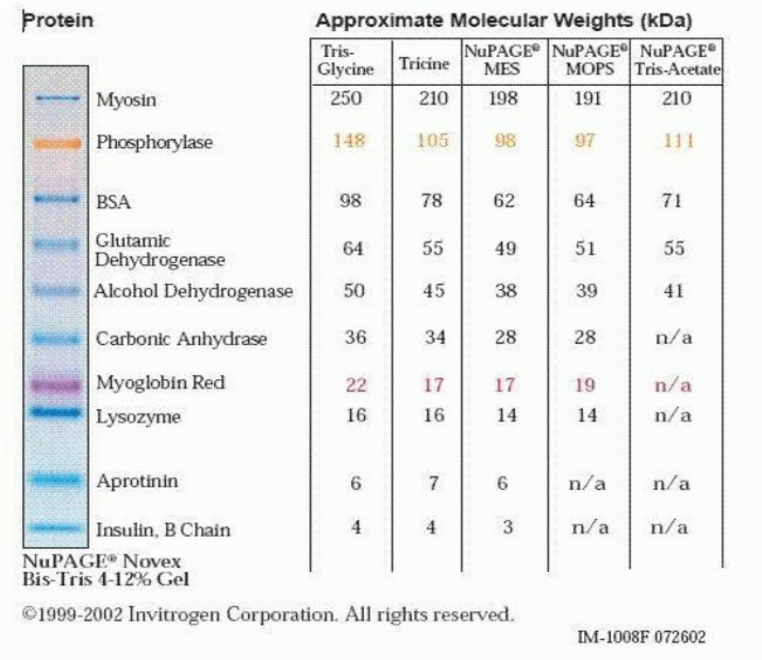

Figur A3. Molecular marker. *SeeBlue® Plus 2 Pre-stained Protein Standard. The molecularmarker is designes for proteins between 3 and 198 kDa. It was used to define the size of proteinmolecules after gelelectrophorase (Thermo Fisher Scientific, n-d).*

Norges miljø- og biovitenskapelige universitet
Noregs miljø- og biovitskapelege universitet
Norwegian University of Life Sciences

Postboks 5003
NO-1432 Ås
Norway